The level of DNA methylation impacts self-renewal capacity and lineage choices of hematopoietic stem cells

DISSERTATION

zur Erlangung des akademischen Grades

doctor rerum naturalium

(Dr. rer. nat.)

im Fach Biologie
eingereicht an der

Mathematisch Naturwissenschaftlichen Fakultät I
der Humboldt Universität zu Berlin
von

Diplom-Biologin Ann-Marie Elisabeth Bröske
geboren am 17.08.1980 in Oldenburg

Präsident der Humbold Universität zu Berlin:
Prof. Dr. Dr. h.c. Christoph Markschies
Dekan der Mathematisch-Naturwissenschaftlichen Fakultät I:
Prof. Dr. Lutz-Helmut Schön

Gutachter:
1. Prof. Dr. Achim Leutz
2. Prof. Dr. Claus Scheidereit
3. Prof. Dr. Harald Saumweber

eingereicht: 13.10.2009

Datum der Promotion: 03.03.2010

Table of Contents

I Abstract

DNA methylation is one of the major epigenetic mechanisms which is known to play a role in embryonic stem cell fate, but its function in somatic stem cells is not well understood. In this thesis two different genetic mouse models were chosen to address the role of DNA methyltransferase 1 (DNMT1) controlled DNA methylation in adult hematopoiesis. First, a conditional knockout approach was used to delete DNMT1 in the adult hematopoietic system. Second, DNMT1 hypomorphic mice with reduced DNMT1 expression were analyzed.

Complete DNMT1 deletion in hematopoietic cells led to severe cytopenia and anemia causing rapid lethality of all animals. Bone marrow analysis revealed an almost complete absence of hematopoietic stem and progenitor cells in DNMT1 ablated primary mice as well as in secondary chimeric mice. These results indicated that DNMT1 controlled maintenance of DNA methylation is indispensable for HSCs preservation and differentiation.

In contrast to complete DNMT1 deletion, mice with hypomorphic DNMT1 expression were viable, but showed low methylation levels in multiple tissues including the hematopoietic system. Detailed phenotypical and functional analysis of the hypomethylated hematopoietic stem cell (HSCs) compartment revealed an impaired homeostasis and self-renewal capacity. Intriguingly, mutant animals had profoundly reduced lymphoid cell compartments, whereas myeloid and erythroid compartments were unchanged. Expression profiling of stem and myeloid progenitor cells unexpectedly demonstrated that reduced DNA methylation forces the HSC to adopt a myeloid lineage identity. These results, showing the inability of hypomethylated HSCs to maintain an undifferentiated state, provided an explanation for their disturbed capability to self-renew and produce lymphocytes.

Taken together, these findings suggest that distinct levels of DNA methylation are required to control different functional programs such as self-renewal and alternative lineage choices in HSCs, thus uncovering a previously unrecognized function for DNMT1 activity.

Keywords: DNA methylation, epigenetic mechanism, hematopoietic stem cell, cell fate decision

II Zusammenfassung

DNS-Methylierung ist ein zentraler epigenetischer Prozess, der essentiell für die Differenzierung embryonaler Stammzellen ist, über dessen Funktion in somatischen Zellen allerdings wenig bekannt ist. In der vorliegenden Doktorarbeit wurden zwei Mausmodelle analysiert, um die Rolle der durch DNS Methyltransferase 1 (DNMT1) hergestellten DNS-Methylierung im adulten hämatopoetischen System zu untersuchen. Als erstes wurde ein „Knockout"-Modell gewählt, um DNMT1 im hämatopoetischen System zu eliminieren. Des Weiteren wurde eine Mausmutante mit reduzierter DNMT1 Expression analysiert.

Die vollständige Entfernung von DNMT1 aus dem hämatopoetischen System adulter Mäuse resultierte in Zytopenie und Anämie, gefolgt vom raschen Tod aller Tiere. Die Analyse des Knochenmarks dieser Mäuse zeigte einen fast vollständigen Verlust von hämatopoetischen Stamm- sowie Vorläuferzellen. Dies zeigt, dass die durch DNMT1 erzeugte DNS-Methylierung essentiell für Homöostase und Differenzierung von hämatopoetischen Stammzellen ist.

Mäuse mit reduzierter DNMT1 Expression hingegen sind lebensfähig und zeigen einen niedrigen Grad an DNS-Methylierung in verschiedensten Geweben, einschließlich des hämatopoetischen Systems. Durch eine detaillierte phänotypische und funktionelle Analyse der hämatopoetischen Stammzellen zeigte sich, dass der veränderte DNS-Methylierungsgrad ein vermindertes Selbsterneuerungspotenzial zur Folge hat. Interessanterweise fehlen DNMT1 hypomorphen Mäusen lymphoide Vorläuferzellen sowie reife lymphoide Zellen, wohingegen myeloide und erythroide Zellpopulationen keine Veränderungen zeigten. Genomweite Expressionsanalysen von Stammzellen sowie myeloiden Vorläuferzellen zeigten, dass hypomethylierte Stammzellen eine verfrühte myeloerythroide Entwicklung vollziehen und liefern damit eine Erklärung für den Verlust des Selbsterneurungspotenzials und der lymphoiden Entwicklung.

Diese Resultate identifizieren eine bis hierhin unbekannte Funktion von spezifischen DNS-Methylierungsgraden für die Steuerung von funktionellen Programmen wie Selbsterneuerung und Differenzierung in hämatopoetischen Stammzellen.

Schlagworte: DNS-Methylierung, Epigenetik, hämatopoetische Stammzellen, Zellschicksalsentscheidung

1 Introduction

1.1 Significance

The developmental process of metazoans requires organization of different genetic programs to give rise to functionally diverse cell types. Since all cells of one individual organism have an identical genetic background, the basis for variable cell development is differential gene expression. However, the detailed molecular mechanisms involved in this process are still poorly understood.

Epigenetic mechanisms, such as DNA methylation, are capable of altering gene expression without changing the underlying DNA sequence. Hence, epigenetic processes are thought to be involved in orchestrating cell type specific genetic programs. Understanding the role of DNA methylation in organizing the molecular network and how it is influencing cell fate decisions is an issue of intensive research and will provide insights in how cell fate decisions are regulated in the nucleus. The hematopoietic system has been used as a model system for many years and is an optimal system to study how developmental processes are governed.

This thesis studies the impact of DNA methylation on hematopoietic stem cell fate decisions and how individual genetic programs are sustained via this epigenetic mechanism. This chapter introduces the hematopoietic system and the principles of gene regulation through DNA methylation.

1.2 Hematopoiesis

Hematopoiesis is the formation and development of blood cells. This is a continuous process throughout life and some 10^{12} hematopoietic cells are given rise to in humans just in steady state every day (Ogawa, 1993). When challenged, this output can rapidly increase at least ten fold to maintain homeostasis and can therefore compensate stress such as bleeding or infection (Kaushansky, 2006). Mature cells from different blood cell lineages carry out a number of functions indispensable for life. Red blood cells (RBC) transport oxygen from the lungs to all parts of the body. Platelets derived from megakaryocytes (Mk) are involved in blood clotting. White blood cells including B cells, T cells, natural killer cells, dendritic cells, granulocytes

and macrophages together form the immune system which protects individuals from infectious disease. Mature blood cells, with the exception of some rarer lymphoid cell types called memory cells, are relatively short lived with a lifespan ranging from hours (granulocytes) to a couple of months (RBCs) (Ogawa, 1993). Therefore, progenitors are required to continuously fill up all the mature cell populations. This general progenitor is the hematopoietic stem cell (HSC). The simplified scheme shown in Figure 1 describes the hierarchy of the hematopoietic system. The hierarchy of progenitor populations cannot be considered to be static, since new investigations show new or altered branching points. Lately, MEPs (megakaryocyte erythrocyte progenitors) were proposed to be the direct origin of HSCs whereas all myeloid and lymphoid progenitors arise from LMPPs (lymphoid myeloid primed progenitors) (Adolfsson, et al., 2005).

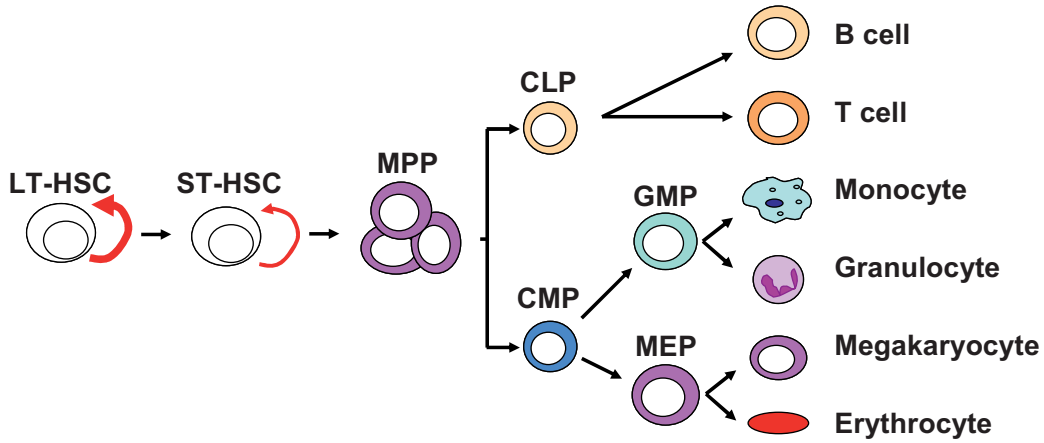

Figure 1: Simplified schematic overview of the hematopoietic hierarchy. All hematopoietic cells are generated from hematopoietic stem cells (HSC) which can self-renew (red arrow). Long term/short term hematopoietic stem cells LT/ST-HSC, multipotent progenitor MPP, common lymphoid progenitor CLP, common myeloid progenitor CMP, granulocyte macrophage progenitor GMP, megakaryocyte erythrocyte progenitor MEP. Adapted from (Rosenbauer and Tenen, 2007).

The function of HSCs in human health and disease is one of the central issues of modern medicine but due to the difficulties in studying human hematopoiesis, animal models, especially mouse models, are extensively used. Even though some differences exist, the major concept of stem cell growth and regulation is likely to be well conserved between mouse and human. Therefore, this thesis is based on findings from studies of the murine hematopoietic system.

1.2.1 Experimental advantages of the hematopoietic system

Choosing the hematopoietic system as a model for stem cell fate regulation offers a lot of advantages. First, it is relatively easy to isolate hematopoietic cells of mice. Hematopoietic cells are found in several organs of the body, namely the bone marrow (BM), which harbors the adult HSCs, all myeloerythroid and B-lymphoid progenitors. The BM largely consists of mature myeloid cells. The majority of mature B and T cells are found in the spleen and lymph nodes, while the thymus largely consist of T cells and T-cell progenitors. Further hematopoietic cell populations are found in the peritoneum and the peripheral blood. A second advantage of the hematopoietic system is that fluorescence activated cell sorting (FACS) and appropriate antibodies coupled to fluorescent dyes enable the experimenter to stain isolated tissues for a variety of surface markers. Subsequently, flow cytometry computer software makes it possible to characterize different hematopoietic cell populations in great detail. For functional characterization, distinct cell populations can be separated and isolated (sorted) based on their surface marker expression. Additionally, functional assays can be carried out with these sorted cells, e.g. *in vivo* transplantation assays and *in vitro* differentiation assays. A third advantage is that a variety of cell populations is well investigated and characterized. Using the method of FACS, it was possible to identify specific myeloid or lymphoid progenitors, which exclusively give rise to myeloid or lymphoid cells, respectively (Akashi, et al., 1999) (Akashi, et al., 2000).

1.2.2 The hematopoietic stem cell

In the hierarchical view of the hematopoietic system, shown in Figure 1, HSCs mark the origin of all mature cell populations. HSCs are defined through different competences. First, being able to extensively self renew. That means they have the ability to generate at least one cell identical to itself upon cell division (Keller and Snodgrass, 1990). Second, being able to give rise to differentiated progeny and to form all different hematopoietic lineages (Dick, et al., 1985) (Keller, et al., 1985) (Lemischka, et al., 1986). These abilities are dependent on the process of asymmetric cell division which balances self-renewal and differentiation allowing the generation of committed daughter cells and the lifelong preservation of the stem cell pool (Congdon and Reya, 2008). Third, being able to functionally replace a damaged

BM, e.g. reconstitute lethally irradiated mice (Lorenz, et al., 1951).

To identify HSCs, their potential of long-term reconstitution of lethally irradiated mice was used in transplantation assays. In the adult mouse, functional HSCs are found in a subset of the BM population that does not express cell-surface markers normally present on lineage-committed (Lin) hematopoietic cells, but expresses high levels of the stem-cell antigen-1 (Sca1) and the c-Kit receptor. Although all functional HSC activity is found in the $Lin^{-}Sca1^{+}c\text{-}Kit^{+}$ (LSK) population, less than 1 out of 10 of these LSK cells has repopulation capacity, suggesting substantial functional heterogeneity within this compartment. Subsequently, these studies were extended using the antiadhesive sialomucin CD34 (a cell-cell adhesion factor) as an additional marker. 1 out of 5 cells in the $LSKCD34^{-}$ compartment show repopulation capacity. The use of two signaling lymphoid activation molecule (SLAM) markers, CD48 and CD150, defines a compartment of $LSKCD48^{-}CD150^{+}$ cells in which 1 out of 2 cells is a HSC with repopulating capacity (Wilson and Trumpp, 2006). The HSC population can be subdivided into long-term (LT) and short-term (ST) reconstituting HSCs. In the LT-HSCs compartment (LSK $CD34^{-/low}Flt3^{-}$) cells are found with the ability to repopulate and rescue a lethally irradiated animal throughout life, whereas in the ST-HSCs compartment (LSK $CD34^{+}Flt3^{-}$) cells are found with the ability to rescue the animal for several weeks only (Morrison, et al., 1995).

Which mechanism enables hematopoietic stem cells to sustain their multipotent state? How is the transition into differentiated progenitor states regulated?

1.2.3 Regulation of the hematopoietic stem cell fate

Homeostasis and plasticity of multipotent HSCs must be tightly controlled. Generation of functionally specialized hematopoietic cells requires the establishment of different genetic programs. However, the molecular details regarding how this is achieved are still poorly understood. Genetic and also epigenetic processes are involved in orchestrating the HSC potential. On the genetic level many transcription factors were shown to have an impact on self-renewal, dormancy, differentiation properties or lineage decisions of HSCs. A short assortment of some of these factors with important functions in the hematopoietic system is shown in Table 1.

Table 1: Hematopoietic cell phenotypes of cells lacking transcriptional regulators. This table lists altered phenotypes as observed after germ line or conditional gene inactivation of each transcription factor. GM granulocytes/macrophages, DC dendritic cells, NK natural killer cells. Adapted from (Laiosa, et al., 2006).

Gene	Phenotype of mutant mice	Reference
Pu.1	Functional defect of HSCs, lack/maturational block of T cells, B cells, GMs and DCs, decrease of NK cells	(Koschmieder, et al., 2005), (Scott, et al., 1994)
Ebf1	Maturational block of B-cell development	(Lin and Grosschedl, 1995)
Id2	Decrease of NK cells and DCs	(Yokota, et al., 1999), (Ikawa, et al., 2001), (Hacker, et al., 2003)
Cebpα	Functional defect of HSCs, lack of GMs	(Zhang, et al., 1997), (Zhang, et al., 2004)
Cebpβ	Functional defect/decrease of B cells, functional defect of GMs	(Chen, et al., 1997), (Tanaka, et al., 1995)
Gata1	Lack/maturational block of MegE	(Takahashi, et al., 2000), (Fujiwara, et al., 1996), (Pevny, et al., 1991)
Pax5	Maturational block in B cell development	(Mikkola, et al., 2002), (Nutt, et al., 1999)
Notch1	Lack of T cells	(Radtke, et al., 1999)
c-myc	Functional defect in HSC homeostasis	(Wilson, et al., 2004)
Pten	Functional defect in HSC maintenance	(Zhang, et al., 2006)

The remaining question is which mechanisms orchestrate the onset of distinct transcription factors and decide about cell fate decisions? As already mentioned, epigenetic mechanisms are capable of altering gene expression without changing the underlying DNA sequence. It was suggested earlier that chromatin remodelling in addition to transcription factor expression is involved in regulating HSC fate (Bonifer, et al., 2006).

1.3 Epigenetics

Historically, the word *epigenetics* was used to describe events that could not be explained by genetic principles. Waddington created the term “epigenetics” as a portmanteau from the words genetic and epigenesis. He defined it as the branch of biology which studies the causal interactions between genes and their products which in the end lead to the phenotype (Waddington, 1942). There are some nameable classical phenomena like paramutation in maize (here, the interaction between two alleles causes heritable changes in one of the alleles) (Hollick, et al., 1997), position effect in the fruit fly *Drosophila* (here, the local chromatin environment of genes influences their expression) (Wakimoto, 1998) and imprinting of specific paternal or maternal loci in mammals (Reik and Walter, 2001).

In a broad sense, epigenetics means the bridge between genotype and phenotype. It describes the phenomenon that epigenetic mechanisms change the final outcome of a gene locus or chromosome (phenotype) without changing the underlying DNA sequence (genotype). This ideally involves a heritable change in gene expression. With this mechanism, it is possible to form a great diversity of cell types with distinct cellular functions although the majority of all cells in a multicellular organism contain an identical genotype. So, the cellular differentiation process could be understood as an epigenetic phenomenon influenced by changes in the epigenetic landscape. This is demonstrated in the classical epigenetic landscape model by Waddington and its modification which illustrates the impact of epigenetic processes on cell fate decisions (Figure 2).

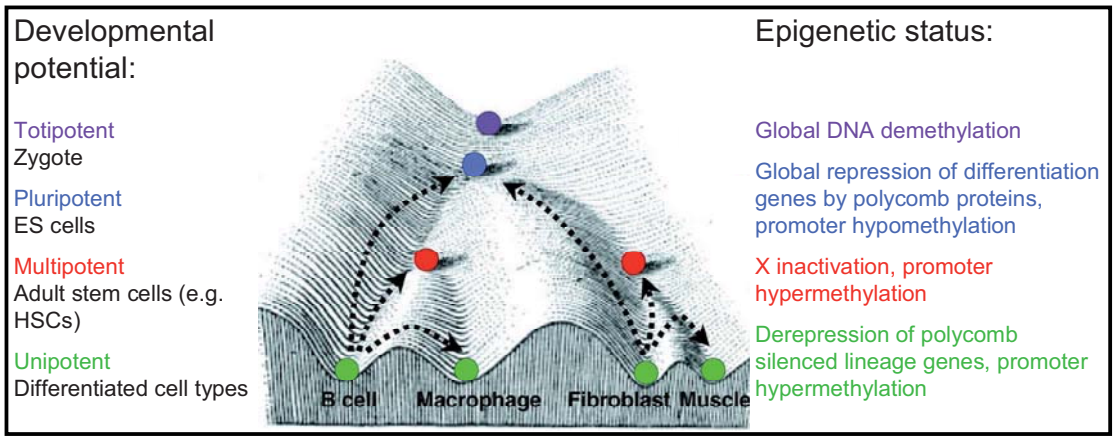

Figure 2: Epigenetic Landscapes. In 1957, Conrad Waddington proposed the concept of an epigenetic landscape to represent the process of cellular decisions during development. (Waddington, 1957). This is a modification of Waddington's epigenetic landscape model, showing cell populations with different developmental potentials (left) and their respective epigenetic states (right). Developmental restrictions can be illustrated as marbles rolling down a landscape into one of several valleys (cell fates). Coloured marbles correspond to different differentiation states. Examples of reprogramming processes are shown by dashed arrows. Adapted from (Hochedlinger and Plath, 2009).

Epigenetic mechanisms influence the overall chromatin structure (complex of DNA and its associated proteins) through covalent and noncovalent modifications of DNA and histone proteins. The components of the main epigenetic chromatin modification and remodeling complexes are:

- DNA cytosine methyltransferases (e.g. DNMT1)
- Methyl-CpG-binding proteins (e.g. MeCP1)
- Histone-modification enzymes (e.g. Suv39h1, G9a)
- ATP-dependent remodeling complexes (e.g. Mi-2/NuRD, SWI/SNF/Brm)

In this thesis, the impact of DNA methylation on cell fate decisions is investigated. Therefore, the introduction will focus on DNA methylation mechanisms and associated processes.

1.3.1 DNA methylation

A major element of epigenetic modifications is the pattern of DNA methylation. DNA methylation is a type of covalent chemical modification on DNA which can be inherited. DNA methylation occurs in plants, fungi, invertebrates and vertebrates

whereas some organisms, such as *S. cerevisiae*, show no methylation or, like *C. elegans*, only in the embryo. In mammals, nearly all DNA methylation occurs on cytosine residues of CpG dinucleotides and results in a 5-methylcytosine (5-mC) (Figure 3).

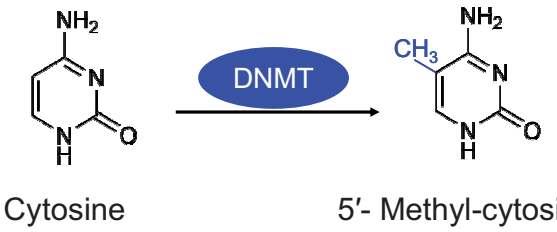

Figure 3: Reaction catalyzed by DNA (cytosine-5′)-methyltransferases. DNMTs place a methyl group at the 5' position of cytosines in CpG dinucleotides. All DNMTs use S-adenosyl methionine (SAM) as the methyl group donor.

80% of the CpG sites in the mammalian genome are in fact methylated (Razin and Szyf, 1984). The occurrence of CpG dinucleotides in the genome is lower than the statistically expected frequency. The cytosine pyrimidine base is vulnerable to spontaneous deamination, which, in case of methylated cytosine, results in a C to T transition. Unmethylated cytosine undergoes formation to uracil which is detected by the DNA repair machinery and, as a non-DNA base, replaced by a thymidine (Cooke, et al., 2003). Due to this mutational pressure, CpG dinucleotides have evolutionarily been reduced.

1.3.1.1 Function of DNA methylation

DNA methylation was shown to be involved in many processes, but the particular function is not completely understood. Two major aspects were commonly stated in the past. First, since transposable elements are methylated to prevent their transposition, DNA methylation is seen as a genome defense against viral DNA. This phenomenon has never been shown for animals but for fungal and plant genomes only (Slotkin and Martienssen, 2007). Second, since DNA methylation is closely coupled to other chromatin modeling mechanisms, it was thought to essentially contribute to the formation of heterochromatin. But even in organisms lacking DNA methylation, such as *D. melanogaster* (Urieli-Shoval, et al., 1982), formation of heterochromatin is seen (Riddle and Elgin, 2008).

The current view of the essential function of DNA methylation is that it stably silences

gene expression through promoter methylation and that transcriptional noise gets reduced through methylation of intragenic regions (Suzuki and Bird, 2008).
Genomic regions which show a high density of CpGs are referred to as CpG islands. Methylation of these ~1000 bp long regions results in transcriptional repression (Goll and Bestor, 2005). CpG islands, but also regions with a lower CpG content, are often associated with genes and were shown to influence gene activity (Weber, et al., 2007). Additionally, DNA methylation is crucial for embryonic development of mammals regulating genomic imprinting, X inactivation and cell differentiation (Reik and Walter, 2001) (Mlynarczyk and Panning, 2000).
In this thesis, the question whether DNA methylation has a function in repressing alternative genetic programs and thereby preserves multipotent HSCs is investigated.

1.3.1.2 DNA methylation in human diseases

DNA methylation patterns were shown to be globally disrupted in cancer, with genome-wide hypomethylation and gene-specific hypermethylation occurring simultaneously in the same cell (Melki and Clark, 2002). Loss of normal imprinting contributes to several inherited genetic diseases in humans. These diseases include Beckwith–Wiedemann, Prader–Willi, and Angelman syndromes, Albright hereditary osteodystrophy (AHO) as well as pseudohypoparathyroidism and transient neonatal diabetes. Abnormal expansion of repeats in the *Fmr1* gene, accompanied by its hypermethylation and silencing, leads to fragile X syndrome. In contrast, reduction and hypomethylation of a larger 3.3 kb repeat leads to facioscapulohumeral muscular dystrophy. But also mutations in the methylation machinery contribute to human diseases. A mutation in the *Dnmt3a* gene leads to immunodeficiency, centromeric instability and facial anomalies (ICF) syndrome. This and other disorders damaging the methylation machinery are characterized by localized disruptions in DNA methylation pattern (Robertson, 2005). These examples show the importance of a tight and accurate regulation of epigenetic mechanisms.

1.3.1.3 DNA methyltransferases (DNMTs)

The DNA methylation pattern is copied by an independent enzymatic machinery, the DNA methyltransferases (DNMTs), during the S1 phase (DNA synthesis) of the cell cycle (Szyf and Detich, 2001). These enzymes catalyze the transfer of a methyl

group from S-adenosylmethionine (SAM) onto the 5′ position of the cytosine ring. The products of this reaction are S-adenosylhomocysteine and methylated DNA (Figure 3).

The first eukaryotic DNA methyltransferase (Dnmt1) was cloned from murine cells in 1988 (Bestor, 1988). During cell cycle, the newly synthesized DNA strand has to be methylated because the parental DNA strand carries the former methylation pattern only. DNMT1 has a 5- to 30-fold preference for hemimethylated DNA (Yoder, et al., 1997) and was shown to carry out a role limited to the maintenance of methylation patterns (Lyko, et al., 1999). This enzyme was shown to be localized in the replication foci (Leonhardt, et al., 1992) and to be associated with the proliferating cell nuclear antigen (PCNA) (Chuang, et al., 1997). It transfers a methyl group to the nascent strand only if a methyl group is present on the parallel position on the parental strand (Gruenbaum, et al., 1982). Therefore, it was postulated to be the enzyme responsible for replicating the DNA methylation pattern during DNA synthesis.

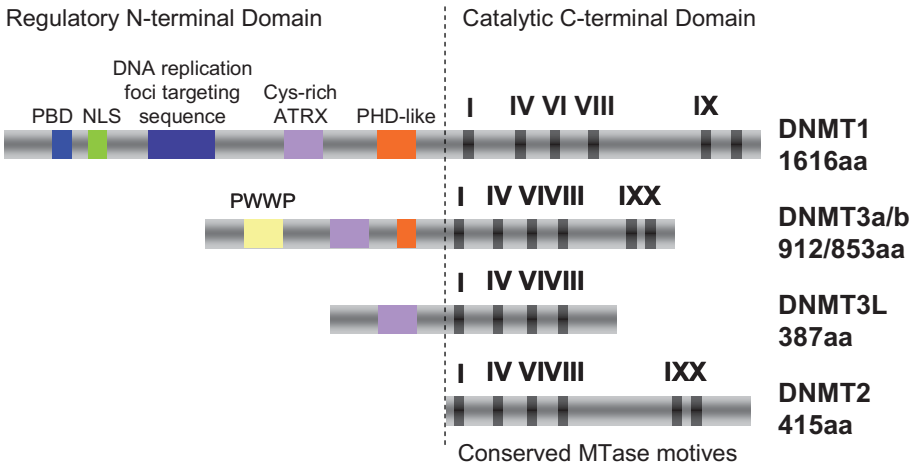

Figure 4: Schematic structure of members of the mammalian DNMT family. Positions of sequence motifs are indicated. The N-terminal domain contains a proliferating cell nuclear antigen-binding domain (PBD), a nuclear localization signal (NLS), an ATRX cysteine-rich zinc finger DNA-binding motif, a polybromo homology domain (PHD) targeting DNMT to the replication foci and a tetrapeptide PWWP, essential for DNMT binding to chromatin. The C-terminal domain includes six conserved motives: I is involved in the formation of the SAM binding site, IV binds the substrate cytosine at the active site, VI contains the glutamyl residue serving as a proton donor, VIII's function is unclear, IX maintains the structure of the substrate-binding site and X participates in the formation of the SAM binding site. aa, number of amino acids. Adapted from (Turek-Plewa and Jagodzinski, 2005)

The residual level of DNA methylation found in *Dnmt1* knock-out mouse embryos (Li, et al., 1992) confirmed the prediction that this enzyme is not the only factor responsible for DNA methylation. *Dnmt3a* and *Dnmt3b* were described as DNA methyltransferases with *de novo* DNA methylation functions (Okano, et al., 1999). A *Dnmt3* like protein (*Dnmt3l*) was shown to have no methyltransferase activity, since it misses the amino acid residues necessary for methyltransferase activity. However, DNMT3L was found to be involved in regulation of DNMT3a and is thought to be required for the establishment of maternal genomic imprints (Jia, et al., 2007).
Another DNA methyltransferase homolog, *Dnmt2*, was found not to be involved in DNA methylation since knockout embryonic stem (ES) cells show no alteration in global *de novo* or maintenance DNA methylation ability (Okano, et al., 1998). Later, DNMT2 was shown to specifically methylate a cytosine in aspartic acid transfer RNA (tRNA(Asp)) (Goll, et al., 2006) and was therefore renamed into TRDMT1 (tRNA aspartic acid methyltransferase 1).
Structure and important sequence motifs of DNMT members are shown in Figure 4.

1.3.1.4 Regulation of Dnmt1

Expression of *Dnmt1* has to be tightly regulated according to cell cycle phases since DNA synthesis, in the absence of DNMT1, would result in loss of the global DNA methylation pattern. Studies of transcriptional regulation of *Dnmt1* revealed activator protein 1 (AP-1) regulatory sequences which are known to be activated by the main mitogenic and proto-oncogenic Ras-c-Jun signaling pathway. Also involvement of retinoblastoma (Rb) (Slack, et al., 2001) and the APC-β catenin-TCF (Laird, et al., 1995) signal pathways were shown to contribute to *Dnmt1* regulation. These data suggest that expression of *Dnmt1* is coordinated with other cellular events that regulate DNA synthesis (Szyf and Detich, 2001).

1.3.1.5 Effects of DNA methylation on gene regulation

Epigenetic mechanisms can cause changes in chromatin conformation. Thus, distinct loci in the genome can get more or less accessible for other regulating machineries involving protein-DNA interactions (Schneider and Grosschedl, 2007). Notably, these chromatin changes are reversible throughout life, giving an opportunity to change the state of a cell whenever it is needed.
How does DNA methylation influence expression of adjacent genes? DNA

methylation or demethylation alone can not change gene expression, since specialized transcriptional machinery is always required to drive expression of a gene. Two major mechanisms influencing the gene expression machinery caused by DNA methylation are presented in the two following paragraphs.

1.3.1.5.1 Direct effects

Genomic sequences, representing binding sites for transcription factors, can be covered by DNA methylation and this in consequence can inhibit specific binding of the respective transcription factors. This effect was shown for multiple cases such as *c-myc* (Prendergast and Ziff, 1991) (Prendergast, et al., 1991), activating protein 2 (AP2) (Comb and Goodman, 1990), cAMP response element CRE (Inamdar, et al., 1991) (Moens, et al., 1993), early gene factor (E2F) (Kovesdi, et al., 1987), NF-κB (Bednarik, et al., 1991) and for the interaction of the genome organizing protein CTCF with insuline-like growth factor 2 (Igf2) (Wolffe, 2000).
Regulation of these genes are examples for a direct transcriptional inhibition through DNA methylation and is based on the existence of transcription factors sensitive to the presence of methylated or non-methylated cytosines within their target sequences. Thus, methylation of regulatory sequences may prevent initiation of transcription. But, not every transcription factor has a CpG site in its binding sequence and not every transcription factor with a CpG site in its binding sequence is sensitive to its methylation status as the example of SP1 shows. SP1 is an ubiquitous transcription factor which is often associated with housekeeping genes and has a CG in its consensus binding site. SP1 is not sensitive for methylation in its recognition site (Holler, et al., 1988).

1.3.1.5.2 Indirect effects

CpG methylation at genomic sites is recognized and bound by methyl-CpG-binding proteins (MBPs). This, in consequence, makes the DNA inaccessible to the transcriptional machinery. Furthermore, MBPs can recruit histone deacetylases (HDACs) to the DNA (Nan, et al., 1998). Deacetylation of lysine groups in histones mediated by HDACs leads to the remodeling of chromatin into an active shape. Known MBPs are: MECP2, MBD1, MBD2, MBD3, MBD4 and Kaiso (Figure 6). Apart from Kaiso, all were identified to carry a methyl-CpG-binding domain (MBD). Except for MBD4, all of them are associated with HDACs and, additionally, a transcriptional

repression mechanism mediated by the recruitment of HDACs has been shown for MeCP2, MBD1 and MBD2 (Nan, et al., 1998) (Ng, et al., 2000). MeCP2 selectively binds CpG dinucleotides in the mammalian genome and mediates transcriptional repression through interaction with histone deacetylase and the corepressor SIN3A (Jones, et al., 1998). MBD2 together with the nucleosome remodeling and deacetylase (NuRD) forms the complex MeCP1 (Ng, et al., 1999). MBD4 is an endonuclease involved in DNA mismatch repair and this enzyme may function to minimize mutation at methyl-CpGs (Hendrich, et al., 1999).

Kaiso, a transcriptional repressor protein lacking an MBD, has also been shown to bind to methylated CpG dinucleotides (Prokhortchouk, et al., 2001). One of these five MBD proteins, the X linked MECP2, is implicated in a human neurological disorder called RETT syndrome (Amir, et al., 1999). A number of studies have shown that not every repression by MBPs could be removed by inhibiting histone deacetylation with the HDAC inhibitor compound Trichostatin A, indicating towards an additional HDAC-independent pathway of transcriptional repression (Yu, et al., 2000).

Taken together, DNA methylation can repress gene expression through direct or indirect blocking of the transcriptional machinery as simplified in Figure 5.

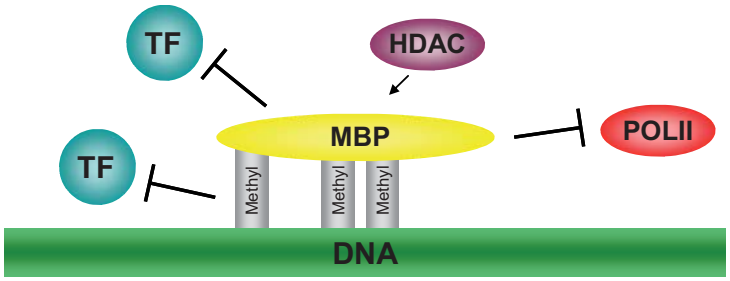

Figure 5: Direct and indirect mechanisms of transcriptional repression by DNA methylation. A stretch of DNA with methyl groups (in grey) is shown. A transcription factor (TF) is unable to bind its recognition site when a methylated CpG is within it. Methyl-CpG-binding proteins (MBP) and histone deacetylases (HDAC), that can be attracted by methylation interfere with the transcription machinery. POLII, polymeraseII.

1.3.1.6 Site specificity of DNMT1

Studies of large numbers of promoters have detected many sequences at which the DNA methylation pattern varies according to the cell type (Suzuki and Bird, 2008). This means that not the global grade of DNA methylation changes during development but DNA sequences are individually methylated or demethylated. These

results allow the hypothesis that distinct DNA sequences are methylated during differentiation. How is a site specific methylation pattern achieved? Is DNMT1 recruited to distinct sequences in a direct or indirect fashion?

DNMT1 was shown to form a complex with Rb, E2F1 and HDAC1 and to repress transcription of E2F-responsive promoters. This finding showed a link between DNA methylation, histone deacetylation and sequence-specific DNA binding activity (Robertson, et al., 2000). Polycomb group (PcG) and trithorax proteins (trithorax group proteins antagonize the repressive effects of PcG proteins) resemble another group of key epigenetic regulators involved in chromatin remodeling. In vertebrates PcG proteins assemble into two discrete chromatin-associated complexes, Polycomb Repressive Complex 1 and 2 (Sauvageau and Sauvageau, 2008). DNMT1 was shown to interact with the PcG protein enhancer of zeste homolog 2 (EZH2) to methylate its target genes, suggesting that EZH2 serves as a recruitment platform for DNA methyltransferases (Vire, et al., 2006). The major histone methyltransferase (G9A) is responsible for dimethylation of H3K9 which in turn serves as a platform for heterochromatin protein 1 (HP1). HP1 was also shown to interact with DNMT1. This interaction involved enhanced methylation of DNA at appropriate target sequences (Smallwood, et al., 2007). These examples show that DNMT1 can indeed be recruited to specific genomic sequences to specifically methylate DNA.

1.3.1.7 Demethylation of DNA

DNA methylation was considered to be the most stable of all heritable epigenetic marks. However, it was shown that DNA methylation is reversible with examples in plant cells, animal development and immune cells (Niehrs, 2009). In mammals, global demethylation occurs in the male pronucleus in the zygote (Howlett and Reik, 1991) and in the primordial germ cells in the early embryo (Rougier, et al., 1998).

Two ways of DNA demethylation must be considered. First, the passive loss of DNA methylation could be achieved through proteins hindering DNMT1 from copying the parental strand pattern during cell cycle. This was shown in an *in vitro* study (Han, et al., 2001) but still remains to be shown *in vivo*. Second, the active removal of methylation marks could be obtained through direct removal of the methyl group of cytosines (Bhattacharya, et al., 1999) through base excision repair or nucleotide excision repair of DNA-containing 5-methylcytosine (Gehring, et al., 2009). The first

protein shown to be responsible for active enzymatic demethylation was Gadd45 in cooperation with the deaminase AID and the glycosylase MBD4 using a zebrafish model (Barreto, et al., 2007) (Rai, et al., 2008).

Taken together, DNA methylation has already been demonstrated to influence gene expression in a really specific manner, but whether it is involved in orchestrating different genetic programs and whether it regulates cell fate decisions has not been shown so far.

1.4 DNMT1 in model systems

Following the isolation of the murine DNA methyltransferase 1, it was deleted from the mouse genome using homologous recombination to test the function of DNMT1 activity *in vivo*. A short summary of the mutant phenotypes of all knockout mice of DNA methyltransferase members is shown in Table 2.

Table 2: Phenotypes of mice with defective DNA methylation enzymes. Adapted from (Li, 2002).

Gene	Mutant phenotype	Reference
Dnmt1$^{-/-}$	Genome wide demethylation and developmental arrest at E8.5	(Li, et al., 1992), (Lei, et al., 1996)
Dnmt3a$^{-/-}$	Malfunction of the gut, spermatogenesis defect, death at ~4 weeks of age	(Okano, et al., 1999)
Dnmt3b$^{-/-}$	Demethylation of minor satellite DNA, mild neural tube defects and embryonic lethality at ~E14.5-18.5	(Okano, et al., 1999)
Dnmt3a$^{-/-}$, 3b$^{-/-}$	Failure to initiate *de novo* methylation after implantation and developmental arrest at E8.5	(Okano, et al., 1999)
Dnmt3l$^{-/-}$	Failure to establish maternal methylation imprints in oocytes and male sterility due to spermatogenesis defects	(Hata, et al., 2002), (Bourc'his, et al., 2001)

Additionally, due to embryonic lethality caused by Dnmt1 deletion, a conditional knockout allele was created (for a detailed description see 2.2.1.1). This was used to delete *Dnmt1* from specific tissues and made it feasible to investigate its role in adult mice.

Conditional deletion of *Dnmt1* via crossbreeding with a *mb1*-Cre strain (*mb1* is expressed only at the early stages of B cell differentiation) results in an almost

complete block in B-cell differentiation (Hobeika, et al., 2006) showing that *Dnmt1* is indispensable for B-cell development. A critical role for *Dnmt1* in T-cell development, function and survival was shown by inactivation of *Dnmt1* by Cre/loxP-mediated deletion at sequential stages of T-cell development (Lee, et al., 2001).

Since *Dnmt1* is expressed at high levels in the central nervous system (CNS) during embryogenesis and after birth (Goto, et al., 1994) and DNA methylation has been associated with at least three mental retardation diseases, including the RETT, ICF, and the fragile X syndromes (Robertson and Wolffe, 2000), the role of DNMT1 activity in the nervous system was studied. With the use of a conditional deletion approach of *Dnmt1* in CNS precursors and in postmitotic CNS neurons it was shown that DNA hypomethylation perturbs the function and survival of CNS neurons in postnatal animals (Fan, et al., 2001). These studies showed that DNA methylation is crucial for development of sensory maps and suggested that epigenetic mechanisms play a role in the development of synaptic plasticity (Golshani, et al., 2005).

Deficiency of *Dnmt1* in ES cells, though with no obvious effect on *in vitro* growth of undifferentiated ES cells, results in genomic hypomethylation, embryonic lethality after gastrulation and loss of monoallelic expression of imprinted genes (Li, et al., 1992) (Li, et al., 1993). Similarly, overexpression of *Dnmt1* in ES cells has no effect on proliferation, but when injected into blastocysts, embryonic lethality of the chimeric embryo is seen. This suggested that DNA methylation has no obvious role in the survival of ES cells but is crucial for normal physiology of somatic cells (Biniszkiewicz, et al., 2002). Conditional knockout of *Dnmt1* in ES cells revealed changes in gene expression that interfere with several pathways, including expression of imprinted genes, cell-cycle control, growth factor/receptor signal transduction and mobilization of retroelements (Jackson-Grusby, et al., 2001). Furthermore, loss of *Dnmt1* has an impact on methylation of repetitive sequences, which is crucial to prevent expression and retrotransposition (Gaudet, et al., 2004).

Complete elimination of *Dnmt1* in a human cancer cell line led to severe mitotic defects and cell death either during mitosis or after arresting in a tetraploid G1 state. These results demonstrated an essential role for DNMT1 in survival and proliferation of human cancer cells (Chen, et al., 2007).

In addition, to study the role of appropriate DNA methylation levels, a mouse model with a knockdown of *Dnmt1* was introduced. In this mouse model, which was also

used in this thesis, a knockout allele was combined with a hypomorphic allele (for a detailed description see 2.2.1.1) resulting in a mouse with decreased *Dnmt1* activity. In contrast to *Dnmt1* knockout animals, *Dnmt1* hypomorphic mice were viable due to substantially higher DNMT1 activity. Nevertheless, *Dnmt1* knockdown mice showed a substantial genome-wide DNA hypomethylation in all tissues. At the age of 4 to 8 months they developed aggressive T cell lymphomas which were possibly caused by chromosomal instability (Gaudet, et al., 2003).

Taken together, the non-replaceable function of DNMT1 was shown with several mouse models. Nevertheless, it is still in question how DNA methylation, achieved by DNMT1, is involved in orchestrating genetic programs. Furthermore, its essential role for differentiation of stem cells was shown but how DNA methylation is specifically influencing (stem) cell fate is still unresolved.

1.5 Epigenetics and cell fate decisions

A number of pluripotency-related genes were shown to be hypomethylated in stem cells and hypermethylated in differentiated cells (Farthing, et al., 2008). This finding suggests that epigenetic regulation of genes promoting pluripotency might be important during differentiation. Demethylation of *Elf5*, acting as a gatekeeper of pluripotency in ES cells, results in loss of stem cell identity (Ng, et al., 2008). *Oct3/4* was shown to be *de novo* methylated by *Dnmt3a* and *3b* mediated by G9A and HP1 in differentiated cells to repress reprogramming and regain of pluripotency (Feldman, et al., 2006). DNA methylation comparison analysis between ES cells and differentiated neurons showed several hundred promoters, including pluripotency and germline-specific genes which became methylated in the lineage-committed progenitor cells (Mohn, et al., 2008). Erasure of epigenetic marks (DNA methylation and histone acetylation) on mammalian somatic chromatin results in a remodeled state which resembles the pluripotent chromatin of ES cells (Bian, et al., 2009). Together, these findings demonstrate that the DNA methylation machinery is able to specifically repress key regulators of pluripotency and stemness in differentiated cells.

How are epigenetic mechanisms involved in establishment of a developmental hierarchy?

For the well established developmental hierarchy of the hematopoietic system,

transcription factors were shown to be the key regulating proteins determining cellular regulation and differentiation (Rosenbauer and Tenen, 2007). Investigations showed that indeed expression of key transcription factors can be regulated through DNA methylation changes in their promoter or regulatory sequences. For example, *C/ebpα* was shown to be downregulated by DNA promoter methylation (Bennett, et al., 2007). Methylation studies of promoters and cis regulatory elements of GATA binding protein 1 (*Gata1*), colony stimulating factor 1 receptor (*c-fms*) and pre T-cell antigen receptor alpha (*ptcrα*) from HSCs and different progenitor cell lineages showed that their DNA methylation patterns correlate with the function in different cell populations. Also, regulation of paired box gene 5 (*Pax5*) (Decker, et al., 2009) and inhibitor of DNA binding 2 (*Id2*) (Ehlers, et al., 2008) was shown to be influenced by DNA methylation. Additionally, an epigenetic characterization of HSCs and progenitor cells revealed histone and DNA modifications being associated with a transcriptional effect at specific regulatory regions of lineage-affiliated genes (Attema, et al., 2007).
Certainly, not all key transcription factors were studied for their sensitivity to modified DNA methylation patterns yet, but the hypothesis that epigenetic gene regulation is involved in stem cell decisions is further evolving.

1.6 Aim of this thesis

DNA methylation, which is achieved by DNA methyltransferases, is a major mechanism in chromatin remodeling. Epigenetic gene regulation is thought to be involved in orchestrating genetic programs during cell fate decisions and cancer. For this reason it is a crucial aim to understand the function of the key modulators in these processes. The aim of this thesis is to investigate the function of DNA methylation, produced by DNMT1, in regulating genetic programs in HSCs.
Particularly, the aim of this thesis is to test the hypotheses whether:

- The loss or reduction of DNMT1 activity is influencing homeostasis and differentiation of HSCs.
- DNMT1 activity is essential for preservation of multipotency of HSCs.
- DNA methylation represents an active mechanism to epigenetically silence differentiation genes.
- Varying threshold levels of DNA methylation are required for establishing different cell fate programs in HSCs.

2 Materials and Methods

2.1 Materials

2.1.1 General equipment

- Mastercycler Gradient (Eppendorf)
- 7300 Real Time PCR System (Applied Biosystems)
- Multicentrifuge 3 S-R (Heraeus)
- Geldoc 2000 (Biorad)
- Flow hood (BDK)
- Microscope DMIL (Leica)
- Nanodrop (PeqLab)
- FACS Calibur (BD)
- FACS LSRII (BD)
- FACS Aria (BD)
- Incubator (Binder)
- Stratalinker 2400 (Stratagene)
- Nylon membrane (Pall Corporation)
- XAR film (Kodak)
- Hybridization oven Hybridiser HB-1D (Techne)
- Agarose gel chambers (Biosteps)
- Power supply EV231 (Consort)
- Microscopy Immersion Oil (Merck)

2.1.2 Cell culture equipment

- Cell culture dishes, sterile, different sizes (TPP or Falcon)
- Centrifuge tubes, sterile, different sizes (TPP or Falcon)
- Serological pipettes (Falcon)
- Neubauer cell-counter chamber (Superior Marienfeld)
- Syringes for single-use, sterile, different sizes (Braun, Omnifix, BS Plastic)
- Needles for single-use, sterile, different sizes (Neoject)
- Disposable scalpel for single-use, sterile (Braun)
- Polystyrene tubes, 5 ml (BD Falcon)
- Cryotubes, sterile, 1.2 ml (Nunc)

- Cell strainer, sterile, different sizes (BD)
- Rotilabo Filter sterile, 0.22 and 0.45 µM PVDF (Roth)

2.1.3 Mouse dissection equipment

- Dissecting board and pins, sterilized
- Scissors and forceps of different sizes and sharpness, sterilized
- Scalpels, sterile
- EDTA-treated canula (Brand)

2.1.4 Chemicals, reagents and buffers

- 20x SSC (3 M NaCl, 0.3 M sodium citrate, 1 mM EDTA)
- 4′,6-Diamidino-2-phenylindol (DAPI) (Sigma Aldrich)
- 50x TAE (242 g Tris base, 57.1 ml Glacial acetic acid, 100 ml 0.5 M EDTA, pH 8.0 in water)
- 6x Loading buffer for agarose gel electrophorasis (0.25% Bromephenol blue, 0.26% Xylene cyanol, 30% Glycerol in water)
- 7-amino-actinomycin D (7AAD) (BD)
- Agarose (Roth)
- Annexin binding buffer (BD)
- Bromphenol blue (Roth)
- BSA (Roth)
- Chloroform/Isoamylalcohol (Roth)
- dNTPs (Fermentas)
- DTT (Fermentas)
- Ethanol absolute
- Ethidium bromide (Roth)
- Ethylenediaminetetraacetate (EDTA) (Roth)
- FACS buffer (2% FCS and 2 mM EDTA in PBS)
- Glacial acetic acid (Roth)
- Glucose-1 (Roth)
- Glycerol (Roth)
- Hematoxylin and Eosin (Sigma Aldrich)
- High molecular weight marker (Fermentas)
- Histofix (Roth)
- Hoechst 33342 (Invitrogen)
- Hoechst buffer (20 mM Hepes, 1 mg/ml Glucose-1, 10% fetal calf serum in PBS)
- Hybri-Quick (Roth)

- Isopropanol (Roth)
- KCl (Roth)
- KH_2PO_4 (Roth)
- Low molecular weight marker (Fermentas)
- $MgCl_2$ (Roth)
- Na_2HPO_4 (Roth)
- NaCl (Roth)
- Nytran SuperCharge Southern/Northernblot membrane (Schleicher&Schuell)
- Phenol (Roth)
- Phosphate buffered saline (PBS) (137 mM NaCl, 2.7 mM KCl, 10 mM Na_2HPO_4, 2 mM KH_2PO_4, pH 7.4 in water)
- poly(I:C) (GE-Healthcare or Invivogen)
- Propidium iodide (Sigma Aldrich)
- Proteinase K (Invitrogen) reconstituted to 10mg/mL in water
- RNase free water (Quiagen)
- Sodium citrate (Roth)
- Sodium dodecyl sulfate (SDS) (Roth)
- Southernblot wash solution I (100 ml 20 x SSC and 10 ml 20% SDS in 890 ml water)
- Southernblot wash solution II (10 ml 20 x SSC and 10 ml 20% SDS in 980 ml water)
- Tail digestion buffer (10 mM Tris-Cl pH 8.0, 10 mM EDTA pH 8.0, 50 mM NaCl, 0.5% SDS, in water)
- TE buffer (10 mM Tris, 1 mM EDTA, pH 7.5 in water)
- Tris base (Roth)
- Tris-Cl (Roth)
- Trizol (PeqLab)
- Trypan blue solution (Sigma)
- 1 M Hepes (PAA)
- Xylene (Roth)
- Xylene cyanol (Roth)
- α32-PdCTP (Amersham)

2.1.5 Cell culture media and reagents

- ACK red blood cells lysis buffer (NH_4Cl 0.15 M, $KHCO_3$ 10 mM, EDTA 0.1 mM, pH 7.3 in water)
- Detoxified Bovine Serum Albumin (StemCell Technologies Inc.)
- Dulbecco's modified Eagle's Medium (DMEM), high Glucose (4.5 g/l) (PAA)

- Dulbecco's Phosphate Buffered Saline 1 x, without Ca & Mg (PAA)
- Fetal Calf Serum (FCS) (Biochrom, BioWhittaker or Sigma-Aldrich)
- Iscove's modified DMEM (IMDM) (PAA)
- MEM Alpha Modification, with L-Glutamine, without Ribonucleosides (PAA)
- MethoCult® M3234 (Stem Cell Technologies Inc.)
- Penicillin/Streptomycin, 100 x Concentrate (PAA)
- Stable Glutamine, 200 mM Concentrate (PAA)
- Trypsin EDTA (1:250) 1 x Concentrate (PAA)
- X-vivo 15 (BioWhittaker)
- Bovine serum albumin (Roth)
- N,N-dimethylsulfoxide (DMSO)
- Freezing medium (FCS with 10% DMSO)
- Polybrene or Hexadimethrine bromide (Sigma-Aldrich)

2.1.6 Enzymes and appending buffers

- Superscript II (Fermentas)
- 5 x First round buffer (Fermentas)
- RNase out (Fermentas)
- DNase I (Fermentas)
- 10 x Dnase I buffer (Fermentas)
- Hpa II (Fermentas)
- Msp I (Fermentas)
- 10 x Tango buffer (Fermentas)
- T4 Ligase (New England Biolabs)
- 10 x T4 Ligase buffer (New England Biolabs)
- Taq polymerase (Fermentas)
- $(NH_4)_2SO_4$ buffer for PCR (Fermentas

2.1.7 Kits

- Genomic DNA Invisorb Kit III (Invitek) for DNA isolation
- Rediprime II DNA Labeling System (Amersham) for radioactive labeling of DNA
- RNeasy Micro Kit (Qiagen) for RNA isolation
- Calcium Phosphate Transfection Kit (Invitrogen) for transient transfection of PLAT-E cells
- Rapace Kit (Invitek) for isolation of DNA fragments

2.1.8 Antibodys and microbeads

- B220 (RA3-6B2)
- CD150 (TC15-12F12.2)
- CD19 (1D3)
- CD34 (RAM34)
- CD3ε (145-2C11)
- CD4 (GK1.5)
- CD48 (HM48-1)
- CD8α (53-6.7)
- c-Kit (2B8)
- FcγRII/III (2.4G2)
- Flt3 (A2F10.1)
- Gr-1 (RB6-8C5)
- IgM (R6-60.2)
- IL-7Rα chain (SB/199)
- Mac-1/CD11b (M1/70)
- Sca1 (E13-161-7)
- Ter119 (TER-119)
- Annexin-V
- NK1.1 (PK136)
- Thy1.2 (30-H12)
- CD25 (PC61)
- CD23 (B3B4)

Antibodys were purchased by BD Biosciences, eBioscience, Biolegend or Caltag Laboratories.

- CD117 microbeads (Miltenyi)
- Dynabeads® Sheep anti–Rat (Invitrogen)

2.1.9 Cytokines

- Murine EPO
- Murine Flt3L
- Murine G-CSF
- Murine GM-CSF
- Murine IL3
- Murine IL6
- Murine IL-7

- Murine Lif
- Murine SCF
- Murine TPO

Cytokines were purchased by Tebu Bio, Prepro Tech Inc., Roche or Amgen Inc.

2.1.10 Cell lines

- OP9 (Kodama, et al., 1994)
- OP9-DL1 (Schmitt and Zuniga-Pflucker, 2002)
- PLAT-E (Morita, et al., 2000)

2.1.11 Mouse strains

- Dnmt1$^{-/chip}$ mice (Gaudet, et al., 2003)
- Dnmt1$^{lox/lox}$ mice (Jackson-Grusby, et al., 2001)
- Mx1Cre transgenic mice (Kuhn, et al., 1995)
- B6.SJL-Ptprca wild-type mice (Taconic)
- 129ola/B6.SJL mice wild-type mice (Taconic)
- CD19Cre mice (C.129P2-Cd19$^{tm1(cre)Cgn}$/J) (Rickert, et al., 1997)
- loxP-STOP-loxP-EYFP transgenic mice (Srinivas, et al., 2001)
- H2K-Bcl-2 transgenic mice (Domen, et al., 1998)

2.1.12 Oligonucleotides

Gene	Oligonucleotide sequence
RHpa24 primer	5'-AGCACTCTCCAGCCTCTCACCGAC-3'
C/ebpα forward	5'-GGC CTC TTC CCC TAC CAG-3'
C/ebpα reverse	5'-CAG GTG CAT GGT GGT CTG-3'
CD 19 cre a	5'-AAT GTT CTG CCA TGC CTC-3'
CD 19 cre b	5'-GTC TGA AGC ATT CCA CCG GAA-3'
CD 19 cre c	5'-CCG GTT ATT CAA CTT GCA CCA-3'
CHIP242R	5'-CTG GTA GCC ACG GAA CTA GG-3'
CHIP48F	5'-CTT GGA GAA CGG AAC ACA CA-3'
Dnmt1 ex32F	5'-ATC TCG GAA ACG CTG TGG GG-3'
Dnmt1 ex32R	5'-CTT ACC TGA GGA AGG AGA CC-3'
DNMT1 lox 1	5'-GGG CCA GTT GTG TGA CTT GG-3'
DNMT1 lox 2	5'-TGA ACC TCT TCG AGG GAC C-3'
DNMT1 lox 3	5'-ATG CAT AGG AAC AGA TGT GTG C-3'

DNMT1lox genotype 2	5’-CCT GGG CCT GGA TCT TGG GGA-3’
Ebf forward	5’-CAA GAC AAG AAC CCT GAA ATG-3’
Ebf reverse	5’-GTA ACC TCT GGA AGC CGT AGT-3’
GM-CSFRα forward	5’-CCA CGG AGG TCA CAA GGT CA-3’
GM-CSFRα reverse	5’-ACT CGC ACG TCG TCG GAC AC-3’
IL7re forward	5’-TTA CTT CAA AGG CTT CTG GAG-3’
IL7re reverse	5’-CTG GCT TCA ACG CCT TTC ACC TCA-3’
Irf8 forward	5’-GCT GAT CAA GGA ACC TTG TG-3’
Irf8 reverse	5’-CAG GCC TGC ACT GGG CTG-3’
Koprimer PGK	5’-GGG AAC TTC CTG ACT AGG GG-3’
M-CSFR forward	5’-AAT GGC AGT GTG GAA TGG GAT GG-3’
M-CSFR reverse	5’-GTG GGG GCT CTG GGT GGA CTC-3’
Pax5 forward	5’-CGG GTC AGC CAT GGT TGT G-3’
Pax5 reverse	5’-GTG CTG TCT CTC AAA CAC G-3’
Rag1 forward	5’-TGC AGA CAT TCT AGC ACT CTG GCC-3’
Rag1 reverse	5’-ACA TCT GCC TTC ACG TCG ATC CGG-3’
β-actin forward	5’-AAG GAG ATT ACT GCT CTG GCT CCT A-3’
β-actin reverse	5’-ACT CAT CGT ACT CCT GCT TGC TGA T-3’
λ5 forward	5’-GCG GAA TTC TCA GCA GAA AGG AGC AGA GCT-3’
λ5 reverse	5’-GCG AAG CTT ACA CAC TAC GTG TGG CCT TGT-3’
EYFP 1	5’-GGC GAC TTC CAG TTC AAC ATC-3’
EYFP 2	5’-AAA GTC GCT CTG AGT TGT TAT-3’
EYFP 3	5’-GCG AAG AGT TTG TCC TCA ACC-3’
MxCre forward	5’-CAA TTT ACT GAC CGT ACA C-3’
MxCre reverse	5’-TAA TCG CCA TCT TCC AGC AG-3’
CD19 Cre	5’-AAT GTT CTG CCA TGC CTC-3’
CD19 Cre	5’-GTC TGA AGC ATT CCA CCG GAA-3’
CD19 Cre	5’-CCG GTT ATT CAA CTT GCA CCA-3’
DNMT1 chip forward	5’-CTT GGA GAA CGG AAC ACA CA-3’
Dnmt1 chip reverse	5’-CTG GTA GCC ACG GAA CTA GG-3’

Oligonucleotides were provided by Biotez or Metabion.

2.1.13 Retroviral expression constructs

- MSCV-Ebf1-ires-Gfp retroviral construct
- MSCV-ires-Gfp

Constructs were provided by B.L. Kee, University of Chicago, Chicago, USA.

2.1.14 Gene expression assays

- Murine Flt3 (Applied Biosystems, TaqMan® Assay probe ID: Mm00438996_m1)
- Murine Gata1 (Applied Biosystems, TaqMan® Assay probe ID:Mm00484678_m1)
- Murine Cebpα (Applied Biosystems, TaqMan® Assay probe ID:Mm00514283_s1)

2.1.15 Software

- CellQuest Pro (BD) flow cytometry analyzing software
- FACSDiva (BD) flow cytometry analyzing software
- FlowJo (Treestar) flow cytometry analyzing software
- 7300 System SDS Software (Applied Biosystems) real time RT PCR analyzing software
- TreeView (EisenSoftware) visualizing software for MassARRAY data

2.2 Methods

2.2.1 Mice

General mouse work such as daily animal care, breeding and offspring separation was carried out in collaboration with the animal core facility of the Max-Delbrück-Center for Molecular Medicine, Berlin, Germany. All mice were housed and bred in specific pathogen-free animal facilities. All animal experiments were approved by the local authorities according to the German Federal Animal Protection Act.

2.2.1.1 Description of the used mouse strains

$Dnmt1^{-/chip}$, $Dnmt1^{lox/lox}$ and transgenic Mx1Cre mice have been described (Gaudet, et al., 2003) (Jackson-Grusby, et al., 2001) (Kuhn, et al., 1995). $Dnmt1^{-/chip}$ mice harbour one *Dnmt1* knockout allele on which exons 3 and 4 are deleted and one *Dnmt1* knockdown allele. The *Dnmt1* knockdown allele was achieved by a cDNA insertion into the locus of the *Dnmt1* knockout allele and is called “chip” (cDNA homologous insertion protocol). A cDNA insertion in a knockout locus restores part of the original gene expression but since intron and exon structures are lost part of the

regulatory network is lost and gene expression is reduced. In Dnmt1$^{lox/lox}$ mice, exons 4 and 5 of *Dnmt1* are flanked by two loxP sites which are used for conditional deletion of *Dnmt1*. In these mice, recombination (excision and consequently inactivation of the target gene *Dnmt1*) occurs only in those cells expressing the cyclization recombination protein (Cre recombinase). Transgenic Mx1Cre mice express Cre recombinase under control of the IFN-inducible *Mx1* promoter (Kuhn, et al., 1995). These strains were crossed to obtain Mx1Cre^{+}Dnmt1$^{lox/chip}$ mice.

Wildtype congenic B6.SJL-Ptprca (CD45.1^{+}) mice were purchased from Taconic and were crossed with 129ola to obtain 129ola/B6.SJL (CD45.1^{+}/CD45.2^{+}) F1 generation animals used as recipients for BM cell transplantation.

To investigate B-cell development, the Dnmt1$^{lox/chip}$ line was crossed with CD19Cre mice (C.129P2-Cd19$^{tm1(cre)Cgn}$/J) (Rickert, et al., 1997), which express the cre recombinase under the promoter of the B-cell specific antigen CD19. Tracing of cells with active Cre recombinase was allowed by crossing in reporter mice carrying an R26R locus with an inducible loxP-Stop-loxP-Eyfp reporter cassette knock-in (Domen, et al., 1998). These mice express the fuorescent marker enhanced yellow fluorescent protein (EYFP) in cells where the Cre recombinase is active.

To assess effects of apoptosis, Dnmt1$^{-/chip}$ mice were crossed with H2K-Bcl-2 transgenic mice (Domen, et al., 1998). H2K-Bcl-2 transgenic mice express the antiapoptotic gene *bcl-2* under the well-characterized H-2K^{b} promoter, active on high levels in HSCs, but also in all other hematopoietic cells.

2.2.1.2 Poly IC treatment

In Mx1Cre mice the Cre recombinase is under the control of the *Mx1* promoter. This promoter is silent in healthy mice but can be induced to high levels of transcription by administration of interferon alpha, interferon beta or synthetic double-stranded RNA (such as poly (I:C)). When combined with a mutant, carrying a gene that is flanked by loxP recognition sites, the expression of Cre recombinase causes the flanked gene to be removed. For induction of excision of floxed *Dnmt1* exons, primary mutant mice or transplanted recipient mice received 300 µg poly (I:C) in PBS per intraperitoneal injection every other day for a total of five injections. 129ola/B6.SJL (CD45.1^{+}/CD45.2^{+}) recipient mice transplanted with *Mx1Cre*$^{-}$Dnmt1$^{lox/chip}$ BM cells were used as controls for nonspecific poly(I:C) effects. Excision efficiency was

analyzed by PCR. The excised Δ-allele generated a 0.25 kilobase (kb) band and the non-excised loxP-flanked allele generated a 0.15 kb band.

2.2.1.3 Genotyping

Tagging of the offspring was carried out according to standard protocols. Mice were genotyped by locus-specific polymerase chain reaction (PCR) on genomic DNA extracted from tail tissue (see 2.2.3.1 and 2.2.3.4).

2.2.1.4 Isolation of mouse organs

After euthanizing the mouse with CO_2, the animal was rinsed with ethanol and pinned down on a dissecting board with the belly facing up. Mice were opened and the upper leg, the lower leg and the upper arm were dissected with scissors and forceps to isolate BM cells. Other organs (spleen, lymph nodes, sternum or thymus) were dissected when needed. All organs were kept in cold PBS until preparation. Single cell suspensions were generated by cutting the organ into small pieces and subsequently filtering it through a cell strainer. BM was isolated by flushing the bones with PBS.
Peripheral blood of living mice was taken from the tail vein with EDTA treated canula.

2.2.1.5 Transplantation experiments

For serial and competitive transplantation assays, adult $CD45.1^+/CD45.2^+$ recipients (8 weeks of age) were irradiated with a lethal dose of 10.5 Gy total body irradiation with the 18-MeV photon beam of a linear electron accelerator with a dose rate of 0.18 Gy/min. These mice were then reconstituted with freshly isolated BM cells within 24 h of irradiation. Therefore, a cell suspension with the desired cell number per 200µl in sterile PBS was prepared and injected intravenously in the tail vein of the fixed animal.
For serial transplantation mice were reconstituted with 5 $x10^6$ BM cells from test or control mice. For competitive transplantation mice were reconstituted with different ratios of test to competitor cells.
For short-term engraftment assays, 10^7 $CD45.2^+$ $Dnmt^{-/chip}$ or $Dnmt^{+/+}$ BM cells were mixed with 10^7 $CD45.1^+$ SJL BM cells and transplanted into lethally irradiated $CD45.1^+/CD45.2^+$ recipient mice. BM analysis of transplanted animals was performed 24 h post-transplantation.

For transplantation of conditional *Dnmt1* mutant cells, 10^7 MxCre$^+$Dnmt1$^{lox/chip}$ or MxCre$^-$Dnmt1$^{lox/chip}$ whole BM cells were mixed with 10^7 CD45.1$^+$ SJL whole BM cells and transplanted into lethally irradiated CD45.1$^+$/CD45.2$^+$ recipient mice. 8 weeks after transplantation, poly(I:C) was administered as described above and peripheral blood was monitored until the experimental endpoint of 20 weeks.

For investigation of the T-cell potential, transplantation with BM depleted of T cells was performed. Therefore, BM of Dnmt$^{-/chip}$ or Dnmt$^{+/+}$ animals was isolated and stained for T-cell markers (CD3ε, CD4, CD8α). Cells positive for these markers were excluded from the BM by cell sorting.

2.2.1.6 Histology (Hematoxylin & Eosin staining)

Hematoxylin stains all acidic or basophile structures in blue, especially the cell nucleus with its DNA and the rough endoplasmatic reticulum. The counterstain eosin stains all basic or acidophile structures in red, especially cell plasmatic proteins.

Mice were euthanized and sterna were removed and fixed in 4% buffered formalin (Histofix). Tissues were dissected and paraffin embedded before staining with hematoxylin and eosin as described previously (Prinz, et al., 2008). The paraffin embedded tissue was taken through brief changes of xylene, alcohol and water to hydrate the tissue. This process was done to give the cells an affinity for the dyes. The tissue slides were stained with the nuclear dye (hematoxylin), rinsed and then stained in the counterstain (eosin). Afterwards they were rinsed, run in the reverse manner as before (taken back through water, alcohol and xylene) and finally coverslipped.

2.2.2 Cell culture

2.2.2.1 Cell lines

The OP9 cell line was established from newborn (C57BL/6 x C3H) F2 -op/op mouse calvaria. These cells do not produce functional macrophage colony-stimulating factor (M-CSF) due to a mutation in the gene encoding M-CSF. Feeder layer of OP9 cells support HSC differentiation to all hematopoietic lineages except T cells (Nakano, et al., 1994) (Cho, et al., 1999). OP9 cells were transduced with the Notch ligand Delta-like-1 resulting in OP9-DL1 cells which support differentiation of HSCs into T cells (de Pooter, et al., 2006) (Schmitt, et al., 2004) (Schmitt and Zuniga-Pflucker, 2002). OP9

and OP9DL cells were cultured in α-MEM with 20% FCS supplemented and were splitted every 2 to 3 days.

2.2.2.2 Thawing of cells

Cells were thawed quickly at 37℃ (e.g. in a water bath) and transferred dropwise to 10 ml medium. After centrifugation (1200 rpm, 5 minutes, room temperature (RT)), supernatant was discarded and pellet was resuspended in 1 ml medium. Cells were plated in an appropriate cell number on culture dishes.

2.2.2.3 Cultivation and cryo-preservation of cell lines and primary cells

All cells were grown in indicated media supplemented with fetal calf serum (FCS) and antibiotics (Penicillin/Streptomycin) in an incubator at 37℃ and 5% CO_2.
For passaging of adherent cells, medium was aspired, cells were washed once with PBS and incubated with 0.05% trypsin-EDTA for approximately 5 minutes at 37℃ (4 ml trypsin per 10 cm dish). Once detached, cells were resuspended in an appropriate amount of medium centrifuged (1200 rpm, 5 minutes, RT) and the cell suspension was transferred in different dilutions to new tissue culture dishes. Suspension cells were passaged and supplied with fresh medium twice a week.
For cryo-preservation, medium was removed, cells were taken up in FCS with 10% DMSO and transferred into cryo-tubes. For 24 h, cryo-tubes were stored in styrophor boxes at -80℃, after which they were placed in liq uid nitrogen.

2.2.2.4 Assessment of cell number and cell viability (Trypan blue)

Cells were harvested, centrifuged (1200 rpm, 5 minutes, RT) and cell pellet was resuspended in 1x PBS. The trypan blue solution was added 1:1 to a small aliquot (e.g. 100 µl) and cells were incubated for 1 minute. An aliquot was transferred to the Neubauer chamber and checked for equal distribution of the cells in all four big quadrants. If more samples were counted, the trypan blue solution was added shortly before counting and cells were placed on ice. Dead cells were blue, viable white.

2.2.2.5 Production of viral supernatants and transduction of cells

Viral supernatants were used to stably transfect hematopoietic cells. Retroviral supernatants were produced by co-transfection of PLAT-E cells with 10 µg of the retroviral construct, a gag-pol construct (10 µg) and an ecotropic env construct (2

µg). Transfection was made using the Calcium Phosphate Transfection Kit according to instructions. Viral supernatants were collected at 48, 72 and 96 h after transfection, filtered through 0.45 µm filters and stored at -80℃.

For retroviral transduction, c-Kit enriched cells were cultured for 24 h at 37℃ in medium (IMDM, 20% FCS, 100 µg/ml of penicillin, 2 mM L-glutamine) containing 50 ng/ml SCF, 20 ng/ml IL-6 and 20 ng/ml Lif. Subsequently, cells were mixed with retroviral supernatants in the presence of 50 ng/ml SCF, 20 ng/ml IL-6, 20 ng/ml LIF and 8µg/ml polybrene and cultured for 48 h at 37℃. Transduced cells were used for B-cell differentiation co-culture assays on OP9 cells (see 2.2.2.6).

2.2.2.6 In vitro clonogenic stem cell differentiation assays

BM cells were harvested and LSKCD34$^-$Flt3$^-$ or LSKCD34$^+$Flt3$^-$ populations were FACS purified and cultured under different conditions as previously described (Mansson, et al., 2007). For evaluating Mk potential, single cells were seeded in 60-well plates in 20 µl X-vivo 15 medium supplied with 0.5% detoxified bovine serum albumin, 10% fetal calf serum and with cytokines (50 ng/ml SCF, 50 ng/ml Flt3L, 50 ng/ml TPO, 5 U/ml EPO and 20 ng/ml IL-3). After 8-10 days of culture, wells were scored for clonal growth and frequency of Mk cells with an inverted light microscope (Kaiho and Mizuno, 1985). For evaluating GM potential, single cells were seeded in 60-well plates in 20 µl X-vivo 15 supplemented with 0.5% BSA and cytokines (SCF, Flt3L, TPO, GM-CSF, all 10 ng/ml, and G-CSF and IL-3, both 20 ng/ml). Wells were scored, with an inverted light microscope, for clonal growth after 8-10 days of culture. For evaluating B- and T-cell potential, single cells were seeded onto ~80% confluent monolayers of OP9 or OP9-DL1 stromal cells (Mansson, et al., 2007). OP9 stromal cocultures were supplemented with 25 ng/ml SCF, 25 ng/ml Flt3L and 20 ng/ml IL-7, whereas OP9-DL1 cocultures were supplemented with 25 ng/ml SCF (only first week) and 25 ng/ml Flt3L. Half of the medium was replaced every week. Visible clones were picked at day 21 and 28 from cocultures and analyzed by FACS for B-cell (B220$^+$CD19$^+$) and T-cell (CD4$^+$CD8α$^+$ and/or NK1.1$^-$Thy1.2^{hi}CD25^{hi}) progeny, respectively. In addition, clones were required to have ≥20 gated events (of indicated cell-surface phenotypes) with appropriate scatter profile to be scored as positive. Small clones were cultured an additional week before being analyzed as described.

2.2.2.7 Methylcellulose assays

To test the potential of stem and progenitor cells methylcellulose assays were performed. Therefore, an appropriate cell number (usually 1.5 x 10^5 BM cells per 1 ml) was mixed with the semi-solid Methocult media supplemented with cytokines. For promotion of myeloid differentiation a mix of 10 ng/ml IL-3, 10 ng/ml IL-6, and 50 ng/ml SCF and for preB-cell differentiation 10 ng/ml IL7 was added to the Methocult media. 1 ml of this suspension was plated onto a 35 mm cell culture dish and three of these dishes were put into one 150 mm cell culture dish together with one dish filled with water to prevent drying of the semi-solid media. Colonies were scored and analyzed 5-10 days after plating.

2.2.3 Molecular biology

2.2.3.1 Preparation of genomic DNA

DNA was extracted following standard protocols. In brief, cells or tissue was digested with tail digest buffer supplemented with 10 µg/ml proteinase K at 56°C for 5-12 h. Genomic DNA was purified with addition of a phenol/chloroform mixture and subsequent centrifugation (13000 g, 5 minutes, 4°C) . Supernatant, which contained the DNA, was transferred into a new tube and precipitated with 1000 µl isopropanol. After centrifugation (13000 g, 20 minutes, 4°C) supernatant was removed and DNA pellet was washed with 1 ml 70% ethanol. After centrifugation (13000 g, 5 minutes, 4°C) supernatant was discarded and the DNA pellet was air-dried until ethanol was completely evaporated. DNA was dissolved in TE buffer.

2.2.3.2 Extraction of RNA

Cells were directly FACS-sorted in Trizol and homogenized through vortexing (for cell numbers up to 5 x 10^5) or through passing through a 16 gauche needle several times. After incubation (5 minutes, RT) 200 µl of Chloroform was added to separate RNA from DNA and proteins. Suspension was vortexed for 15 seconds and incubated (5 minutes, RT). After centrifugation (13000 g, 15 minutes, 4°C), RNA that remained in the colorless aqueous phase was transferred to a new tube. To precipitate RNA, 500 µl isopropanol was added to the samples, incubated (10 minutes on ice) and centrifuged (13000 g, 10 minutes, 4°C). Supernatant was removed and pellet was washed with 1 ml 70% ethanol. After centrifugation (13000

g, 10 minutes, 4℃) supernatant was discarded and pellet was air-dried until ethanol was completely evaporated. RNA was re-dissolved in RNase free H_2O and incubated (10 minutes, 55℃). In general, RNA was stored at - 80℃. All buffers, solutions, tips and other equipment were RNase free.
Alternatively, RNA was extracted using RNAeasy Kit according instructions.

2.2.3.3 cDNA synthesis

First, RNA was treated with DNase to destroy remaining DNA. Therefore, 5.2 µl RNA was incubated with 1 µl DNase I, 0.8 µl 10 x DNase I buffer and 1µl RNase out (15 minutes, RT). DNase was inactivated by adding 1 µl EDTA (25 µM) and incubated (65℃, 10 minutes). First strand cDNA synthesis was achieved by incubating the RNA with 2 µl dNTPs (10 mM) and 1 µl random hexameres (300 nM) (65℃, 5 minutes). After quick chill on ice, 4 µl 5 x first strand buffer, 2 µl DTT(mM) and 1 µl RNase out were added and the mixture was incubated (10 minutes, 25℃). cDNA synthesis was started with adding 1 µl Sperscript II and incubation (42℃, 50 minutes). Reaction was stopped through incubation (70℃, 15 minutes). cDNA was stored at -20℃. As a control, no RT samples (RNA samples which undergone DNase treatment but no reverse transcription) were generated exemplarily and used as a negative control in real time RT PCR analysis.

2.2.3.4 Polymerase chain reaction (PCR) and quantitative (real time) RT PCR

PCR was carried out following standard procedures. For all reactions solutions of 10 µM forward primer, 10 µM reverse primer, 10 µM dNTPs, 10 mM $MgCl_2$, 1 x NH_4 buffer and 5 U/µl Taq polymerase were used as stock solutions. Either genomic DNA or cDNA was used as template. Oligonucleotides used for quantitative PCR were designed exon/exon spanning to reduce false positive signals. For semi-quantitative PCR, aliquots were taken at 5 cycles intervals to ensure that PCR remained within the exponential range of amplifications. For real time RT PCR 2 x Taqman mix and 20 x Taqman assays was used according instructions. 7300 System SDS Software was used to analyze results.
Amplified PCR products were separated and visualized on 1-2% agarose gels containing 1 µg/ml ethidiumbromide.

2.2.3.5 Agarose gel electrophoresis

Agarose gels were prepared according to the following procedure. Aagarose was dissolved in 1 x TAE at the desired concentration and boiled in a microwave until the solution looked crystal clear. Ethidiumbrodmide was added in the appropriate concentration. After casting the gel, hardening occurred within 10-15 minutes. Gel chamber was filled with 1x TAE and aliquots of the PCR samples including the corresponding amount of loading buffer were loaded into the slots. To determine DNA length of the fragments, an appropriate standard marker was used. Depending on the size of the supposed bands, the gel was run 20-45 minutes (100-160V). DNA was visualized by UV-light.

2.2.3.6 Quantitative RT PCR analysis of single cells

Single-cell RT PCR analysis was performed as previously described (Adolfsson, et al., 2005). Single cells were sorted in 96 well plates provided with 4 µl cell lysis buffer (10% NP40, 10 mM dNTP, 0.1 mM DTT, 0.2 U Rnase out) each. Plates were kept on ice before sorting. After sorting, plates were frozen at -80℃. Reverse transcription (first strand sythesis) was done with 2 µl 5 x first strand buffer, 0.125 µl of each reverse primer, 0.25 µl superscript II in a total volume of 10 µl. For the first round of PCR, 40 µl of a mastermix containing polymerase buffer, dNTPs, forward primers and polymerase was added to each well. For the second round of PCR, 1 µl of the first round PCR was used as template and added to a mastermix containing polymerase buffer, dNTPs, inner primers and polymerase. PCR products were visualized on agarose gels.

2.2.3.7 Southern blot analysis

For analysis of global DNA methylation levels, genomic DNA was digested with excess amounts of methylation-sensitive HpaII or the methylation-insensitive isoschizomer MspI, purified by phenol extraction and precipitated with ethanol. After quantification of each sample, specified amounts of samples were run in a 0.7% agarose gel. DNA in the gel was capillary-blotted onto a nylon membrane and blotted DNA was cross-linked to the membrane by UV light using a quantitative cross-linker. An intracisternal A particle (IAP) cDNA probe (Walsh, et al., 2002) was prepared by random-labeling with [α-32P]dCTP using the Rediprime Labeling Kit. The IAP

sequence is normally methylated by DNMT1. Hybridization was carried out for 8-12 h in Roti-Hybri-Quick at 60℃ and filters were washed twice in 2 x SSC, 0.1% SDS and twice in 1 x SSC, 1% SDS at 60℃ for 15 minutes eac h. Washed filters were exposed to Kodak XAR film.

2.2.3.8 Detection of DNA methylation levels by PCR

Genomic DNA of sorted hematopoietic cell populations was digested with HpaII or MspI overnight. After digestion, products were purified with the Rapace Kit and ligated to a RHpa adaptor (Ushijima, et al., 1997). Ligation was performed in the presence of T4 Ligase and 1 x T4 Ligase buffer. 0.1 volume of the ligation products was amplified with RHpa24 primer using a 25 cycle program of 1 minute at 95℃ and 3 minutes at 72℃ per cycle. DNA methylation status of each cell population was determined by electrophoresing the PCR products in a 1% agarose gel.

2.2.4 Fluorescence activated cell sorting (FACS)

2.2.4.1 General flow cytometry and cell sorting.

For staining of cell surface antigens, about 5 x 10^5 cells were incubated with 1 µg antibody in 100 µl PBS at 4℃ for 20-40 minutes. Subsequently, cells were washed twice in 1 ml PBS and, if necessary, the procedure was repeated with a secondary antibody. Non-specific binding was reduced by preincubation with unconjugated anti-FcγRII/III (2.4G2).

Analysis and sorting of HSCs and intermediate progenitors was done as described (Mansson, et al., 2007) (Kiel, et al., 2005) (Akashi, et al., 2000). Before sorting of progenitor populations, lineage depletion of BM cells was achieved with a lineage “cocktail” of antibodies against CD3ε, CD4, CD8α, B220, CD19 and Gr-1. Subsequently, cells positive for these markers were depleted with immunomagnetic beads conjugated to anti-Rat. Alternatively, c-Kit-enrichment was perfomed with CD117 microbeads. For B-cell progenitor analysis, the lineage “cocktail” contained antibodies against CD3ε, CD4, CD8α and Gr-1. Finally, cells were resuspended in 200 µl PBS and fluorescence intensity was measured with a FACSCalibur cytometer equipped with CellQuestPro software or a LSRII cytometer and Diva software. Data analysis was performed with FlowJo software. To discriminate between living and dead cells, staining with propidium iodide (PI) or 4’,6-diamidino-2-phenylindole

(DAPI) was accomplished by adding the substances to the cell suspension 10 minutes before measurement without a washing step.
Cell sorting was done with a high-speed multicolour cell sorter (FACSAria) using standard protocols. Before sorting, cells were filtered with a cell strainer.

2.2.4.2 Annexin-V staining

The plasma membrane of cells is build asymmetrically. Loss of this asymmetry is an early sign for programmed cell death (apoptosis). During apoptosis, phosphaditylserine (PS), which is located on the cytoplasmatic side of the cell membrane under living conditions, occurs more often at the outer side of the membrane. Annexin-V binds specifically to PS. Membranes of necrotic cells are porous and Annexin-V can also bind to inner PS molecules, therefore a counterstain with PI is necessary. Cells staining double positive for PI and Annexin-V are dead or necrotic, Annexin-V single positive cells are apoptotic.
For Annexin-V staining, freshly isolated BM cells were stained with the appropriate antibodies, washed in Annexin binding buffer and incubated for 20 minutes at 4℃ in the dark with an anti-Annexin-V antibody.

2.2.4.3 Cell cycle analysis of living cells

Surface marker staining was performed as described above but incubation time was performed at 37℃. Afterwards, the cell cycle statu s of HSCs was determined by staining at 37℃ for 30 minutes with Hoechst 33342 in Hoechst buffer (Cheshier, et al., 1999). Staining with DAPI was used for exclusion of dead cells. Cells were analyzed on a LSR II cytometer equipped with a violet laser (407 nm).

2.2.5 MassARRAY

Quantitative DNA methylation analysis at single CpG units was performed by MassARRAY as previously described (Ehrich, et al., 2005) and schematically described in Figure 6. Therefore, 500 ng (sorted primary cells) or 1 µg (cell lines) of genomic DNA was treated with sodium bisulfite, PCR-amplified, *in vitro* transcribed, cleaved by RNase A and subjected to matrix-assisted laser desorption/ionization time-of-flight mass spectrometry. Methylation standards (0, 20, 40, 60, 80 and 100% methylated genomic DNA) and correction algorithms based on the R statistical computing environment were used for data normalization.

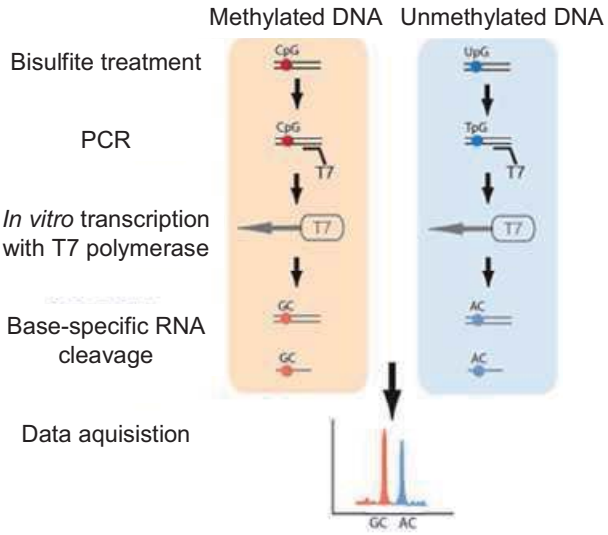

Figure 6: Schematic illustration of the MassARRAY technique. Genomic DNA undergoes bisulfite conversion followed by PCR in which a T7 promoter tag is introduced. Next, *in vitro* RNA transcription is performed on the reverse strand, followed by a base specific cleavage. The resulting cleavage pattern depends on the presence of methylated cytosine in the original genomic DNA. The cleavage products are automatically and quantitatively analyzed by MALDI-TOF mass spectrometry. This results in a distinct signal pattern from the methylated and non-methylated template DNA.

2.2.6 Gene expression profiling

2.2.6.1 Microarray procedure

35000 HSC ($Flt3^{-}LSK$) and myeloid progenitors (MP) ($CD34^{+}LK$) were sorted from BM of three independent pools of $Dnmt1^{+/+}$ and $Dnmt1^{-/chip}$ mice, consisting of 3-4 animals at the age of 8-12 weeks each. Additionally, 35000 B-cell progenitors (BP) ($CD19^{+}IgM^{-}$) were sorted from BM of $Dnmt1^{+/+}$ mice. RNA was extracted according to the RNeasy Micro Kit optimized for small amounts of RNA. For linear amplification of RNA, a strategy of two rounds of reverse transcription followed by T7 promoter-dependent *in vitro* transcription was applied according to Affimetrix instructions. 10 µg of amplified RNA was labeled and then hybridized to an Affymetrix Mouse Genome 430 2.0 Array that covers ~45000 transcripts, according to Affimetrix instructions. Results were obtained by scanning.

2.2.6.2 Microarray analysis

All microarray analysis was performed using tools contained in the Bioconductor project (http://www.bioconductor.org) that is available for the R statistical programming language (http://www.r-project.org). Raw expression values were

normalized using RMA, and differential expression was determined using the limma library. All probe set annotation information comes from the mouse4302.db library, version 2.2.0. Microarray quality was assessed using the affyQualityMetrics library. To determine the total number of genes up- and down-regulated in HSCs and MPs, one representative probe set for each gene was selected by choosing the alphabetically first probe set that mapped to a given gene. Probe sets that were not associated to any gene symbol according to current annotation were assumed to map to a single unique gene. Genes with a false discovery rate of less than 0.05 were considered differentially expressed (controlled using the procedure of Benjamini and Hochberg (Benjamini and Hochberg, 1995). Presence and absence of each gene was determined using the MAS 5.0 Calls algorithm. Principle components analysis was performed using the affycoretools library, and divisive clustering of the complete arrays was performed using the diana function contained in the cluster library. Expression values were converted to probe set Z-scores by taking the expression value and subtracting the probe set's mean expression across all arrays, and dividing this number by the probe set's standard deviation across all arrays. The probe sets were then clustered according to these Z-scores and visualized as heat maps. When defining stem and myeloid signature probe sets, probe sets that were differentially expressed with a false discovery rate (controlled using the procedure of Benjamini and Hochberg) of 0.001 or less and $\log_2$ fold change of greater than 2.0 were chosen, with HSC signature probe sets being more highly expressed in HSCs and MP signature probe sets being more highly expressed in MPs. Density plots of the signature probe sets were generated using the sm library.

2.2.7 Statistical analysis

Student's t-test was carried out to determine the statistical significance of experimental results. *P≤0.05 and **P≤0.001

3 Results

Results from collaborations are outlined when discussing the respective data.

- Immunohistology

done in cooperation with Marco Prinz, University of Freiburg

- Single-cell RT PCR and single-cell *in vitro* differentiation assay

done in cooperation with Shabnam Kharazi and Sten E. Jacobsen, University of Lund

- RNA isolation for genome wide mRNA expression profiling
- *In vitro* amplification and labeling of mRNA for genome wide expression profiling
- Hybridization and scanning of Affymetrix microarrays

done by Imagenes, Berlin, Germany

- Bioinformatics of the Affymetrix microarray raw data

done in cooperation with Matthew Huska and Miguel A. Andrade-Navarro, Max Delbrück Center Berlin

- Performance of the MassARRAY

done by Sequenom, Hamburg, Germany

- General mouse care and genotyping

done in cooperation with Victoria Malchin, Christin Graubmann, Lotte Huismann, Nancy Endruhn and Jann-Felix Zinke, Max Delbrück Center Berlin

3.1 Studies with the *Dnmt1* knockout mouse model

3.1.1 Validation of the *Dnmt1* conditional knockout mouse model

To test the function of DNMT1 during early steps in hematopoiesis, mice in which exons 4 and 5 were flanked by loxP sites (Jackson-Grusby, et al., 2001) were bred with animals expressing the Cre recombinase under control of the type I interferon-inducible Mx1 promoter (Kuhn, et al., 1995) (see 2.2.1.1.) This strategy allowed inducible deletion of the catalytic DNMT1 domain upon administration of the interferon-γ inducer polyinosinic-polycytidylic acid (poly(I:C)), thus, creating a functional knockout of the gene in hematopoietic cells.

To validate excision of the loxP site flanked part of the *Dnmt1* gene, a genotyping PCR was performed on genomic DNA of various organs of poly(I:C) treated Dnmt1$^{lox/lox}$Mx1Cre^{+} and Dnmt1$^{lox/lox}$Mx1Cre^{-} control animals. Figure 6A shows efficient excision of *Dnmt1* in all Mx1Cre^{+} animals in hematopoietic tissues such as spleen and bone marrow (BM), but not in other tissues such as the brain. Furthermore, efficient excision in the liver was revealed, which is in line with reports showing that the Mx1 promoter is also active in this tissue (Kuhn, et al., 1995). To confirm the functional loss of DNMT1 activity in Dnmt1$^{lox/lox}$Mx1Cre^{+} animals after poly(I:C) treatment, a southern blot detecting global DNA methylation levels was performed. In this assay, genomic DNA was digested with the methylation-sensitive (Hpa II) or the methylation-non-sensitive isoschizomeric (Msp I) restriction enzyme as a control. The methylation sensitive restriction enzyme only cuts at its recognition sites if they are not methylated. Hence, in a DNA fraction with reduced methylation levels Hpa II will cut more often than in a wild-type (WT) DNA fraction. This effect is shown in Figure 7B.

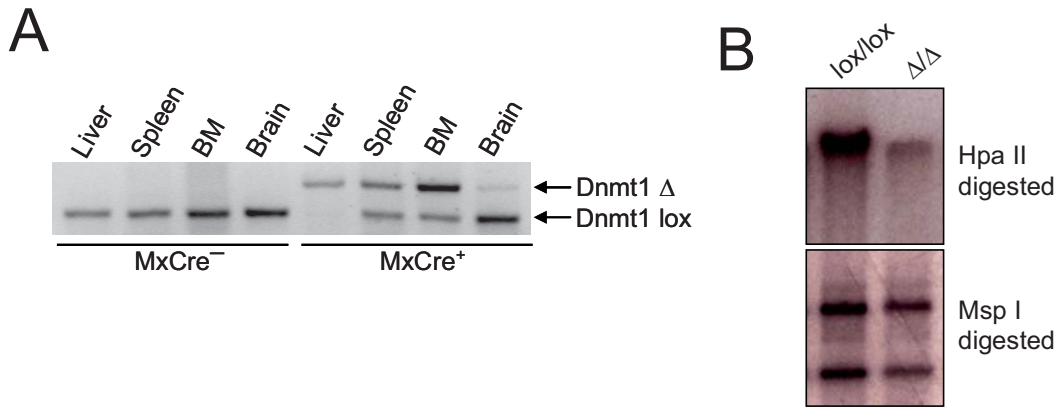

Figure 7: Inducible deletion of *Dnmt1* in adult hematopoiesis. A) Genomic PCR analysis of *Dnmt1* deletion in various organs of Dnmt1$^{lox/lox}$MxCre^{-} and Dnmt1$^{lox/lox}$MxCre^{+} mice 5 days after poly(I:C) injection. The upper band indicates the deleted *Dnmt1*$^{\Delta}$ allele, the lower band indicates the undeleted allele. **B)** Southern blot analysis showing the DNA methylation status of whole BM cells from Dnmt1$^{lox/lox}$MxCre^{-} (lox/lox) and Dnmt1$^{lox/lox}$MxCre^{+} (Δ/Δ) mice 5 days after poly(I:C) injection using a random intracisternal A particle cDNA probe. Genomic DNA was digested with the methylation-sensitive enzyme Hpa II or the methylation-non-sensitive isochizomere Msp I respectively.

The reduction of high molecular weight fragments and the appearance of more low weight fragments in the Hpa II digested fraction demonstrated an impaired DNA methylation ability in *Dnmt1* deficient cells.

3.1.2 Complete loss of *Dnmt1* leads to rapid hematopoietic crisis

Poly(I:C) injection of 6-week-old Dnmt1$^{lox/lox}$MxCre^{+} mice (hereafter designated Dnmt1$^{\Delta/\Delta}$) resulted in rapid death of all animals (Figure 8A). In contrast, all equally treated Dnmt1$^{lox/lox}$MxCre^{-} control mice (hereafter designated Dnmt1$^{lox/lox}$) survived this procedure. Peripheral blood samples of moribund Dnmt1$^{\Delta/\Delta}$ mice showed anemia and cytopenia (Table 3).

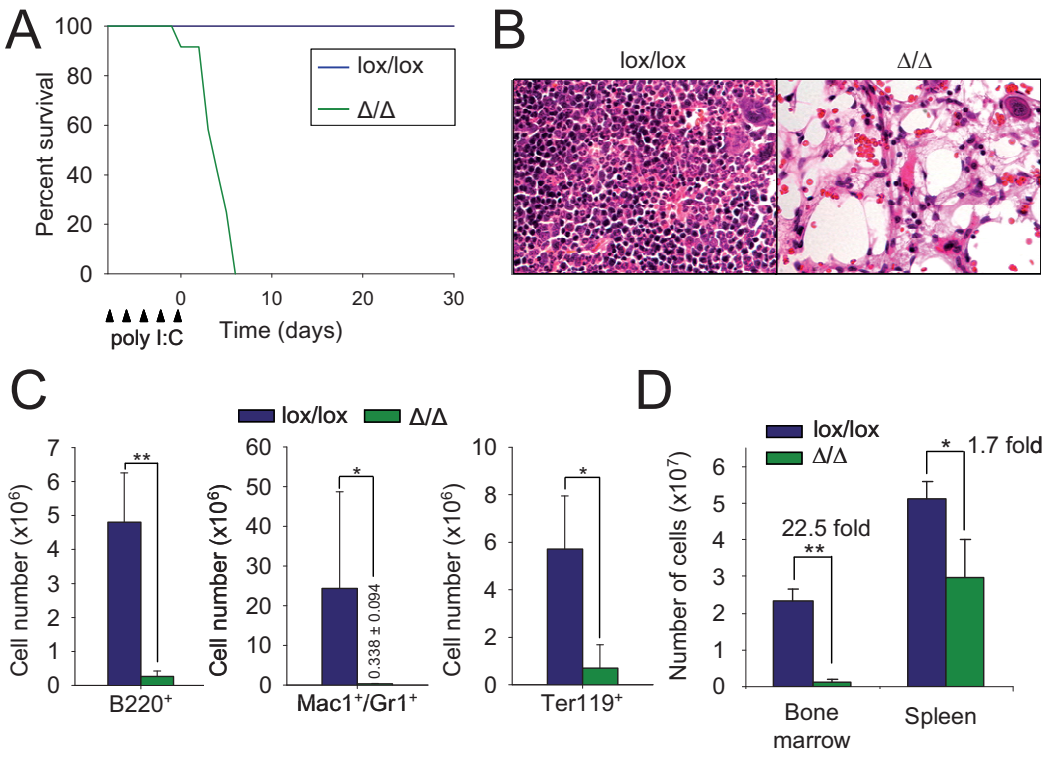

Figure 8: DNMT1 is indispensable for early hematopoiesis. A) Cumulative survival curve of poly(I:C) injected Dnmt1$^{lox/lox}$MxCre^{+} (Dnmt1$^{\Delta/\Delta}$, n=21) and Dnmt1$^{lox/lox}$MxCre^{-} control mice (Dnmt1$^{lox/lox}$, n=19). Arrowheads indicate time points of poly(I:C) administration. **B)** Histological analysis of sternum sections stained with hematoxylin and eosin. Original magnification 400 x. Analysis was performed in cooperation with Marco Prinz, University of Freiburg, Germany. **C)** Graphs showing numbers of B-lymphoid (B220^{+}), myeloid (Mac1^{+}Gr1^{+}), and erythroid (Terr119^{+}) cells in the BM of Dnmt1$^{\Delta/\Delta}$ and Dnmt1$^{lox/lox}$ mice as determined by FACS. n=4 **D)** Bar graphs showing total cell numbers in BM and spleen of Dnmt1$^{lox/lox}$ (lox/lox) and Dnmt1$^{\Delta/\Delta}$ (Δ/Δ) mice 5 days after poly(I:C) injection (n=3). **C)** and **D)** Values are mean ± s.d * P≤0.05, ** P≤0.001

Table 3: Blood count of *Dnmt1* conditional mice seven days after *Dnmt1* deletion in comparison to control animals.

Genotype	Number of mice	Hematoglobin [g/dl]	White blood cells [x10^3/µl]	P value
Dnmt1$^{lox/lox}$	7	12.6+1.7	11.2+3.6	0.001
Dnmt1$^{\Delta/\Delta}$	7	7.9+2.5	2.9+1.4	<0.001

Histological analysis of sternum sections with a Haematoxylin & Eosin staining (in which the cell nucleus stains blue and other parts of the cell appear light-pink to pink) revealed a profound BM loss. In Figure 7B, massive BM hypoplasia and cytopenia is detected in moribund Dnmt1$^{\Delta/\Delta}$ mice 7 days after the first p(I:C) injection in contrast to normal BM morphology in Dnmt1$^{lox/lox}$ animals.

The eradication of the BM was caused by a depletion of cells from all major BM lineages such as B, myeloid and erythroid cells (Figure 8C). Total cell numbers of BM and spleen suspensions confirmed hematopoietic pancytopenia (reduction of red and white blood cells as well as platelets) (Figure 8D).

Furthermore, the BM fraction staining negative for any lineage marker such as CD19, B220, Gr1, CD3ε, CD4 and CD8α (hereafter designated as lineage negative or Lin$^-$) was analyzed by FACS. This analysis revealed a nearly complete absence of phenotypic HSCs and early progenitors in Dnmt1$^{\Delta/\Delta}$ mice (Figure 9A). To test the ability of *Dnmt1* deficient BM progenitors to generate progeny, an *in vitro* methylcellulose differentiation assay was performed. In this assay, mutant BM cells were unable to generate myeloid and B-lymphoid colonies, indicating that DNMT1 ablation completely disrupted the differentiation potential of hematopoietic stem and progenitor cells (Figure 9B).

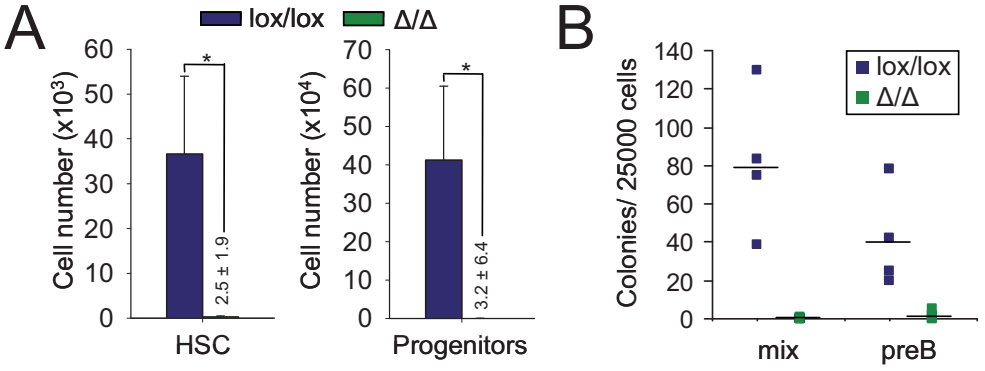

Figure 9: Loss of *Dnmt1* ablates HSCs and progenitors. A) Bar graphs of FACS results demonstrating near complete absence of phenotypic HSCs ($Lin^-Sca\text{-}1^+c\text{-}kit^+$) and progenitors ($Lin^-Sca\text{-}1^-c\text{-}kit^+$) from the BM of $Dnmt1^{\Delta/\Delta}$ mice 7 days after p(I:C) administration. Values are mean ± s.d. (n=4) *P≤0.05, **P≤0.001. **B)** DNMT1 loss blocks myeloid and B lymphoid differentiation *in vitro*. BM from $Dnmt1^{lox/lox}$ or $Dnmt1^{\Delta/\Delta}$ mice was plated in methylcellulose. Each dot represents the average colony number of one animal from triplicate platings. Bars indicate mean values. P≤0.001 each.

To test whether the severe hematopoietic phenotype was caused by cell intrinsic effects of DNMT1 loss, an *in vivo* transplantation assay was performed. For this purpose, chimeric animals were generated by transplanting 1-2 x 10^6 total BM cells from untreated $Dnmt1^{lox/lox}Mx1Cre^+$ and $Dnmt1^{lox/lox}Mx1Cre^-$ control mice into lethally irradiated congenic WT recipients. Stable engraftment of donor cells was confirmed by FACS of peripheral blood cells 8 weeks post-transplantation (Figure 10A). Subsequently, poly(I:C) was administered to delete *Dnmt1* in hematopoietic cells. As in primary $Dnmt1^{\Delta/\Delta}$ mutants, DNMT1 loss in chimeric mice led to profound hematopoietic cell depletion, followed by the rapid death of all animals (Figure 10B). With these data, the severe effect of *Dnmt1* loss in the hematopoietic system is demonstrated. All other tissues, which also show Mx1 activity in the $Dnmt1^{lox/lox}Mx1Cre^+$ mice, are of the recipient WT genotype and have no alterations in DNA methylation following poly(I:C) injection. Thus, in this transplantation experiment, exclusively the hematopoietic tissue is devoid of DNMT1 activity after poly(I:C) treatment.

Taken together, DNMT1 activity is indispensable for establishment and maintenance of the hematopoietic system in a cell autonomous manner.

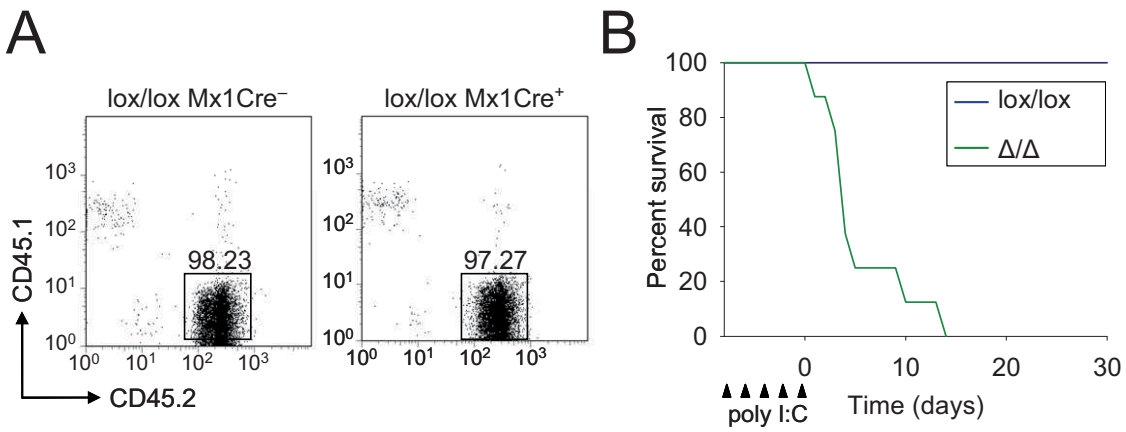

Figure 10: Cell intrinsic effect causes rapid lethality of *Dnmt1* ablated cells. A) Peripheral blood FACS analysis confirming stable donor cell engraftment of Dnmt1$^{lox/lox}$MxCre^{-} or Dnmt1$^{lox/lox}$MxCre^{+} BM cells 8 weeks after transplantation prior to poly(I:C) injection. **B)** Rapid lethality by hematopoietic cell intrinsic DNMT1 loss. Stably engrafted mice were injected 5 times with poly(I:C) (arrowheads) 8 weeks post transplantation. Survival was followed (n=8-9).

Finally, staining of BM cells from primary Dnmt1$^{\Delta/\Delta}$ mice with an antibody against cell surface Annexin-V, a marker for early apoptotic cells (Vermes, et al., 1995), revealed that rapid BM failure was caused by apoptosis (Figure 11). Apoptotic cells (Annexin-V^{+}, DAPI^{-}) were 2-fold enriched and a drastic incline of mean fluorescence intensity (MFI) of Annexin-V illustrates the enlarged proportion of apoptotic cells in *Dnmt1* depleted BM cells.

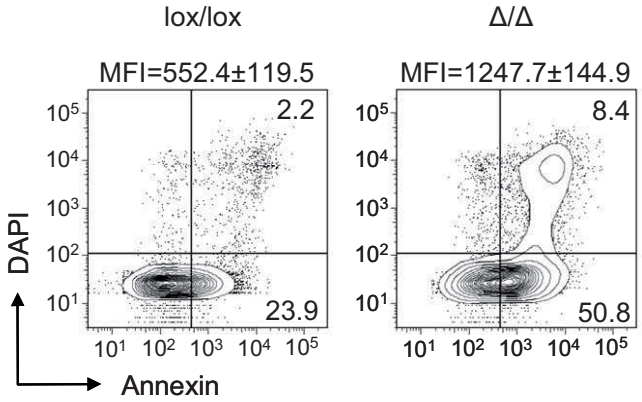

Figure 11: Loss of *Dnmt1* leads to apoptosis of hematopoietic cells. Rates of apoptotic cells were determined in BM of Dnmt1$^{\Delta/\Delta}$ and Dnmt1$^{lox/lox}$ mice by Annexin-V/DAPI co-staining. Values are mean percentages (n=2). Mean fluorescence intensities (MFI) for Annexin-V are indicated on top of each plot.

Results shown in Figures 8-10 demonstrate that complete elimination of DNMT1 activity in the hematopoietic system fully eliminates HSCs and BM progenitors. Additional analysis shown in Figure 11 revealed that this effect is induced by cell-autonomous apoptosis.

3.2 Studies with the *Dnmt1* knockdown mouse model

3.2.1 Validation of the *Dnmt1* knockdown mouse model

The short life span and complete HSC loss in Dnmt1$^{\Delta/\Delta}$ animals made it impossible to investigate the role of DNA methylation levels in regulation of stemness and development of the blood system. Therefore, a hypomorphic Dnmt1 (chip) allele was combined with a null allele (see 2.2.1.1) and these *Dnmt1* hypomorph Dnmt1$^{-/chip}$ mice were used for further experiments.

As reported before, Dnmt1$^{-/chip}$ mice were viable, expressed low amounts of DNMT1 and were hypomethylated in multiple tissues at levels substantially milder than *Dnmt1* null cells (Gaudet, et al., 2003). Figure 12A shows the results of a RT-PCR analysis to quantify *Dnmt1* expression. These results confirmed that Dnmt1 $^{-/chip}$ animals had a 2.9 fold down-regulation of *Dnmt1* expression in Lin$^-$ BM cells.

In a southern blot analysis, genomic DNA from Dnmt1$^{-/chip}$ BM showed an increase of DNA fragments with lower weight when digested with the methylation sensitive restriction enzyme Hpa II (Figure 12B left). This result indicated a hypomethylated status since Hpa II cuts more often on unmethylated DNA. Control cells were taken from Dnmt1$^{+/chip}$ littermate animals, which behaved like WT mice in all analyses made (data not shown). A linker-mediated PCR on genomic DNA from Dnmt1$^{-/chip}$ LT-HSCs produced more PCR fragments after Hpa II digest (Figure 11B right), indicating more frequent cutting with the methylation sensitive enzyme Hpa II and a subsequent higher amount of ligation products used as a template for PCR. These results demonstrate a global loss of DNA methylation in BM and LT-HSCs of Dnmt1$^{-/chip}$ mice.

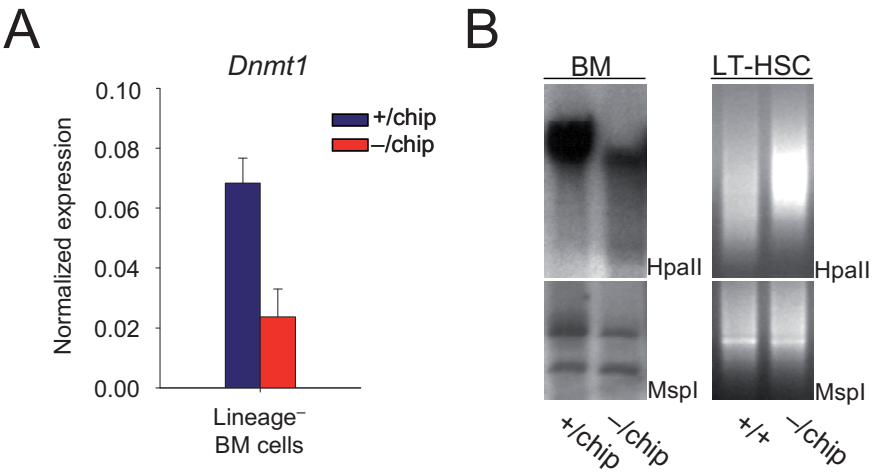

Figure 12: Reduced expression of *Dnmt1* and DNA hypomethylation in Dnmt1$^{-/chip}$ hematopoietic cells. A) Real time RT-PCR of Lin$^-$ BM cells confirmed down-regulation of *Dnmt1* expression. Data were normalized to the expression of *β-actin*. Results represent the mean ± s.d. of two independent experiments. **B)** Genomic DNA was digested with the methylation sensitive HpaII enzyme or its methylation non-sensitive isochizomere MspI. Left: Southern blot analysis showing hypomethylation in whole BM cells of Dnmt1$^{-/chip}$ mice using an IAP cDNA probe. Right: Linker-mediated genomic PCR performed on sorted LT-HSCs (LSKCD34$^{-/low}$Flt3$^-$) of Dnmt1$^{+/+}$ and Dnmt1$^{-/chip}$ mice.

3.2.2 DNA methylation maintains homeostasis within the HSC pool

To test if DNA hypomethylation has an impact on HSC frequency or phenotype, FACS analysis of the BM was performed. All HSC subgroups are harbored in the population of LSK (Lin$^-$Sca1$^+$cKit$^+$) cells. In the BM of Dnmt1$^{-/chip}$ mice normal LSK cell frequencies were detected (Figure 13A). Thus, hypomorphic *Dnmt1* expression is apparently sufficient to rescue HSC formation. However, separation of LSK cells using Flt3 and CD34 markers revealed a markedly skewed distribution of mutant HSC subpopulations. While frequencies of ST-HSCs (LSKCD34$^+$Flt3$^-$) were not significantly changed, LT-HSC (LSKCD34$^{-/low}$Flt3$^-$) frequencies were 2.7 fold enriched (P=0.018). The hematopoietic cell population showing the earliest stage of lymphoid transcriptional priming (Adolfsson, et al., 2005) (Mansson, et al., 2007), the lymphoid myeloid primed progenitor (LMPP, (LSKCD34$^+$Flt3$^+$)), was virtually absent in Dnmt1$^{-/chip}$ mice (Figure 13B). The frequency of LMPPs was 156 fold reduced (P=0.0018).

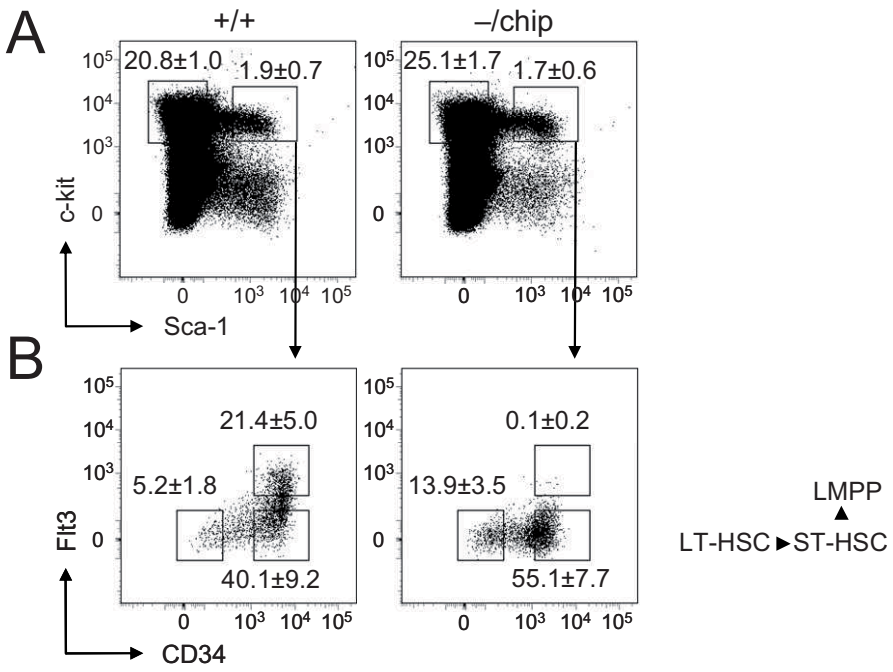

Figure 13: Distribution of HSC subpopulations. A) Total LSK ($Lin^{-}Sca\text{-}1^{+}cKit^{+}$) from $Dnmt1^{+/+}$ and $Dnmt1^{-/chip}$ mice were separated into **B)** LT-HSCs ($LSKCD34^{-/low}Flt3^{-}$), ST-HSCs ($LSKCD34^{+}Flt3^{-}$) and LMPPs ($LSKCD34^{+}Flt3^{+}$). Numbers represent the mean ± s.d. of 3 mice each. Three independent experiments were performed.

Figure 14A shows that Flt3 mRNA expression was normal in $Dnmt1^{-/chip}$ LT-HSCs and ST-HSCs compared to WT controls. According to that, the lack of LMPPs can most likely not be due to reduced Flt3 transcript expression.

The LT-HSC compartment was further characterized using the surface marker most stringent for HSCs, CD150, a SLAM family protein (Kiel, et al., 2005). FACS analysis shown in Figure 14B revealed that $Dnmt1^{+/+}$ and $Dnmt1^{-/chip}$ LT-HSCs expressed CD150 at similar levels. This result demonstrates that both subsets were uniform populations of phenotypic stem cells.

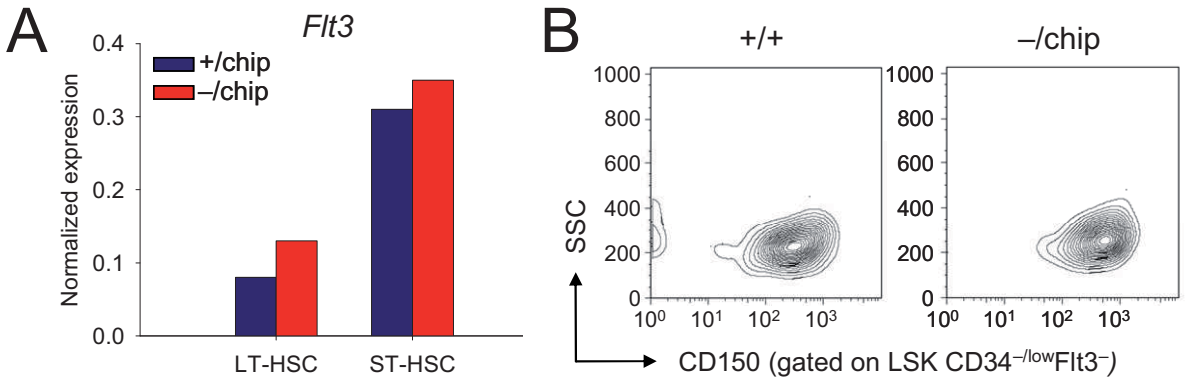

Figure 14: Expression of Flt3 and CD150 in Dnmt1$^{-/chip}$ HSCs. A) *Flt3* transcript numbers were quantified in LT-HSCs (LSKCD34$^{-/low}$Flt3$^-$) and ST-HSCs (LSKCD34$^+$Flt3$^-$) from Dnmt1$^{+/+}$ and Dnmt1$^{-/chip}$ mice using real time RT-PCR. Data were normalized to expression of *Hprt*. Results represent means of technical triplicates. **B)** LT-HSCs of Dnmt1$^{+/+}$ and Dnmt1$^{-/chip}$ mice were co-stained with an anti-CD150 antibody and analyzed by FACS. One representative plot of three independent experiments is shown.

3.2.3 DNA hypomethylation does not alter proliferation or rate of apoptosis

To test the probability whether hypomethylated HSCs have an altered cell cycle phase distribution, Hoechst 33342 staining, a dye for DNA in living cells, was performed. The distribution of cells in the respective cell cycle phase was not significantly different in LSK cells of Dnmt1$^{+/+}$ and Dnmt1$^{-/chip}$ mice (P>0.8) (Figure 15A). An Annexin-V staining was performed to test the possibility of an apoptotic effect in Dnmt1$^{-/chip}$ HSCs as seen in the *Dnmt1* conditional knockout mice. No significant alterations in apoptosis rates of Dnmt1$^{-/chip}$ HSCs were detected (Figure 15B).

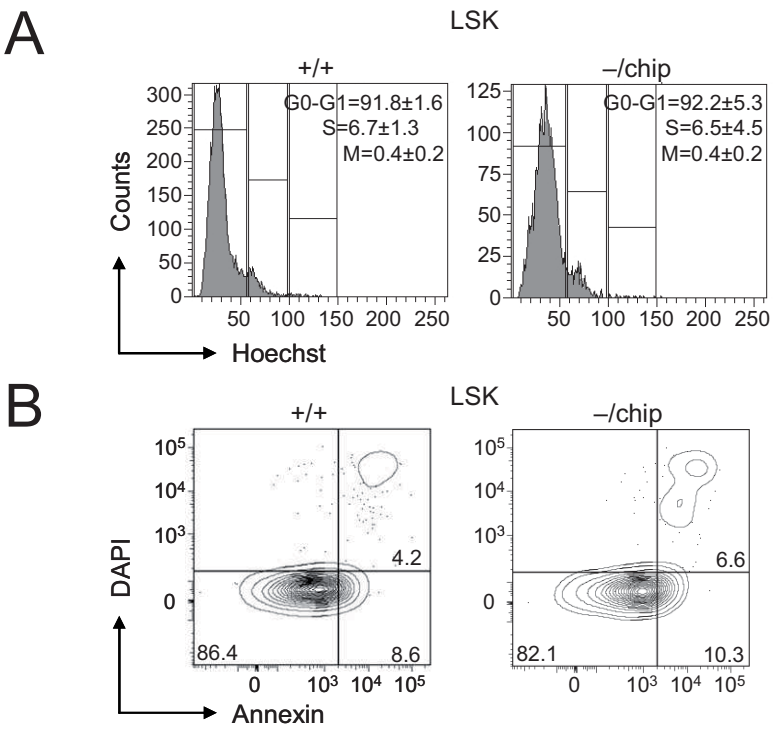

Figure 15: Apoptosis and cell cycle analyses of HSCs from Dnmt1$^{-/chip}$ mice. A) Cell cycle analysis of LSK cells as assessed by DNA staining (Hoechst 33342). Values are mean ± s.d. (n=4). Experiment was performed twice independently. **B)** Annexin-V/DAPI co-staining revealed equal apoptotic rates in LSK cells of Dnmt1$^{+/+}$ and Dnmt1$^{-/chip}$ mice. Numbers in quadrant gates indicate percent cells of one representative animal. Experiment was performed twice independently with n=3 each.

To more rigorously test the contribution of apoptosis to the altered HSC compartment in Dnmt1$^{-/chip}$ mice, a second strategy was performed by testing a possible rescue effect of an anti-apoptotic gene. However, crossbreeding of the anti-apoptotic H2K-bcl2 transgene (Domen, et al., 1998) into the Dnmt1$^{-/chip}$ strain failed to correct the mutant HSC phenotype. Dnmt1$^{-/chip}$ animals positive for *bcl2* still showed a loss of LMPPs and an enlarged LT-HSC compartment (Figure 16).

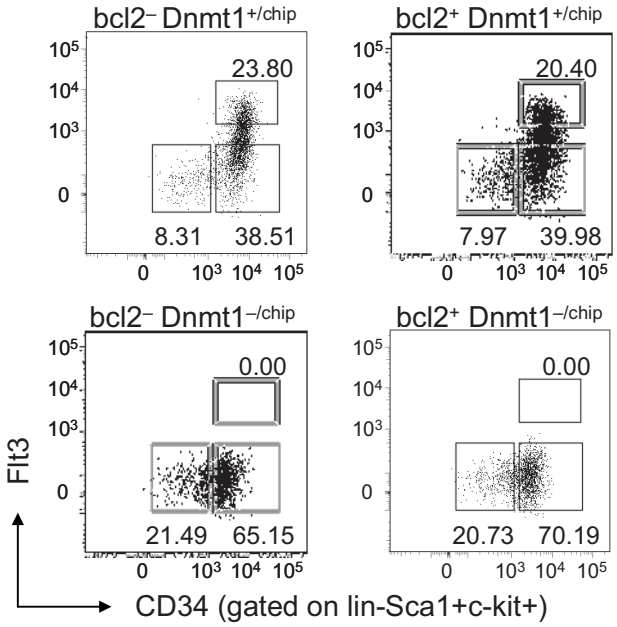

Figure 16: Crossbreeding of bcl2 transgenic mice with Dnmt1$^{-/chip}$ mice failed to rescue the altered HSC phenotype. FACS analysis of BM cells of the designated genotypes. Numbers indicate percent cells of one representative animal (n=4). Experiment was performed twice independently.

Taken together, results shown in Figure 13-16 demonstrate that gradually reduced DNMT1 activity alters HSC homeostasis by a mechanism independent from effects on cell cycle or apoptosis.

3.2.4 Hypomethylation entails impaired stem cell function

Results shown in the previous chapter demonstrated that hypomethylated HSCs exhibit an altered phenotype. The following chapter shows results of a series of transplantation assays, used to test whether Dnmt1$^{-/chip}$ HSCs have an altered HSC function. A scheme of employed transplantation assays is shown in Figure 17. The functional potential of HSCs is measured in a competitive transplantation assay. This study provides qualitative information about the HSCs within a given population. In a serial transplantation assay, the most stringent test of HSC potential, the ability of HSC self-renewal is tested (Purton and Scadden, 2007).

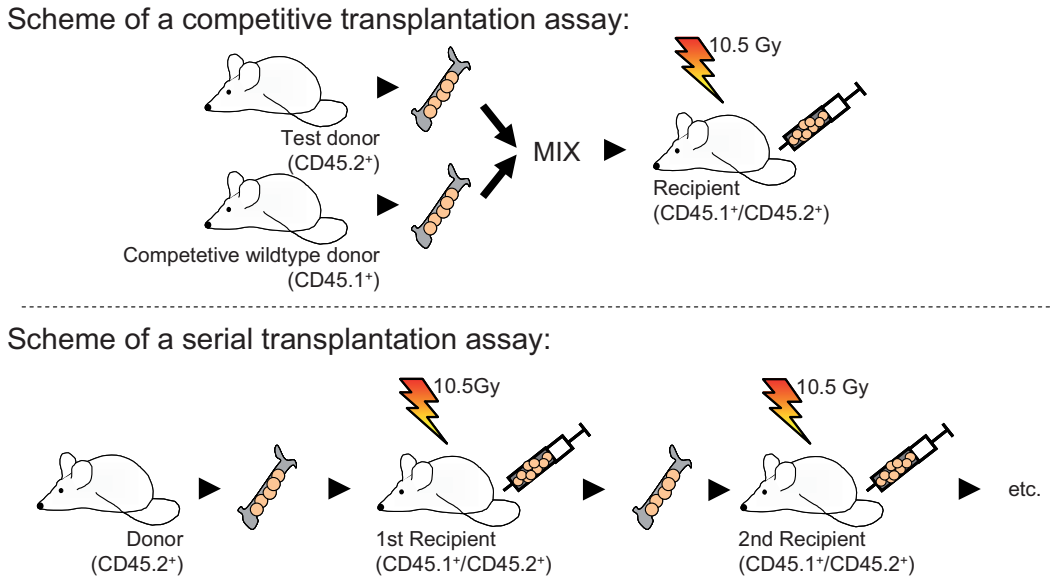

Figure 17: Experimental setup of transplantation assays performed. Donor and recipient cells can be distinguished by FACS analysis of the peripheral blood after transplantation via differential CD45 marker expression (given in brackets). Gy gray.

First, the competitive repopulation potential of BM cells from Dnmt1$^{-/chip}$ mice was tested using different ratios of test : competitor cells. For this assay 1.6 x 10^7 (1:4), 4 x 10^6 (1:1) or 8 x 10^5 (5:1) B6SJL CD45.1$^+$ WT competitor cells were mixed with 4 x 10^6 CD45.2$^+$ test cells from Dnmt1$^{-/chip}$ or Dnmt1$^{+/chip}$ control mice and injected into lethally irradiated F1 129ola/B6.SJL CD45.1$^+$/CD45.2$^+$ WT recipient mice. FACS plots in Figure 18A demonstrate a severely decreased repopulation ability of Dnmt1$^{-/chip}$ HSCs compared to the Dnmt1$^{+/chip}$ control in a 1:1 competition. Dnmt1$^{-/chip}$ donor cells had >200-fold (1:1 competition) reduced ability to reconstitute hematopoietic cells, indicating that hypomethylation disrupts HSC repopulation ability. Even in a 5:1 competition (5 times more Dnmt1$^{-/chip}$ BM cells than WT competitor cells) hypomethylated HSCs were not able to reconstitute the recipients with more than 2% progeny (Figure 18B). This result revealed that Dnmt1$^{-/chip}$ HSCs were functionally impaired.

Second, a serial transplantation assay was performed to test the self-renewal ability of the Dnmt1$^{-/chip}$ HSCs. For this experiment, four rounds of transplantation with 5 x 10^6 BM cells each were performed in 12-16 weeks intervals. Donor chimerism was monitored weekly in peripheral blood samples. While control donor-derived hematopoiesis remained at a constant level throughout the transplantation series, repopulating efficiency of Dnmt1$^{-/chip}$ cells progressively decreased with each

generation (Figure 18C). This result demonstrated that low activity of Dnmt1$^{-/chip}$ HSCs was caused by impaired self-renewal.

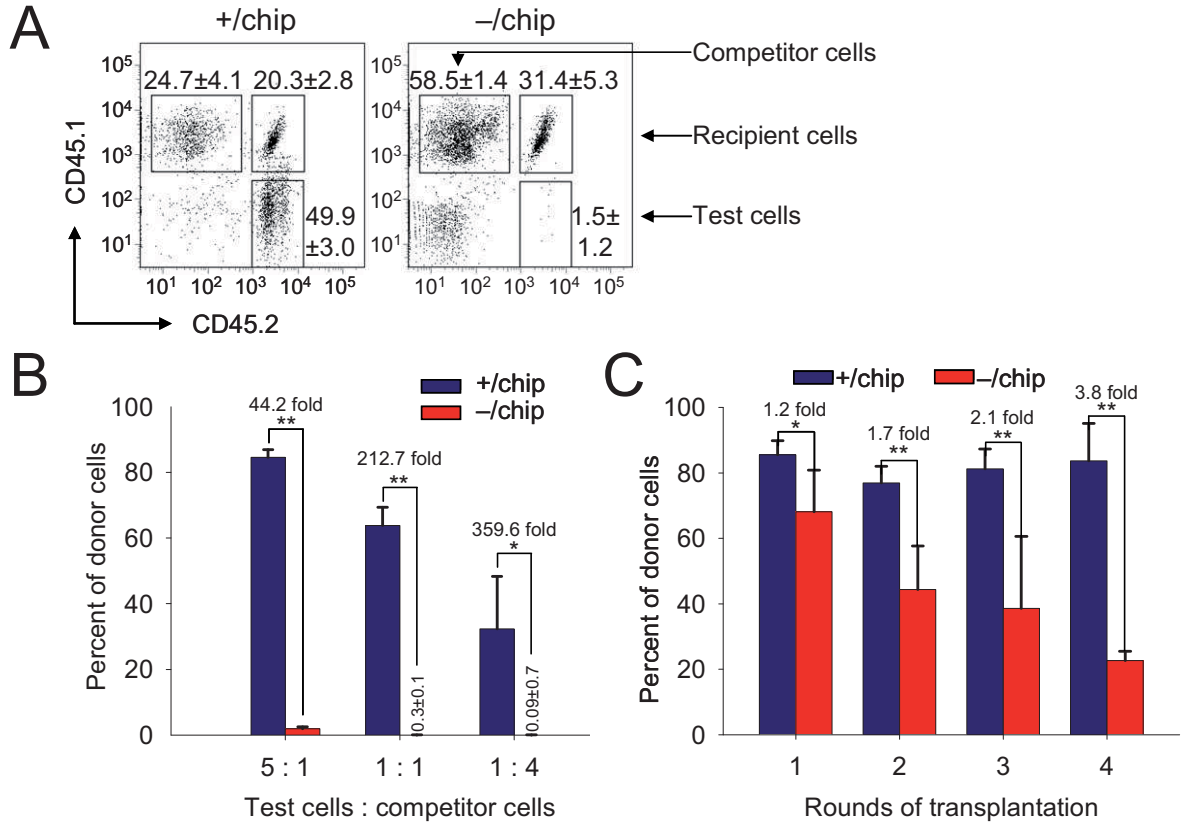

Figure 18: DNA methylation is required for HSC homeostasis and self-renewal. A) Distribution of CD45.2^{+} test and CD45.1^{+} competitor derived cells in the peripheral blood of a CD45.1^{+}/CD45.2^{+} recipient mouse that was transplanted with a test to competitor BM cell ratio of 1:1 12 weeks after transplantation. Values are mean ± s.d. (n=4). **B)** BM cells from Dnmt1$^{-/chip}$ mice are out-competed by WT cells in competitive transplantation assays. Bars represent frequencies of CD45.2^{+} donor cells in peripheral blood of the recipients 16 weeks after transplantation for the respective test to competitor ratio (n=3-5). **C)** Dnmt1$^{-/chip}$ HSCs harbor an impaired long-term reconstitution capacity in serial transplantation assays (n=5-7). **B)** and **C)** Values are mean ± s.d. *P≤0.05, **P≤0.001

A competitive short-term engraftment assay was used to investigate the homing capacity of hypomethylated stem cells, to test whether the phenotype described above was due to impaired homing. In this assay 10^7 test cells, either Dnmt1$^{-/chip}$ or Dnmt1$^{+/+}$, were transplanted along with 10^7 competitor cells into lethally irradiated recipient mice. BM analysis of recipients was performed after 24 h. Results shown in Figure 19A revealed that BM cells from Dnmt1$^{-/chip}$ and control mice equally contributed to the BM progenitor chimerism in recipients, indicating that HSC homing

is not affected by hypomethylation.

A conditional genetic approach was used to exclude that the impaired HSC activity was caused by altered homing or repopulation ability. Thus, Dnmt1$^{lox/chip}$Mx1Cre^{+} and Dnmt1$^{lox/chip}$Mx1Cre^{-} control mice were generated (see 2.2.1.1) and their untreated BM cells were used for repopulation. This experimental approach allows normal homing of all HSCs. 1 x 10^6 BM cells from not induced Dnmt1$^{lox/chip}$Mx1Cre^{+} and Dnmt1$^{+/+}$Mx1Cre^{-} mice (CD45.2^{+}) were transplanted along with 1 x 10^6 WT BM cells (CD45.1^{+}) into lethally irradiated recipients. Stable donor cell engraftment was confirmed 8 weeks after transplantation (Figure 19B). Afterwards, poly(I:C) was injected to induce hypomethylation upon Cre-mediated excision of the Dnmt1^{lox} allele (hereafter termed Dnmt1$^{\Delta}$). Figure 19C shows that following poly(I:C) administration, numbers of Dnmt1$^{\Delta/chip}$ donor-derived peripheral blood cells decreased. The inducible BM chimeras confirmed an intrinsic deficiency in long-term maintenance of hypomethylated HSCs. Importantly, analysis of the donor-derived BM compartment at the experimental endpoint revealed a 10 fold decline in hypomethylated donor HSCs (LSK) (Figure 19D). Transplantation assays normally always imply stress for the transplanted BM cells because cells were removed from their niche and have to repopulate a new one. The conditional approach, described in Figure 19, circumvents this stress impulse by reducing DNMT1 activity not until stable repopulation has taken place.

Together, these results demonstrate that constitutive DNA methylation is important for self-renewal and maintenance of the HSC self-renewal program, even in the absence of transplantation stress.

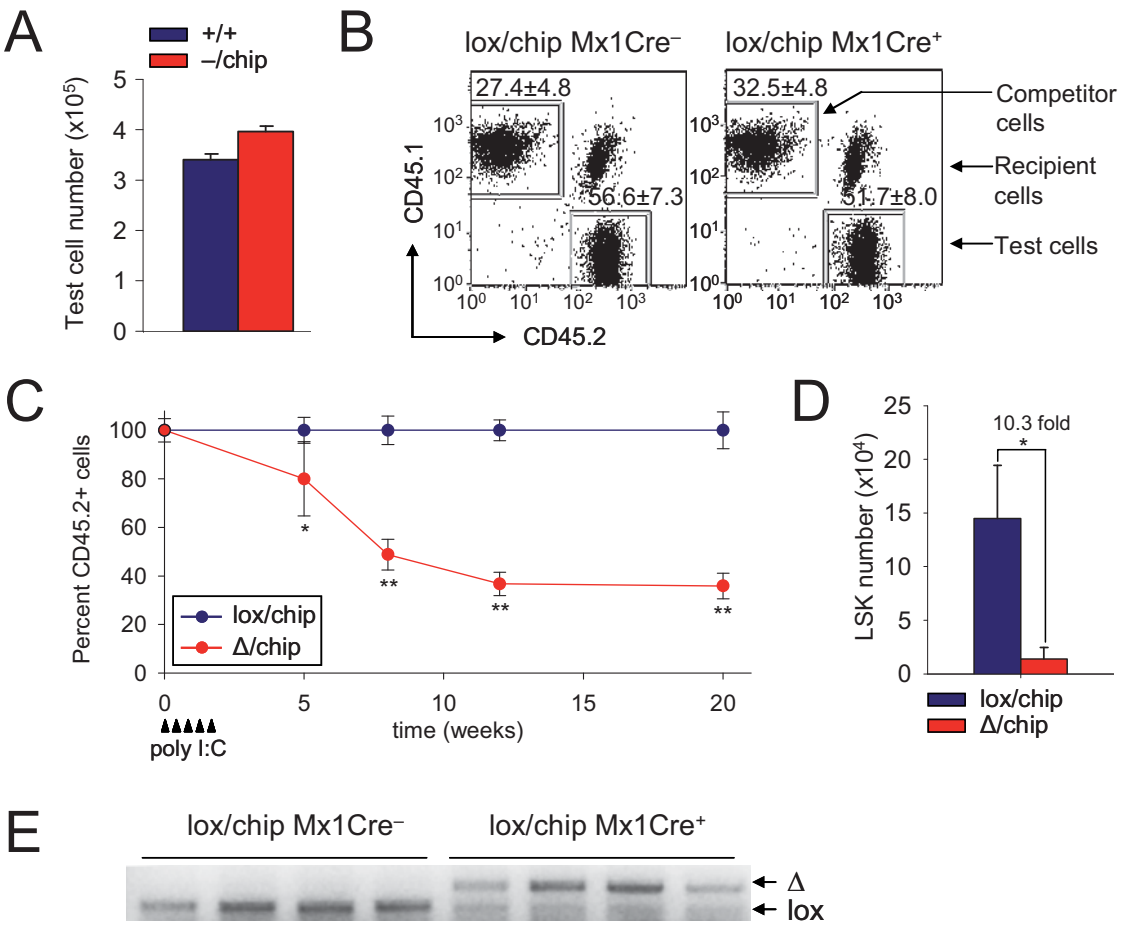

Figure 19: Long term reconstitution, but not homing, is affected by hypomethylation. A) FACS analysis of recipient BM 24 h post transplantation revealed equal short-term engraftment ability of Dnmt1$^{-/chip}$ and Dnmt1$^{+/+}$ donor cells (n=4). **B)** Peripheral blood FACS analysis confirming stable donor cell engraftment of Dnmt1$^{lox/chip}$Mx1Cre^{-} or Dnmt1$^{lox/chip}$Mx1Cre^{+} cells prior to poly(I:C) injection. The experiment was performed twice independently (n=4). **C)** After stable donor cell engraftment, mice were injected 5 times with poly(I:C) (arrow heads) and CD45.2^{+} cells were monitored in peripheral blood. The average value of CD45.2^{+} control cells was set to 100% at each time point (n=4). **D)** FACS analysis of LSK cells of the chimeras described in 19C 20 weeks after poly(I:C) induction (n=4). **A)**, **B)**, **C)** and **D)** Values are mean ± s.d. *P≤0.05, **P≤0.001 **E)** Genomic PCR analysis of *Dnmt1* deletion in BM of poly(I:C) treated chimeras that had received Dnmt1$^{lox/chip}$MxCre^{-} (lox/chip) or Dnmt1$^{lox/chip}$MxCre^{+} (Δ/chip) BM.

3.2.5 Lymphoid pathway establishment is dependent on DNA methylation

Recently, it was demonstrated that megakaryocyte-erythroid (MkE) potential is lost in LMPPs (Mansson, et al., 2007). Mansson et al. showed that MkE genes were downregulated during transition from the HSC state to the LMPP state, whereas common lymphoid genes were upregulated. Additionally, in functional experiments LMPPs were shown to functionally lose MkE potential (Adolfsson, et al., 2005). These results predicted LMPPs as the first transcriptionally primed lymphoid progenitor population. Consequently, the absence of LMPPs in Dnmt1$^{-/chip}$ mice suggested an unanticipated effect of the DNA methylation status on myeloerythroid versus lymphoid lineage choice.

Indeed, investigation of lineage distribution in various hematopoietic tissues by FACS, as shown in Figure 20A, revealed that B cells were profoundly reduced in Dnmt1$^{-/chip}$ mice while frequencies of differentiated myeloid and erythroid cells were not affected. Similarly, myeloerythroid progenitor frequencies such as common myeloid progenitors (CMPs), granulocyte macrophage progenitors (GMPs) and megakaryocyte erythrocyte progenitors (MEPs) were comparable in Dnmt1$^{-/chip}$ and control mice. In contrast, common lymphoid progenitors (CLPs) as well as B- and T-lineage-restricted progenitors were drastically diminished (Figure 20A, 20B and 20C).

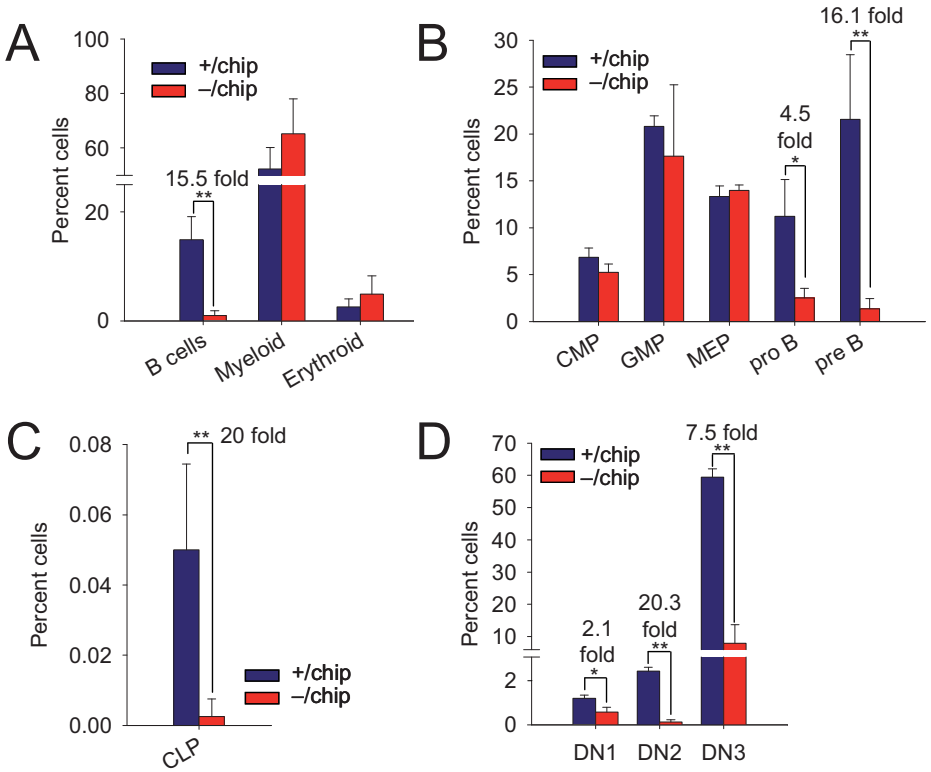

Figure 20: Multiple-color FACS analysis of hematopoietic lineages in *Dnmt1* hypomorph mice. A) Frequencies of B ($CD19^+$) and myeloid cells ($Mac1^+$) in BM and erythroid cells ($Ter119^+$) in spleen were analyzed in $Dnmt1^{-/chip}$ and $Dnmt1^{+/chip}$ mice by FACS. (n=3-7) **B)** CMPs ($lin^-Sca\text{-}1^-c\text{-}kit^+CD34^+Fc\gamma RII/III^{low}$), GMPs ($lin^-Sca\text{-}1^-c\text{-}kit^+CD34^+Fc\gamma RII/III^+$), MEPs ($Lin^-Sca\text{-}1^-c\text{-}kit^+CD34^-Fc\gamma RII/III^-$), preB cells ($Lin^-IgM^-B220^+CD43^-$) and proB cells ($Lin^-IgM^-B220^+CD43^+$) were analyzed from BM. (n=3-4) **C)** CLPs ($Lin^-Sca\text{-}1^{low}c\text{-}kit^{low}IL7R\alpha^+$) were analyzed from BM. **D)** Double negative (DN) T-cell progenitor stages DN1 ($CD3\varepsilon^-CD4^-CD8\alpha^-CD44^+CD25^-$), DN2 ($CD3\varepsilon^-CD4^-CD8\alpha^-CD44^+CD25^+$) and DN3 ($CD3\varepsilon^-CD4^-CD8\alpha^-CD44^-CD25^+$) were analyzed from thymuses. (n=3-4). **A)**, **B)**, **C)** and **D)** percentages are mean ± s.d. *P≤0.05, **P≤0.001.

To exclude that only phenotypic markers are lacking on hypomethylated BM cells, an expression profile of genes characteristic for different lineages was determined. Figure 21A shows the result of the RT PCR profiling of Lin^- BM cells. These results demonstrated that $Dnmt1^{-/chip}$ progenitors had reduced expression of genes indicative for lymphocyte progenitors, whereas myeloid progenitor genes were expressed at normal levels. Strikingly, $Dnmt1^{-/chip}$ progenitors lacked detectable expression of essential B-cell factors (e.g. Pax5 (Busslinger, 2004) and Ebf (Medina and Singh, 2005)), indicating that DNA methylation is essential for establishing the transcriptional B-cell program.

To evaluate whether loss of lymphoid potential was a cell intrinsic effect, BM

chimeras described in Figure 18C were analyzed by FACS. Transplanted Dnmt1$^{-/chip}$ donor cells reconstituted myeloid cells with a two-fold decrease resembling the impaired HSC function. In contrast, these cells were totally incompetent to generate B cells.

Mature T cells are known to undergo substantial homeostatic proliferation, therefore, a steady state measurement in the adult Dnmt1$^{-/chip}$ mouse would not quantitatively evaluate the ability of hypomethylated HSCs to generate T-cell progeny. Because of this, Dnmt1$^{-/chip}$ BM cells depleted from all T cells (CD3ε^{+}/CD4^{+}/CD8α^{+}) were used in an additional transplantation assay. After transplantation, the ability of Dnmt1$^{-/chip}$ cells to generate T cells was analyzed. For this experiment, 1.5 x 10^{6} T-cell depleted BM cells were transplanted into lethally irradiated WT recipients. Figure 23C shows that the fraction of CD45.2^{+} donor cells contained fewer T cells (CD3ε^{+}, CD4^{+} and/or CD8α^{+}) in mice reconstituted with Dnmt1$^{-/chip}$ cells 8 weeks after transplantation. This approach revealed that Dnmt1$^{-/chip}$ progenitors had impaired capacity to regenerate T cells.

Taken together, these data demonstrate that the selective inefficiency of Dnmt1$^{-/chip}$ precursors to generate lymphocytes is cell intrinsic *in vivo*.

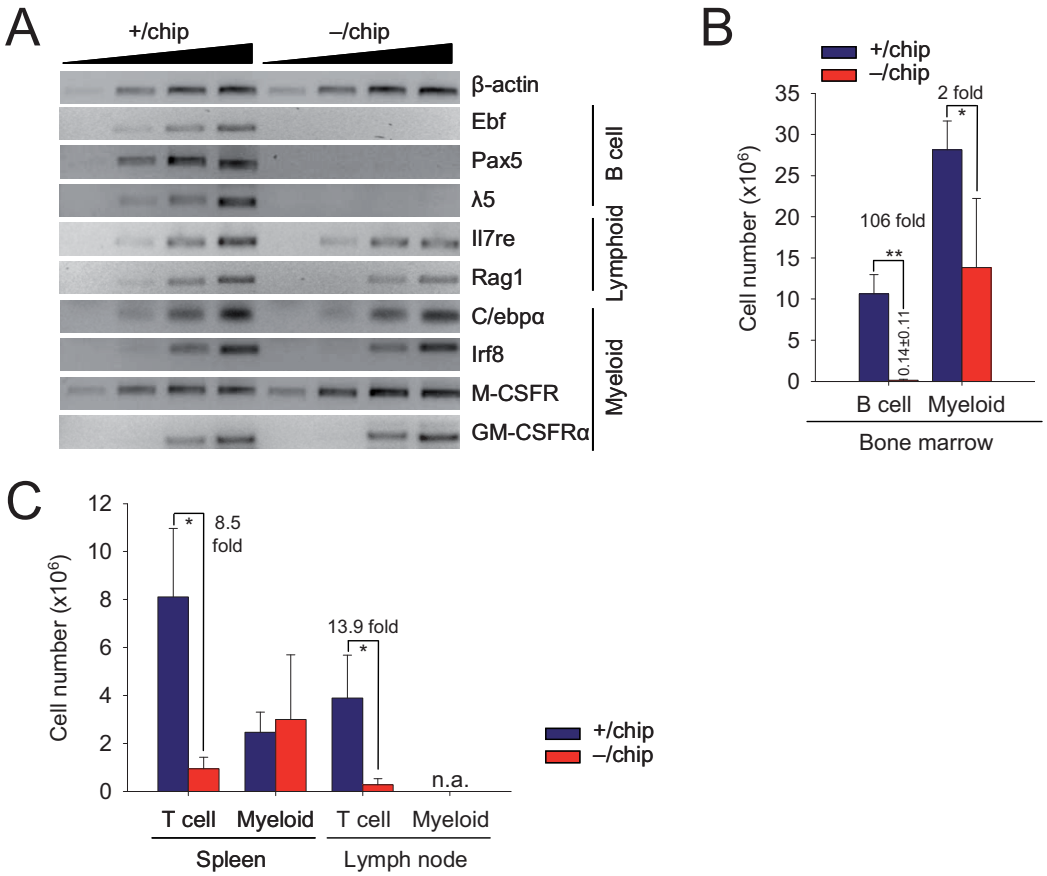

Figure 21: Transcriptional lymphoid cell program and *in vivo* generation of B and T cells is disturbed in *Dnmt1* mutants. A) Semi-quantitative RT PCR on Lin^- BM cells of marker genes for B cells, early lymphocytes and myeloid cells. *β-actin* was used as a positive control for equal cDNA input. Samples were taken at four cycle intervals. One representative out of 3 independent experiments is shown. **B)** Loss of B-lymphoid potential is cell intrinsic. BM of first generation chimeras described in Figure 18C was analyzed for presence of donor-derived B ($B220^+$) and myeloid ($Mac1^+$ and/or $Gr1^+$) cells 12 weeks after transplantation. (n=5-7) **C)** DNA hypomethylation impairs T-cell reconstitution. Analysis of donor generated T cells ($CD3\varepsilon^+$, $CD4^+$ and/or $CD8\alpha^+$) and myeloid cells ($Mac1^+$) in mice reconstituted with $Dnmt1^{-/chip}$ or control cells depleted from mature T cells 8 weeks after transplantation. (n=4) **B)** and **C)** Values are mean ± s.d. *P≤0.05, **P≤0.001

To quantify lineage potential of purified LT- and ST-HSCs, a clonal single-cell *in vitro* differentiation assay was performed. For this approach, ST- and LT-HSCs were subjected to single cell differentiation assays. Cloning frequencies with indicated lineage potential were scored at week 3 to 4 for T and B cells and at day 8 to 10 for GM (granulomonocytic) and Mk (megakaryocytic) cells. Lineage affiliations of individual clones were determined by morphology (GM and Mk) or FACS (T cell = $NK1.1^-Thy1.2^{hi}CD25^{hi}$, B cell = $B220^+CD19^+$). Results shown in Figure 22A and 22B

revealed that both Dnmt1$^{-/chip}$ LT- and ST-HSCs had normal potential to differentiate into granulomonocytic and megakaryocytic lineages. In contrast, they had reduced capacity to generate T and B cells.

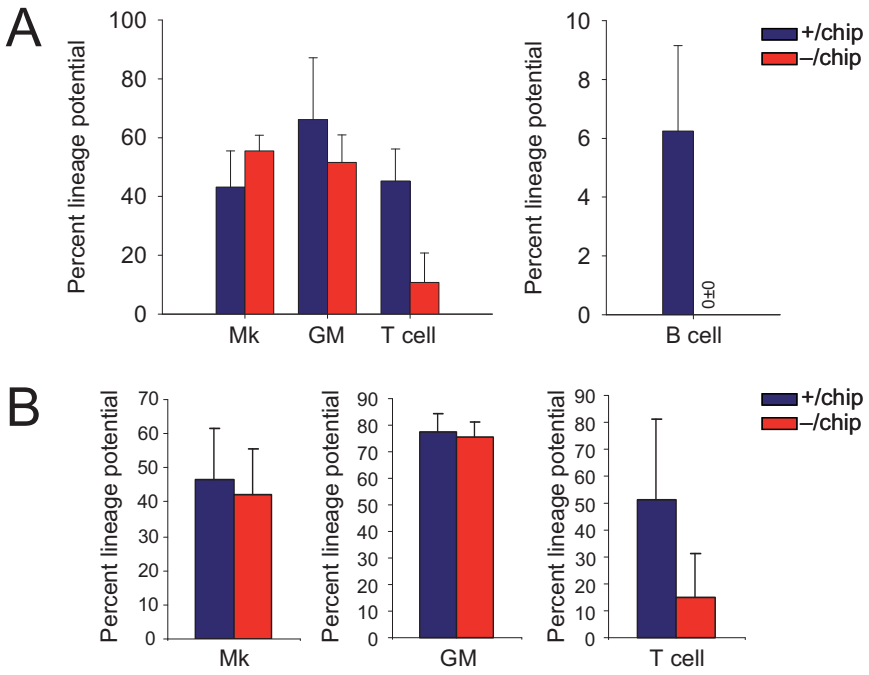

Figure 22: *In vitro* measured lineage potential of Dnmt1$^{-/chip}$ HSCs. A) LT-HSC and **B)** ST-HSC cloning frequencies with indicated lineage potentials are shown. Mk megakaryocytic, GM granulomonocytic. Values are mean ± s.d. (n=2-3). One of at least two independent experiments is shown. In vivo differentiation assays were performed in cooperation with S. Kharazi and S.E. Jacobsen, Lund Stem Cell Centre, Sweden.

Additionally, the effect of *Dnmt1* reduction on lineage diversification could be tested in a fully established hematopoietic system in adult animals using Dnmt1$^{lox/chip}$Mx1Cre^{+} mice (already introduced in the previous chapter). Animals with a conditional Dnmt1$^{-/chip}$ genotype (Mx1Cre^{+}Dnmt1$^{lox/chip}$) were treated with poly(I:C) to induce excision of the *Dnmt1* allele (afterwards designated as Dnmt1$^{\Delta/chip}$). Both, LMPP and B cell frequencies were reduced in poly(I:C) treated Dnmt1$^{\Delta/chip}$ mice in contrast to control Dnmt1$^{lox/chip}$ animals (Figure 23). These results revealed that DNA methylation is required not only for establishing, but also maintaining lymphoid potential in HSCs.

Taken together, these results demonstrate a crucial and previously unexpected

methylation dosage effect in the control of myeloerythroid versus lymphoid lineage choice in HSCs.

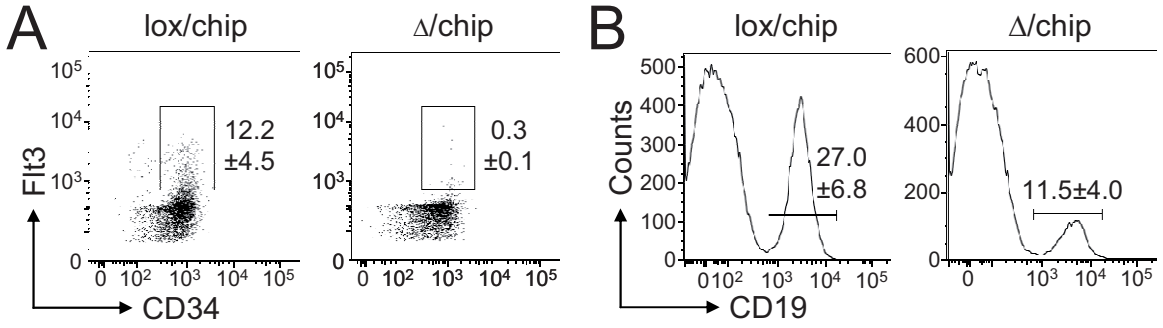

Figure 23: Effect of DNA methylation reduction on a fully established hematopoietic system in adult animals. A) LMPPs (LSKCD34^{+}Flt3^{high}) and **B)** B cells (CD19^{+}) of Dnmt1$^{\Delta/chip}$ (Δ/chip) mice were significantly (P≤0.05) reduced 3 weeks after poly(I:C) administration. Values are mean percentages ± s.d. (n=4). The experiment was performed twice independently.

3.2.6 Impaired lymphoid development is not caused by apoptosis

One possible reason for the loss of lymphoid potential could have been that these cells undergo intrinsic apoptosis during development. To evaluate this possibility, crossbreeding of Dnmt1$^{-/chip}$ with H2K-bcl2 transgenic mice was performed. With this approach, it was tested whether *bcl2* expression could rescue the lymphoid pathway in Dnmt1$^{-/chip}$ mice. Importantly, the absence of B cells in the BM of Bcl2^{+}Dnmt1$^{-/chip}$ mice (Figure 24) demonstrated that *bcl2* failed to rescue the disrupted lymphopoiesis. This finding suggested that lymphopenia was not caused by enhanced hypomethylation-induced apoptosis of lymphocytes.

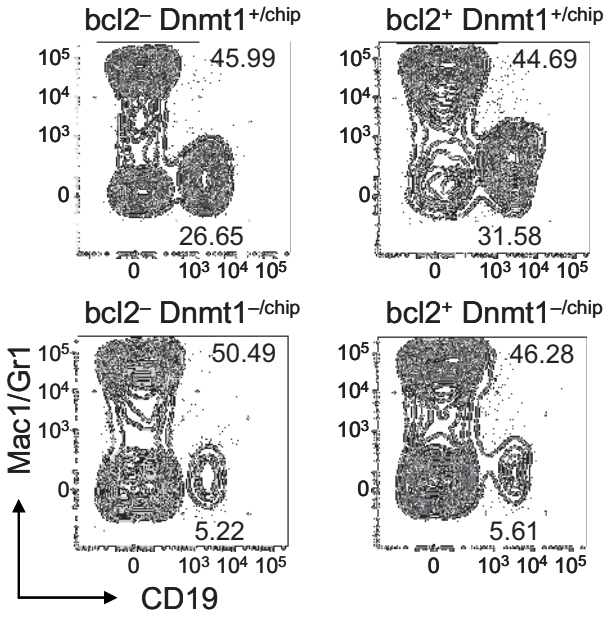

Figure 24: Crossbreeding of Bcl2 transgenic mice with Dnmt1$^{-/chip}$ mice failed to rescue lymphopenia. FACS analysis of BM of the indicated genotypes. Numbers indicate percent cells of one representative animal (n=4). Experiment was performed twice independently.

3.2.7 Committed B cells do not require DNA methylation for maturation and homeostasis

To determine whether constitutive methylation is continuously required throughout lymphopoiesis, Dnmt1$^{lox/chip}$ mice were crossbred with CD19Cre mice (see 2.2.1.1). The CD19Cre genotype facilitates the induction of DNA hypomethylation after onset of CD19 expression and thus, after commitment to the B-cell lineage has occurred. Addition of a R26R allele carrying an inducible loxP-Stop-loxP-Eyfp reporter cassette knock-in (see 2.2.1.1) allowed tracing of cells with active Cre recombinase.

In contrast to the almost complete absence of B cells in Dnmt1$^{-/chip}$ mice, normal numbers and an undisturbed homeostasis of EYFP^{+} B cells was detected in Dnmt1$^{\Delta/chip}$CD19Cre^{+} animals (Figure 25A and 25B). FACS analysis of splenocytes from Dnmt1$^{\Delta/chip}$CD19Cre^{+} and Dnmt1$^{\Delta/+}$CD19Cre^{+} mice showed an equal distribution of marginal zone B cells (CD21^{hi}CD23^{-}) and follicular B cells (CD21^{+}CD23^{+}) (Figure 25C) as an example for two fully mature B cell populations. Complete excision of the *Dnmt1* allele in sorted EYFP^{+} splenocytes of Dnmt1$^{\Delta/chip}$CD19Cre^{+} mice was confirmed by PCR on genomic DNA.

These results demonstrate that a lower DNA methylation threshold is sufficient to

maintain B-cell identity and maturation once the B-cell program has initially been established.

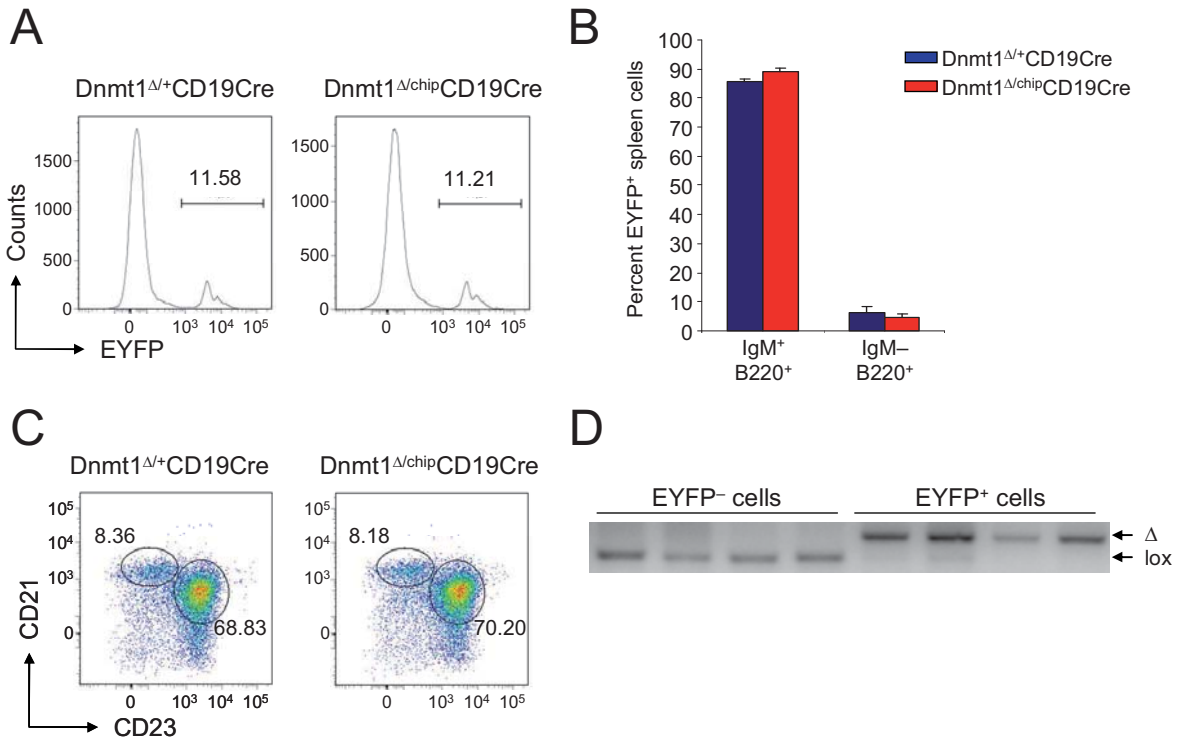

Figure 25: Normal specification of B cells after CD19Cre induced DNA hypomethylation. A) FACS analysis of Dnmt1$^{\Delta/chip}$CD19Cre^{+} and Dnmt1$^{\Delta/+}$CD19Cre^{+} spleen cells carrying an additional loxP-Stop-loxP-Eyfp knockin R26R allele revealed equal frequencies of EYFP^{+} cells. Numbers indicate percent cells of one representative animal (n=4). **B)** Unchanged numbers of EYFP^{+}B220^{+}IgM^{+} and EYFP^{+}B220^{+}IgM^{-} splenic B cells of Dnmt1$^{\Delta/chip}$CD19Cre^{+} and control mice. Values are mean ± s.d. (n=4). **C)** FACS plots of EYFP^{+}B220^{+} splenocytes from Dnmt1$^{\Delta/chip}$CD19Cre^{+} and control mice with marginal zone B cells (CD21^{hi}CD23^{-}) and follicular B cells (CD21^{+}CD23^{+}). One representative animal from each group is shown (n=3). **D)** Excision of the *Dnmt1* allele in sorted EYFP^{+} splenocytes of Dnmt1$^{\Delta/chip}$CD19Cre^{+} mice was confirmed by PCR on genomic DNA.

3.2.8 Hypomethylated HSCs show a severely altered gene expression pattern

Results described in the previous chapters revealed an unexpectedly specific effect of loss of DNA methylation on HSC activity, maintenance and lineage decisions. To gain insight into the molecular basis of these defects in Dnmt1$^{-/chip}$ stem cells, genome-wide mRNA expression profiles were utilized. Profiles of Dnmt1$^{-/chip}$ HSCs (=Lin^{-}Sca-1^{+}c-Kit^{+}Flt3^{-}) and Dnmt1$^{-/chip}$ myeloerythroid progenitors (MPs=Lin^{-}Sca-1^{+}c-Kit^{+}Flt3^{-}) as well as WT control populations were generated. For expression

profiles, mRNA of 35000 sorted cells (HSCs or MPs) was extracted and linearly amplified (see 2.2.6.1). Additionally, $CD19^{+}IgM^{-}$ B-cell progenitors (BPs) were sorted from WT BM as a third control population. RNA extraction, linear amplification, array hybridization and scanning was performed in cooperation with Imagenes, Berlin, Germany.

The array data shown in Figure 26A confirmed that *Dnmt1* mRNA levels in $Dnmt1^{-/chip}$ HSCs and MPs are decreased by a similar degree. In contrast, *Dnmt3a* and *Dnmt3b* levels were not significantly changed in either population, suggesting that neither enzyme compensated for the diminished DNMT1 activity (Figure 26B).

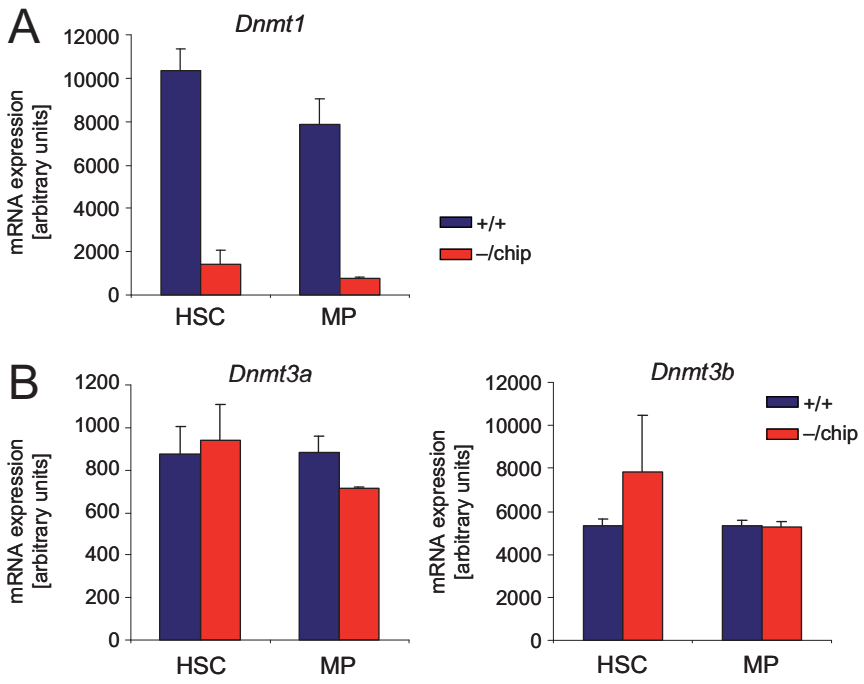

Figure 26: mRNA expression of *Dnmt1*, *3a*, and *3b*. A) mRNA levels of *Dnmt1* and **B)** *Dnmt3a* (left) and *b* (right) in HSCs ($LSKFlt3^{-}$) and MPs ($LKCD34^{+}$) from $Dnmt1^{+/+}$ and $Dnmt1^{-/chip}$ mice were measured by Affymetrix Mouse Genome 430 2.0 arrays and are shown in Affymetrix GenArray arbitrary units. Bar graphs represent mean values ± s.d. of n=3 for each population except +/+ HSCs which were n=2. Shown are data from representative array probes sets (probe ID *Dnmt1*: 1435122; probe ID *Dnmt3a*: 1460324; probe ID *Dnmt3b*: 1449052).

Comparison of the whole genome expression profiles of mutant HSCs and MPs with their WT counterparts demonstrated a striking difference in the number of deregulated transcripts between hypomethylated HSCs and MPs (Figure 27A). While the expression levels of 1186 unique transcripts (11.4% of all expressed) were different between $Dnmt1^{+/+}$ and $Dnmt1^{-/chip}$ HSCs, only 44 (0.4% of all expressed)

were different between the MP populations. Principle components analysis (PCA) was performed to explore the relationships between WT and mutant HSCs and MPs based on the comparison of their transcriptomes (Landgrebe, et al., 2002). A PCA plot illustrates the similarity and dissimilarity of gene expression profiles between all investigated populations in a plane dimension. The PCA plot shown in Figure 27B demonstrated that Dnmt1$^{-/chip}$ HSCs reside at a midpoint between Dnmt1$^{+/+}$ HSCs and both Dnmt1$^{+/+}$ and Dnmt1$^{-/chip}$ MPs. This analysis revealed the increased transcriptional similarity of Dnmt1$^{-/chip}$ HSCs to myeloerythroid cells. Additionally, the PCA approach showed a clear separation of Dnmt1$^{-/chip}$ HSCs from their WT counterparts, while mutant and WT MPs remained closely related. Intriguingly, Dnmt1$^{-/chip}$ HSCs had an increased transcriptional similarity with MPs, but not with BPs. This demonstrated that hypomethylated HSCs do specifically adopt a myeloid progenitor fate. Figure 27C illustrates an unbiased cluster analysis in a tree diagram (dedrogram), which further confirmed the increased relationship between Dnmt1$^{-/chip}$ HSCs and MPs.

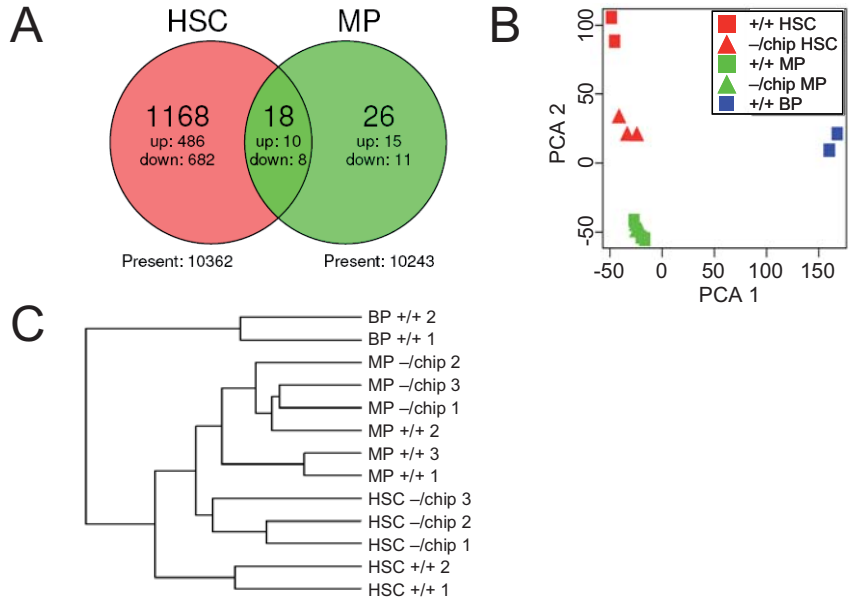

Figure 27: Venn diagram and analysis of relationships between the five profiled populations. **A)** Genome-wide mRNA expression profiles of HSCs (LSKFlt3^{-}) and myeloerythroid progenitors (MPs LKCD34^{+}) were generated using Affymetrix Mouse Genome 430 2.0 Arrays. The number of up- and down-regulated genes in HSCs and MPs from Dnmt1$^{+/+}$ and Dnmt1$^{-/chip}$ mice was compared using a Venn diagram. Numbers below circles indicate total unique transcripts expressed in HSCs or MPs respectively. **B)** Expression of profiled populations was compared using principal components analysis.**C)** The branching points of the dendrogram display that Dnmt1$^{-/chip}$ HSCs are transcriptionally more similar to MPs than Dnmt1$^{+/+}$ HSCs. Bioinformatic analysis was performed in cooperation with M. Huska and M. Andrade-Navarro, Max-Delbrück-Center Berlin, Germany.

3.2.9 DNA hypomethylation causes myeloerythroid gene activation in HSCs

To visualize the different gene expression profiles of the four profiled populations (HSCs and MPs of WT and Dnmt1$^{-/chip}$) gene signatures were calculated in an unbiased approach. Gene signatures specific for HSCs or MPs were generated by subtracting the genes expressed in WT MPs from those expressed in WT HSCs or vice versa. Hereby, cell population signatures were created which contain genes highly expressed in the individual WT cell population. Strikingly, 96.57% of the HSC signature genes showed decreased expression in Dnmt1$^{-/chip}$ HSCs, while 3.43% were increased (Figure 28A). In contrast, only 10.30% of the MP signature genes decreased in expression, while 89.71% increased in Dnmt1$^{-/chip}$ HSCs. Density plots, shown in Figure 28B, further illustrated reciprocal expression shifts of HSC and MP signature genes in Dnmt1$^{-/chip}$ HSCs.

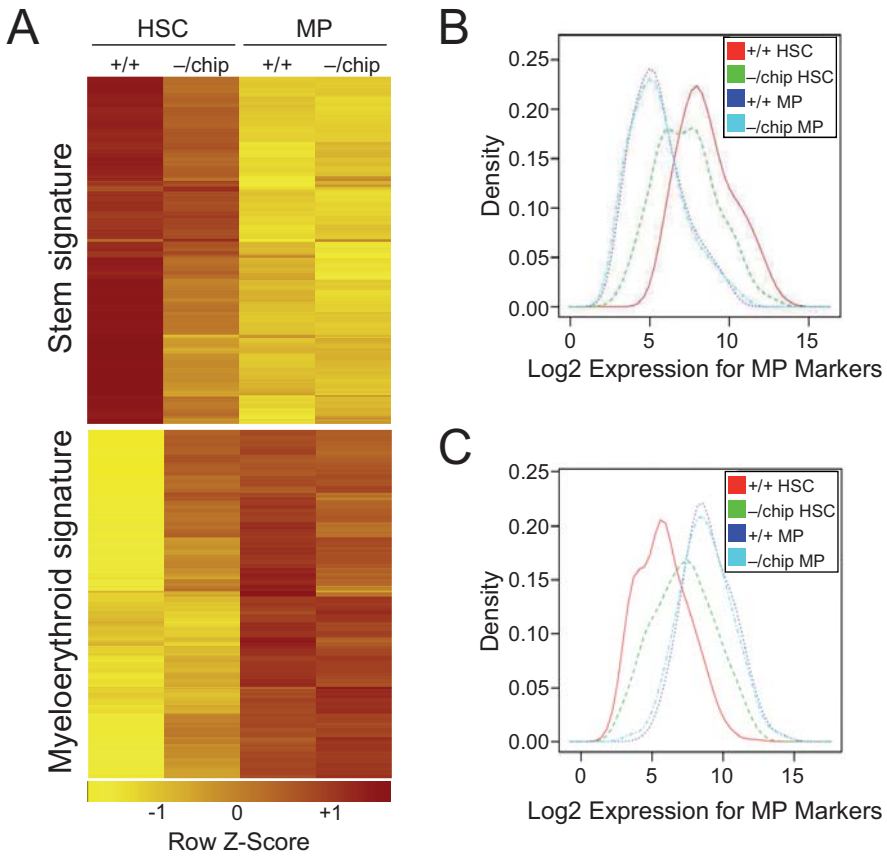

Figure 28: DNA hypomethylation leads to derepression of myeloerythroid genes in HSCs. A) HSC and MP signature probe sets were defined as probe sets that were differentially expressed between Dnmt1$^{+/+}$ HSCs and MPs as calculated by a false discovery rate <0.001 and a log fold change >2.0. Absolute expression values were transformed to probe set Z-scores before visualization. Density plots show expression levels of **B)** HSC and **C)** MP signature genes of Dnmt1$^{+/+}$ and Dnmt1$^{-/chip}$ HSCs and MPs. All bioinformatic analysis was performed in cooperation with M. Huska and M. Andrade-Navarro, Max-Delbrück-Center Berlin, Germany.

Additionally, a biased approach was chosen to evaluate the differential expression of genes with known function for stemness, myeloid or lymphoid differentiation in HSCs. Figure 29 depicts the expression levels of three selected sets of genes in the profiled cell populations. In contrast to the increased expression of MP genes, most genes known to control self-renewal and/or lymphoid differentiation were downregulated in mutant HSCs.

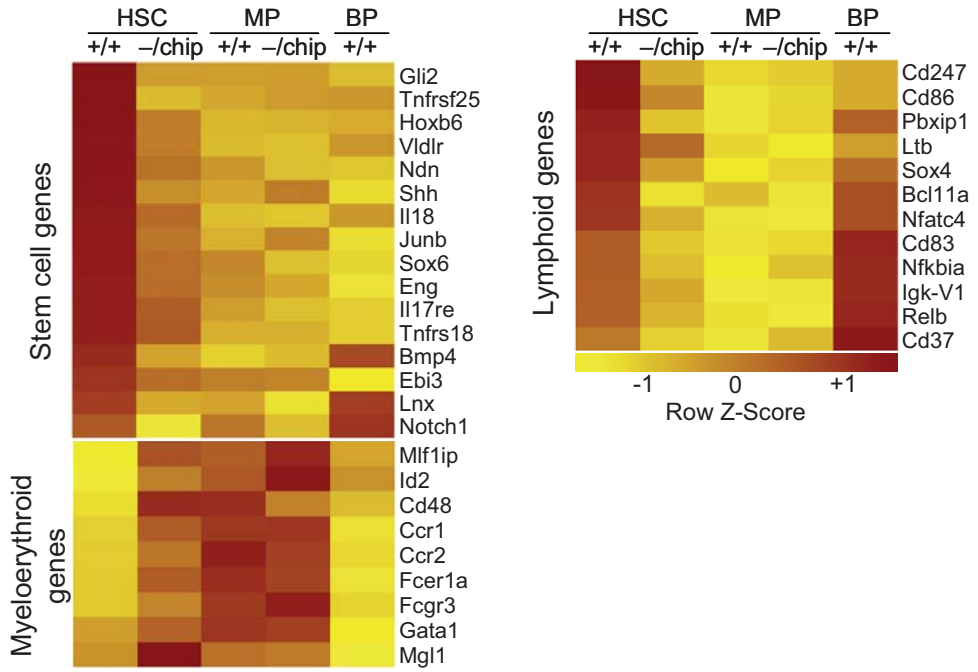

Figure 29: Enhanced expression of myeloerythroid and decreased expression of stemness and lymphoid genes. Expression values of representative genes with known functions in HSCs, myeloerythroid cells or lymphoid cells are shown for the five profiled populations. Bioinformatic analysis was performed in cooperation with M. Huska and M. Andrade-Navarro, Max-Delbrück-Center Berlin, Germany.

Taken together, hypomethylated HSCs show a severely altered gene expression pattern which is similar to a more differentiated myeloerythroid gene expression pattern. This might serve as an explanation for the impaired function of Dnmt1$^{-/chip}$ HSCs.

3.2.10 Validation of the microarray data

Many genes with known functions in myeloerythroid differentiation were among the most highly upregulated genes in Dnmt1$^{-/chip}$ HSCs. These included the potent transcription factors *Gata1, Id2* and *C/ebp*α (Figure 30A and B). Remarkably, *Gata1* was expressed by a greater frequency of Dnmt1$^{-/chip}$ HSCs, as shown by single cell RT PCR (Figure 30C).

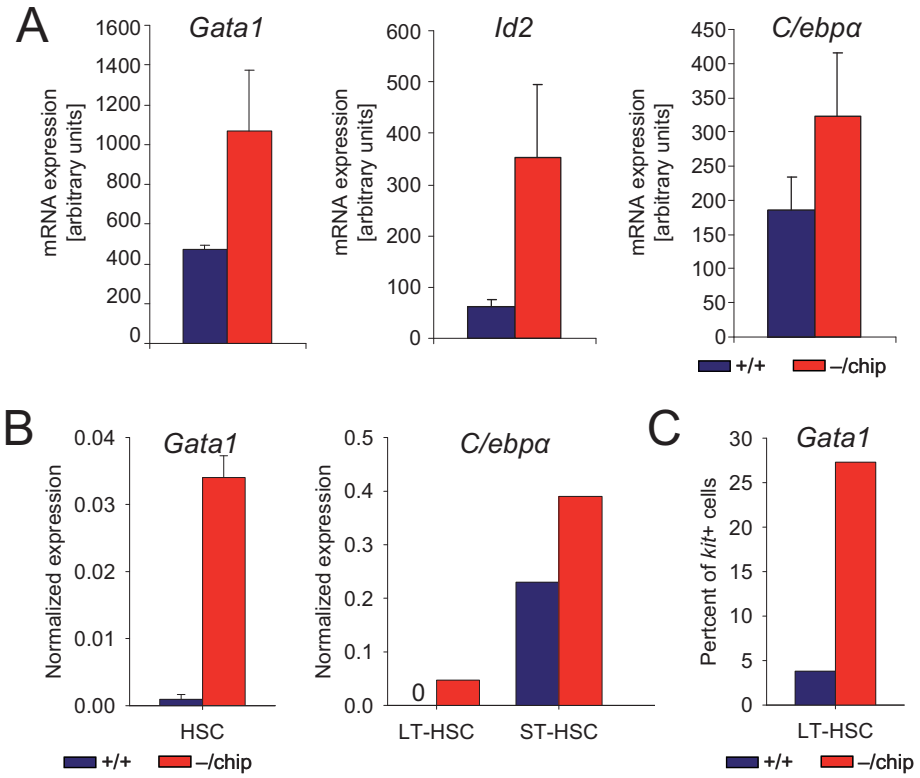

Figure 30: Dnmt1$^{-/chip}$ HSCs show enhanced expression of key myeloerythroid transcription factors. A) mRNA expression of *Gata1, Id2* and *C/ebpα* in HSCs of *Dnmt1*$^{+/+}$ and *Dnmt1*$^{-/chip}$ mice. mRNA levels were measured by Affymetrix arrays and are shown in Affymetrix GeneArray arbitrary units. Bar graphs represent mean values ± s.d. of n=3 for Dnmt1$^{-/chip}$ and n=2 for Dnmt1$^{+/+}$. Data from representative array probes sets are shown (probe ID *Gata1*: 1449232; probe ID *Id2*: 1435176; probe ID *C/ebpα*: 1418982). **B)** Quantitative RT PCR analysis of expression of *Gata1* in HSCs (LSK) and *C/ebpα* in LT-HSCs (LSKCD34$^{-/low}$Flt3^{-}) and ST-HSCs (LSKCD34^{+}Flt3^{-}) from Dnmt1$^{+/+}$ and Dnmt1$^{-/chip}$ mice. Data were normalized to the expression of *Gapdh*. 0 = no detectable expression after 45 cycles of PCR. **C)** Result of single-cell RT PCR for *Gata1* on LT-HSCs from Dnmt1$^{+/+}$ and Dnmt1$^{-/chip}$ mice. Expression of *Kit* served as an internal positive control for the RT-PCR, thus, only cells being *Kit* mRNA positive were further analyzed.

FACS analysis of LT-HSCs was performed to test whether the myeloerythroid lineage identity of mutant HSCs, determined with genome wide mRNA expression profiles, is in consequence leading to an altered protein expression.

Several surface receptors known to be expressed on differentiated cells, but normally not on HSCs, were upregulated in Dnmt1$^{-/chip}$ HSCs. Two of these surface receptors with upregulated mRNA levels were FcγRII/III (Akashi, et al., 2000) and CD48 (Kiel, et al., 2005). FACS analyses of surface expression of these markers are shown in Figure 31. These results demonstrated that both were expressed on Dnmt1$^{-/chip}$ LT-

HSCs at unusually high levels, comparable to that of WT MPs. This experiment confirmed that increased transcription of MP genes also led to an increase in protein expression.

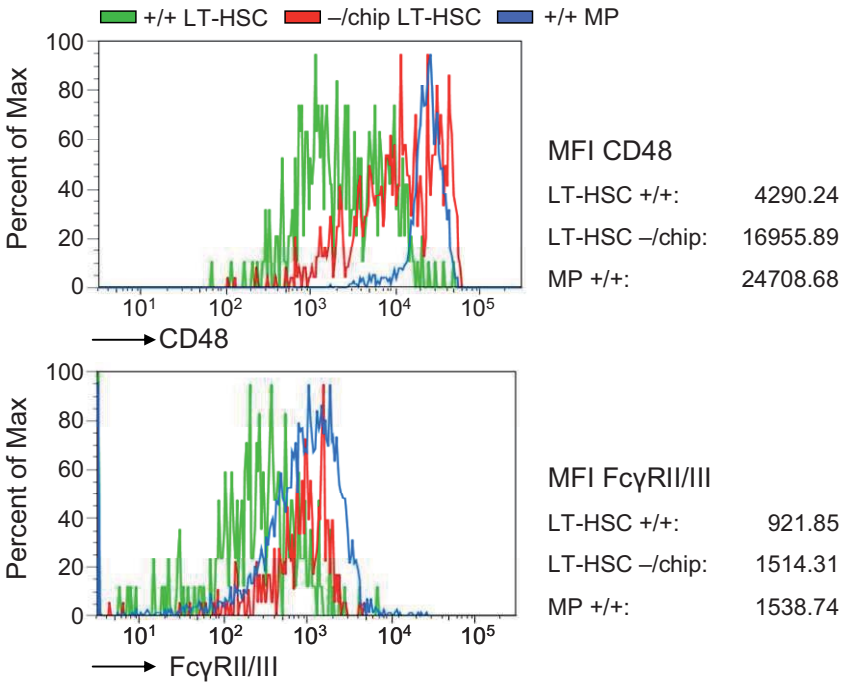

Figure 31: Enhanced expression of myeloerythroid surface markers. Representative FACS plots demonstrate increased surface expression of CD48 and FcγRII/III on LT-HSCs of Dnmt1$^{-/chip}$ mice as compared to their counterparts of Dnmt1$^{+/+}$ mice. MPs of Dnmt1$^{+/+}$ animals served as high expression control. Mean fluorescence intensity (MFI) values are indicated for each sample.

Taken together, these data confirmed the results of the microarray and demonstrate that the diminished stem cell identity could be an explanation for deficiencies in HSC activity, maintenance and lineage commitment in Dnmt1$^{-/chip}$ mice.

3.2.11 Myeloerythroid gene activation in Dnmt1$^{-/chip}$ HSCs by promoter demethylation

To test the relation between gene expression and the CpG methylation status in Dnmt1$^{-/chip}$ HSCs, a MassARRAY was performed. With this method it is feasible to investigate the CpG methylation status within a defined sequence. Thus, promoter sequences of genes deregulated in Dnmt1$^{-/chip}$ HSCs, *Gata1*, *Id2*, *C/EBPα*, and *Cd48*, were analyzed using MassARRAY technology. The MassARRAY was performed in cooperation with Sequenom, Hamburg, Germany. First, the CpG

methylation status in WT HSCs was tested. *Gata1* and *Cd48* promoters showed CpG methylation in WT HSCs, whereas *Id2* and *C/EBPα* showed no CpG methylation at the analyzed regions (data not shown). Second, CpG methylation status was analyzed in HSCs of Dnmt1$^{-/chip}$ mice. Erythrocytes (Ter119) and T cells (CD3) from WT mice were used as control populations which are known to express *Gata1* or *Cd48*. Importantly, methylation of *Gata1* and *Cd48* promoters was reduced in Dnmt1$^{-/chip}$ HSCs compared to Dnmt1$^{+/+}$ HSCs (Figure 32).

This finding demonstrate a direct link between enhanced expression of myeloerythroid genes in Dnmt1$^{-/chip}$ HSCs and their CpG methylation status.

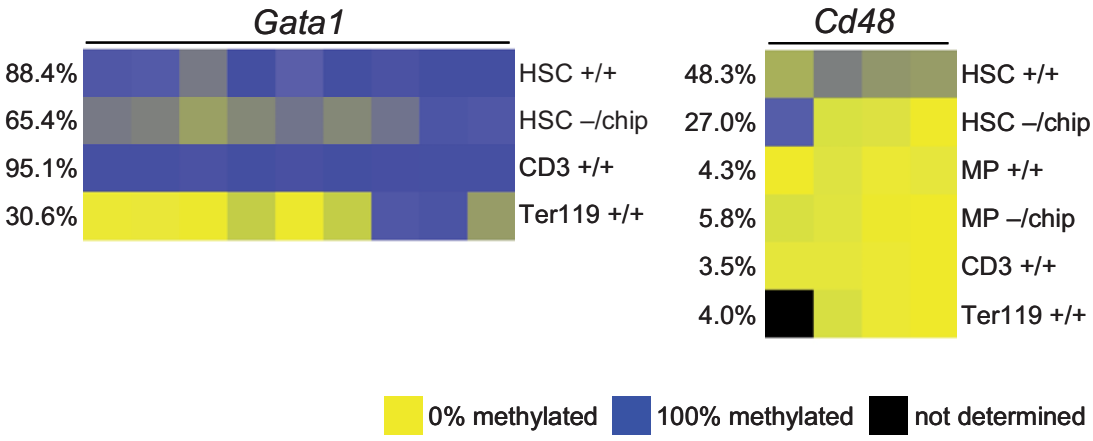

Figure 32: MassARRAY profiles showing methylation statuses of *Gata1* and CD48 promoters in Dnmt1$^{+/+}$ and Dnmt1$^{-/chip}$ HSCs and MPs. Profiles of T cells (CD3^{+}) and erythrocytes (Ter119^{+}) of *Dnmt1*$^{+/+}$ animals are shown for control. Every box illustrates one CpG of the investigated sequence. The percentage of methylated CpGs is indicated. Genomic localizations of the analyzed promoter regions are: *Gata1*: ChrX 7545431-7545769 and ChrX: 7553755-7554238, *Cd48*: Chr1: 173612289-173612577.

3.2.12 Ebf1 expression restores B-cell potential of Dnmt1$^{-/chip}$ HSCs

Dnmt1$^{-/chip}$ HSCs were shown to express myeloerythroid genes to a higher extend than WT HSCs. Some of these factors are known to block lymphoid differentiation by repression of lymphoid genes. For example, C/EBPs were shown to inhibit the B-cell commitment transcription factor Pax5 (Xie, et al., 2004) and GATA1 activity was shown to induce lineage conversion of lymphoid progenitors into the megakaryocyte erythroid lineage (Iwasaki, et al., 2003). Consequently, the defect in lymphoid development might be a direct result of the incompetence of Dnmt1$^{-/chip}$ HSCs to upregulate critical lymphoid genes, owing to their disability to epigenetically silence

predominant myeloerythroid factors. To test this hypothesis, c-Kit enriched BM progenitors of Dnmt1$^{-/chip}$ and WT mice were infected with a retrovirus carrying a potent lymphoid transcription factor, the early B cell factor 1 (EBF1). Subsequently, these cells were cultured on OP9 stroma cells promoting lymphoid cell growth. *Ebf1* was chosen because it is a key transcription factor for early B-cell development (Pongubala, et al., 2008) and was shown to be repressed in Dnmt1$^{-/chip}$ BM precursors (Figure 21). Figure 33A demonstrates that ectopic expression of EBF1 in Dnmt1$^{-/chip}$ progenitor cells was able to generate lymphoid progeny at numbers comparable to that of WT precursors. In contrast, control virus infected Dnmt1$^{-/chip}$ cells were still incompetent of generating B cells. Figure 34B reveals that the B220^{+} cells in Figure 34A also expressed another B cell marker, CD19.

Taken together, the block in lymphoid differentiation in Dnmt1$^{-/chip}$ progenitor cells could be overcome by forced expression of a potent lymphoid transcription factor.

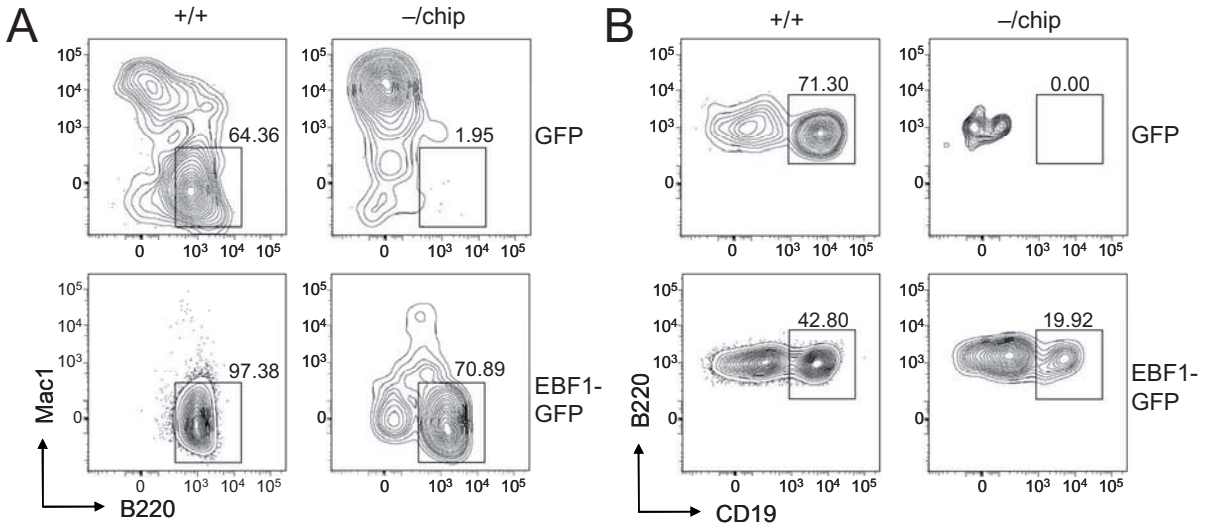

Figure 33: Rescue of Dnmt1$^{-/chip}$ B-cell differentiation by ectopic expression of the early B-cell factor 1 (EBF1). c-Kit^{+} BM cells were purified from Dnmt1$^{+/+}$ and Dnmt1$^{-/chip}$ mice, infected with a MSCV-Ebf1-ires-Gfp or a MSCV-ires-Gfp retrovirus and cultured on OP9 stroma cells in the presence of Il7, Flt3L and SCF. Representative FACS plots show cells after 19 days of co-culture. Gated on **A)** GFP^{+} or **B)** GFP^{+}Mac^{-} cells Numbers indicate frequencies of **A)** GFP^{+}B220^{+}Mac1^{-}or **B)** GFP^{+}B220^{+} CD19^{+}Mac1^{-} B cells. The experiment was performed twice independently.

4 Discussion

One major question was addressed in this thesis. Does loss or reduction of the maintenance DNA methyltransferase 1 (DNMT1) have an impact on HSC homeostasis and differentiation potential in an *in vivo* mouse model? In particular, it was investigated whether and how regulation between "stemness" and differentiation in HSCs is affected by DNA methylation. The results obtained in this study will be discussed in the following sections.

4.1 Role of DNMT1 in preservation of hematopoietic cell hierarchy

4.1.1 DNMT1 is indispensable for cell-autonomous survival of HSCs

Complete abolishment of *Dnmt1* from the hematopoietic system results in a severe crisis of all existing hematopoietic cells. It could be shown that numbers of various mature cell lineages, and therefore also cell numbers of various organs, decline in the short time frame of approximately seven days after *Dnmt1* ablation. Phenotypic analysis and functional assays revealed that HSCs and lymphoid as well as myeloid progenitor cells are missing shortly after *Dnmt1* depletion. In an additional transplantation assay, this effect was shown to be cell intrinsic. In case of a full loss of DNMT1 activity, apoptosis was shown to be the mechanism triggering the death of nearly all hematopoietic cells in the BM.

In a previous work, conditional knockout of *Dnmt1* in a human cancer cell line was shown to cause checkpoint defects, massive DNA damage and chromosomal instability (Chen, et al., 2007). Chen et al. suggested that increased levels of hemimethylated DNA may be recognized by the cell as a damage which initiates an apoptosis response. It can be hypothesized that severe demethylation in the $Dnmt1^{\Delta/\Delta}$ mouse model also leads to the rapid depletion of hematopoietic stem and progenitor cells and thus, severely damaged cells are prevented from staying alive.

A recent analysis of HSCs depleted of *Dnmt3a* and *3b* demonstrated that *de novo* methylation is needed for self-renewal but not for differentiation of blood cell lineages (Tadokoro, et al., 2007). In contrast to the *Dnmt3a* and *3b* knockout, the pre-existing

methylation pattern achieved by *Dnmt1* appeared crucial for both, self-renewal and differentiation. Comparison of these results suggested that *de novo* methylation might represent a fail-safe mechanism to replace lost methylation marks during HSC renewal. Additionally, these data manifest individual roles for *de novo* and maintenance DNA methylation processes in self-renewal and differentiation capacities of HSCs. Furthermore, this demonstrated that these two enzymes, DNMT1 and DNMT3, perform non-redundant functions in maintaining CpG methylation in HSCs as it was hypothesized earlier (Rhee, et al., 2002).
Taken together, DNMT1 was shown for the first time to be absolutely indispensable for cell-autonomous survival of HSCs.

4.1.2 The HSC self-renewal program requires constitutive DNA methylation

Analysis of the stem cell compartment of mice with reduced *Dnmt1* expression revealed an enlarged phenotypic LT-HSC compartment. Additionally, the absence of the earliest progenitor population with evident lymphoid transcriptional priming, the LMPP, was observed. Since these observations rely on phenotypic analysis of surface marker expression, appropriate functional assays were performed subsequently. Thus, long-term repopulation assays were utilized and analysis was performed 12 to 16 weeks after transplantation to ensure measuring stem cell potential instead of progenitor potential. A competitive repopulation assay was performed to measure the functional potential of the mutant HSCs against WT HSCs. With this experiment, qualitative information about the repopulation capacity of HSCs compared to the competing BM were obtained, but no distinction between the number of HSCs or their quality could be made (Purton and Scadden, 2007). For this reason, the most stringent test for HSC potential was applied by performing a serial transplantation assay. This assay provides information about the most immature HSC which is capable of sustaining hematopoiesis throughout serial transplantation (Lemischka, et al., 1986). Additionally, a short-term engraftment assay was performed to investigate the capacity of HSCs to home towards the stem cell niche located in the BM (Adams and Scadden, 2006). Remarkably, *Dnmt1* hypomorphic HSCs demonstrated surprisingly specific defects. While they showed normal homing capacity, their repopulation potential was severely impaired under transplantation-induced proliferation stress in competitive as well as in serial transplantation assays.

Under steady state conditions, implying that *Dnmt1* was depleted after transplantation and repopulation, HSCs were diminished after a time period of 16 weeks. Hence, hypomethylation led to an intrinsic repopulation deficiency of HSCs caused by a proliferation stress-independent decrease in self-renewal potential. Together, these results revealed that the self-renewal program of HSCs requires constitutive maintenance of a critical threshold of DNA methylation.

As discussed earlier, HSCs devoid of DNMT1 activity underwent rapid apoptosis. This was fully blocked by reintroduction of the hypomorphic $Dnmt1^{chip}$ allele. No enhanced apoptosis was observed in the compartment of HSCs in the *Dnmt1* hypomorph mice. Also, transgenic introduction of the anti-apoptotic gene *bcl2* which protects HSCs from many apoptotic stimuli (Domen and Weissman, 2000), was not able to rescue the phenotypic change in the HSC compartment, demonstrating that other mechanisms than apoptosis must be responsible for the HSC defect.

A steady state analysis of the cell cycle status demonstrated that *Dnmt1* hypomorphic HSCs do not contain a higher proportion of cycling cells, suggesting that exhaustion of HSCs can not be an explanation for their impaired self-renewal capacity.

4.1.3 DNA methylation governs myeloerythroid versus lymphoid cell fate

Since the earliest lymphoid primed progenitor, the LMPP, is phenotypically absent in the HSC compartment of mice with reduced *Dnmt1* expression, it was a crucial aim to investigate whether *Dnmt1* hypomorph HSCs are competent of giving rise to lymphoid lineages.

LMPPs are characterized by the expression of the surface marker Flt3 (Adolfsson, et al., 2005). Flt3 surface marker expression was shown to be lost in *Dnmt1* hypomorphic mice, but normal mRNA levels of *Flt3* were detected in *Dnmt1* hypomorphic LT- and ST-HSCs. This result indicated a comprehensive loss of lymphoid lineage potential but not loss of a phenotypic lineage marker only. Additionally, results from functional experiments, discussed in the following part, revealed a clear defect in lymphoid cell development.

$Dnmt1^{-/chip}$ HSCs were competent to form myeloid and erythroid progeny but they were severely impaired to commit to lymphoid differentiation in *in vitro* and *in vivo* assays. Mature B cells as well as T-cell and B-cell progenitors were diminished in

Dnmt1$^{-/chip}$ animals. Transplantation experiments showed that the impairment of Dnmt1$^{-/chip}$ cells to establish lymphoid cell types is a cell intrinsic defect. In single cell *in vitro* assays, this was validated to be in particular a defect of LT- and ST-HSCs. Again, transgenic introduction of the anti-apoptotic gene *bcl2* was not able to reverse this effect, indicating a developmental effect rather than programmed cell death of established lymphoid cells. Knockdown of *Dnmt1* in a fully established adult hematopoietic system with the help of the conditional *Dnmt1* knockout allele resulted in a similar phenotype, supporting the idea that especially the lymphoid lineage needs a higher threshold of DNMT1 activity.

Together, these observations demonstrated that methylation-dependent control mechanisms differentially regulate myeloerythroid versus lymphoid lineage choice, thus, uncovering a previously unrecognized gradual DNA methylation sensitivity of opposing lineage programs.

Accumulating evidence indicates that chromatin remodeling mediated by DNA methylation and demethylation plays an important role in regulating the immunoglobulin gene segment rearrangement as achieved by recombinases. DNA methylation is involved in recruitment of chromatin-modifying complexes followed by changes in the chromatin structure which influences recombinase accessibility (Schlissel, 2004) (Inlay and Xu, 2003). Strikingly, conditional induction of DNA hypomethylation in CD19 expressing B-cell progenitors led to normal numbers of mature B cells. This result demonstrated that a high methylation threshold is required for lymphoid commitment in HSCs, yet a lower threshold is sufficient to maintain the lymphoid program once it has been established in progenitors. Dnmt1$^{-/chip}$ mice already lacked the earliest lymphoid progenitor state with no reported immunoglobulin rearrangement (LMPP) (Adolfsson, et al., 2005) (Janeway, 2001). This finding revealed that DNA hypomethylation blocked lymphoid lineage choice before lymphoid transcriptional priming was initiated. Hence, a failure in immunoglobulin locus rearrangement can not be the cause for the defect in lymphoid lineage development in Dnmt1$^{-/chip}$ mice.

Together, these data strongly argue for a fundamental difference in the role of DNA methylation in HSCs and lineage specific progenitors.

4.1.4 DNA hypomethylation causes derepression of myeloerythroid genes

To address the question of how DNA methylation is capable of preserving HSC functions and which underlying mechanisms are triggered upon loss or reduction of DNA methylation in the hematopoietic system, whole genome RNA expression arrays of HSCs and myeloid progenitors (MPs) were utilized. Data generated here revealed that DNA hypomethylation caused wide-spread transcriptional deregulation in HSCs. In sharp contrast, transcription was only mildly disturbed in MPs, supporting the idea that methylation is most relevant at the stem cell level and loses importance after lineage commitment.

The expression profiles of the four populations, WT and DNA hypomethylated HSCs and MPs, demonstrated that hypomethylated HSCs depict a striking drift towards the WT MPs. In a dendrogram, picturing the genetic relations between these populations, hypomethylated HSCs are clustering more closely with WT and mutant MPs than with WT HSCs. Additionally, a principal components analysis, depicting the transcriptional distance between the different populations in a 2D manner, demonstrated that hypomethylated HSCs were located between WT MPs and HSCs. To investigate whether this was a true shift in direction towards the WT MP expression profile or displacement from WT HSCs, signatures specific for each cell population were designed.

The majority of genes of a myeloerythroid gene signature (normally highly expressed by WT MPs and not by HSCs) was upregulated in Dnmt1$^{-/chip}$ HSCs, whereas stem cell signature genes (highly expressed by WT HSCs and not by MPs) were mostly downregulated. This result illustrated that the genetic identity of hypomethylated HSCs moved away from the stem cell identity towards a myeloerythroid identity.

Hand picked lists of genes with known functions in lymphoid, myeloerythroid or stem cell differentiation and their differential expression in the mutant cell populations revealed that DNA hypomethylation induced transcriptional changes were surprisingly specific. For example, Dnmt1$^{-/chip}$ HSCs demonstrated an increase in the expression of many myeloerythroid genes, including the transcription factors *Gata1*, *Id2* and *C/ebp*α, but a decrease in the expression of “stemness” and lymphoid genes. Protein expression of the myeloerythroid surface markers CD48 and FcγR was increased on Dnmt1$^{-/chip}$ HSCs confirming the microarray data. However, the stem

cell antigen CD150 was still expressed at a high level on Dnmt1$^{-/chip}$ HSCs indicating that the investigated cells were phenotypically true stem cells and not progenitors. Moreover, other differentiation markers such as CD34, IL7Rα and Flt3 were not upregulated, demonstrating a specific deregulation of myeloerythroid factors.

Taken together, the global reduction of DNA methylation levels in HSCs led to a systemic upregulation of myeloerythroid related genes.

Assessment of DNA methylation of *Gata1* and *Cd48*, which were upregulated in Dnmt1$^{-/chip}$ HSCs, revealed that promoter regions of these two genes were strongly methylated in normal HSCs. Interestingly these sequences showed reduced CpG methylation in Dnmt1$^{-/chip}$ HSCs. No promoter methylation was detected in case of two other up-regulated genes, *Id2* and *C/ebpα*. Nevertheless, it is possible that these genes were activated by demethylation of more distally located regulatory elements which were not investigated here. Both, *Id2* and *C/ebpα* were identified to be silenced by methylation in cancer cells earlier, supporting the idea that their expression is controlled by methylation-dependent mechanisms (Flotho, et al., 2009) (Ehlers, et al., 2008) (Hackanson, et al., 2008).

Data on the CpG methylation status of myeloerythroid genes and the associated expression data suggested a role for DNA methylation in repression of myeloerythroid genes in HSCs to preserve “stemness” and to allow lymphoid differentiation upon its initiation. Consequently, reduction of the global DNA methylation status entailed a differentiation stimulus towards myeloerythroid cell fate, a block of lymphoid differentiation and a reduction of HSC potential. Intriguingly, forced expression of a critical transcription factor for early B-cell development, EBF1, restored the potential of Dnmt1$^{-/chip}$ HSCs to differentiate into B cells. EBF1 was previously shown to be transcriptionally repressed by GATA1 and C/EBPα (Iwasaki, et al., 2003) (Xie, et al., 2004). Moreover, *Ebf1* was shown to be repressed in Dnmt1$^{-/chip}$ BM precursors. Hence, expression of one critical lymphoid transcription factor was able to overcome the block in B-cell development in Dnmt1$^{-/chip}$ HSCs. This result demonstrated for the first time that DNA hypomethylated HSCs are blocked to switch on critical lymphoid genes which is caused by the failure of silencing myeloerythroid genes through DNA methylation.

In summary, these data provide a molecular explanation for the narrowed functional repertoire of Dnmt1$^{-/chip}$ HSCs.

4.2 Relevance and implications

Recent data suggested that the transition of stem cells from self-renewal to differentiation is accompanied by extensive changes in their methylation pattern (Bibikova, et al., 2008) (Meissner, et al., 2008). However, this observation leaves the important issue unanswered whether changes in methylation are of causal relevance for changes in stem cell fate. This question was addressed in this thesis by using the hematopoietic system which provides a valuable model for understanding how genetic programs are established to decide cell fates in multipotent stem cells. Here, it was demonstrated that alternative functional stem cell programs require distinct threshold levels of DNA methylation as summarized and illustrated in Figure 34.

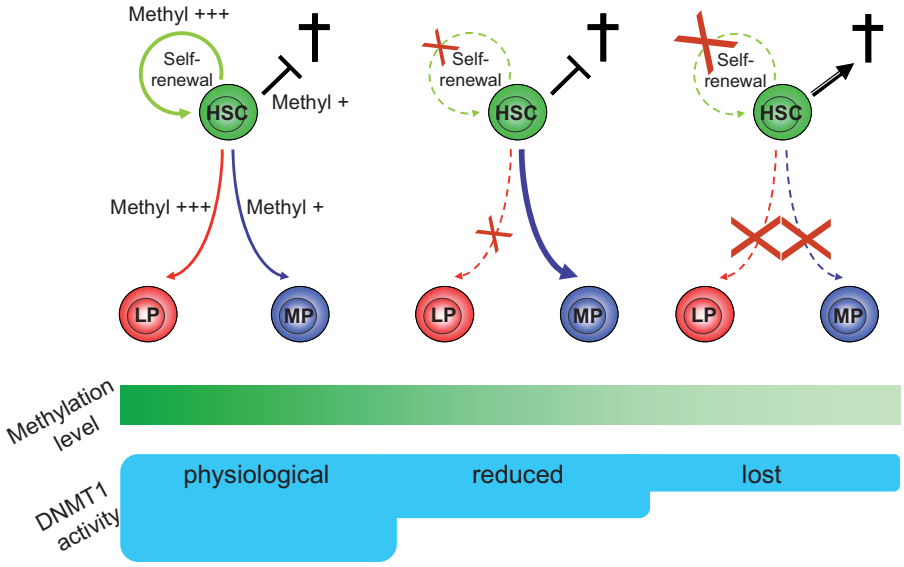

Figure 34: Hematopoietic stem cell fate is regulated through DNA methylation levels. Schematic summary of results obtained in this thesis. LP, lymphoid progenitor, MP, myeloid progenitor, HSC, hematopoietic stem cell, Methyl +++, high methylation level required; Methyl +, low methylation level required, †, apoptosis.

In previous studies, it was suggested that stem cells exhibit a more “open” chromatin state. An “open” chromatin state would provide accessibility for transcription factors at multiple loci at the DNA. Consequently, this should allow enhanced flexibility in cell fate commitments at a multipotent developmental stage (Akashi, 2005). Although there is a strong correlation between “open” chromatin and the undifferentiated state of stem cells, it remains unknown whether “open” chromatin is necessary for stem cell potential. Recently, it has been shown that the chromatin remodeller Chd1

(chromodomain helicase DNA-binding protein) is indeed an essential regulator of "open" chromatin and of pluripotency of ES cells (Gaspar-Maia, et al., 2009). Furthermore, ES cells lacking epigenetic regulators like EZH2 (enhancer of zeste homolog 2, a part of the polycomb repressor complex) were found to be delayed in differentiation because they fail to shut down pluripotency factors such as *Nanog* or *Oct4* through chromatin remodelling (Shen, et al., 2008). On the contrary, data presented in this thesis encourages an additional aspect of correlation between DNA methylation and multipotency in the model system of HSCs. In fact, data presented here, indicate that HSCs need a distinct level of DNA methylation to suppress factors driving differentiation in order to preserve their multipotent state. These results characterize the multipotent state as actively controlled through DNA methylation, contradicting the view of a more "open" chromatin state as prerequisite for multipotency. Based on these findings, the role and function of DNA methylation, as introduced in chapter 1.2.1.1, can be added with a superoridinated function in controlling cell fate decisions and lineage programs in HSCs.

Additionally, the possibility that DNA methylation might have been relevant for evolution of the immune system is encouraged. A previous study already revealed the myeloid gene expression program as a default pathway and showed that lymphoid commitment requires activation of additional sets of genes (Miyamoto, et al., 2002). These results were in line with reports showing that the first hematopoietic cells, arising during embryonic development, are competent to produce primitive erythroid cells as well as macrophages but appear to be devoid of lymphoid cell-forming potential (Cumano and Godin, 2001). Also, macrophage-erythroid-like cells precede lymphoid cell formation during evolution (Hansen and Zapata, 1998). Taken together, DNA methylation might have been utilized through evolution to suppress the default myeloerythroid differentiation pathway to allow for the newly acquired lymphoid function to evolve.

4.3 Perspective

Data presented in this thesis provides evidence that DNA methylation represents an epigenetic mechanism for preservation of "stemness" in HSCs. One crucial remaining question is how DNA methylation at key myeloerythroid genes is controlled to avoid loss of "stemness" and simultaneously enable a myeloerythroid lineage decision?

Further insights into the network of epigenetic gene expression control would help to answer this question. For this approach, it would be of importance to compare the existing genome-wide RNA expression data with a genome-wide CpG methylation pattern. To achieve this, an unbiased approach could be applied by methylated DNA immunoprecipitation (MeDIP) combined with a large scale analysis using microarrays (Mohn, et al., 2009). Importantly, previous studies showed that regulatory gene elements must not only be limited to the gene promoter, but can be located several kb upsteam or downstream, e.g. as demonstrated for the beta-globin locus (Grosveld, et al., 1987). Thus, not only promoter regions must be analyzed in terms of CpG methylation to draw conclusions of gene activity, but also relevant sequences in the periphery. With the two sets of data, global RNA expression profile and global CpG methylation pattern, the network of epigenetically regulated factors could be understood.

Further on, it would be of importance to verify the direct effect of CpG methylation on gene activity. Klug et. al. reported a useful tool to test for the regulatory impact of CpG methylation on adjacent genes (Klug and Rehli, 2006). In this method *in vitro* DNA methylation and a successive luciferase assay is used to investigate the effect of CpG methylation at specific sequences on gene activity. This approach enables to verify the impact of CpG methylation at regulatory sites of myeloerythroid transcription factors. Findings from such experiments would also strengthen the statement that genes, e.g. *Gata1* or *Cd48*, are upregulated in Dnmt1$^{-/chip}$ HSCs as a result of decreased DNMT1 activity.

Additionally, investigations of how DNA demethylation of myeloerythroid key factors is achieved and controlled during development are of great interest. Is demethylation achieved through a passive mechanism during cell division or through an active enzyme-mediated demethylation process? Uncovering the process of demethylation and subsequent upregulation of key myeloerythroid factors during lineage decisions in the HSC would be of great interest. These new insights would also help to understand of how CpG methylation is controlled specifically.

Finally, since epigenetic changes are a hallmark of cancer, the influence of DNA methylation changes on cancer cells is of crucial interest. Epigenetically induced chromatin changes are reversible throughout life. This provides the opportunity to change the state of a cell whenever it is needed. Especially in cancer, DNA

methylation changes are commonly observed contributing to reprogramming events often associated with a regain of “stemness” and uncontrolled growth of cells (Krivtsov, et al., 2006). It must be a substancial aim for further investigations to understand the function of DNA methylation in cancer formation and progression. Since demethylating agents are already used in cancer therapy, the detailed understanding of reduction of DNA methylation on “stemness” might help to improve the effect of demethylating drugs.

4.4 Concluding remarks

Data presented here, demonstrates an indispensable role for DNMT1 catalyzed DNA methylation in hematopoietic stem cell homeostasis and differentiation. Furthermore, data revealed that DNA methylation actively preserves hematopoietic stem cell multipotency. This thesis provides the first evidence for a tight correlation between loss of DNA methylation and subsequent loss of multipotency of hematopoietic stem cells.

However, a number of important questions remain unresolved. The probably most intriguing being whether the same mechanisms could be transferred to leukaemic stem cells, which are characterized by similar abilities as normal hematopoietic stem cells. It would be of particular interest whether the leukaemic stem cell could also be targeted through reduced DNA methylation, which was not shown so far. This will be the main focus of future investigations.

Bibliography

Adams, G. B. and Scadden, D. T. (2006): The hematopoietic stem cell in its place, Nat Immunol (vol. 7), No. 4, pp. 333-7.

Adolfsson, J.; Mansson, R.; Buza-Vidas, N.; Hultquist, A.; Liuba, K.; Jensen, C. T.; Bryder, D.; Yang, L.; Borge, O. J.; Thoren, L. A.; Anderson, K.; Sitnicka, E.; Sasaki, Y.; Sigvardsson, M. and Jacobsen, S. E. (2005): Identification of Flt3+ lympho-myeloid stem cells lacking erythro-megakaryocytic potential a revised road map for adult blood lineage commitment, Cell (vol. 121), No. 2, pp. 295-306.

Akashi, K. (2005): Lineage promiscuity and plasticity in hematopoietic development, Ann N Y Acad Sci (vol. 1044), pp. 125-31.

Akashi, K.; Traver, D.; Kondo, M. and Weissman, I. L. (1999): Lymphoid development from hematopoietic stem cells, Int J Hematol (vol. 69), No. 4, pp. 217-26.

Akashi, K.; Traver, D.; Miyamoto, T. and Weissman, I. L. (2000): A clonogenic common myeloid progenitor that gives rise to all myeloid lineages, Nature (vol. 404), No. 6774, pp. 193-7.

Amir, R. E.; Van den Veyver, I. B.; Wan, M.; Tran, C. Q.; Francke, U. and Zoghbi, H. Y. (1999): Rett syndrome is caused by mutations in X-linked MECP2, encoding methyl-CpG-binding protein 2, Nat Genet (vol. 23), No. 2, pp. 185-8.

Attema, J. L.; Papathanasiou, P.; Forsberg, E. C.; Xu, J.; Smale, S. T. and Weissman, I. L. (2007): Epigenetic characterization of hematopoietic stem cell differentiation using miniChIP and bisulfite sequencing analysis, Proc Natl Acad Sci U S A (vol. 104), No. 30, pp. 12371-6.

Barreto, G.; Schafer, A.; Marhold, J.; Stach, D.; Swaminathan, S. K.; Handa, V.; Doderlein, G.; Maltry, N.; Wu, W.; Lyko, F. and Niehrs, C. (2007): Gadd45a promotes epigenetic gene activation by repair-mediated DNA demethylation, Nature (vol. 445), No. 7128, pp. 671-5.

Bednarik, D. P.; Duckett, C.; Kim, S. U.; Perez, V. L.; Griffis, K.; Guenthner, P. C. and Folks, T. M. (1991): DNA CpG methylation inhibits binding of NF-kappa B proteins to the HIV-1 long terminal repeat cognate DNA motifs, New Biol (vol. 3), No. 10, pp. 969-76.

Benjamini, Yoav and Hochberg, Yosef (1995): Controlling the False Discovery Rate: A Practical and Powerful Approach to Multiple Testing, Journal of the Royal Statistical Society. Series B (Methodological) (vol. 57), pp. 289-300.

Bennett, K. L.; Hackanson, B.; Smith, L. T.; Morrison, C. D.; Lang, J. C.; Schuller, D. E.; Weber, F.; Eng, C. and Plass, C. (2007): Tumor suppressor activity of CCAAT/enhancer binding protein alpha is epigenetically down-regulated in head and neck squamous cell carcinoma, Cancer Res (vol. 67), No. 10, pp. 4657-64.

Bestor, T. H. (1988): Cloning of a mammalian DNA methyltransferase, Gene (vol. 74), No. 1, pp. 9-12.

Bhattacharya, S. K.; Ramchandani, S.; Cervoni, N. and Szyf, M. (1999): A mammalian protein with specific demethylase activity for mCpG DNA, Nature (vol. 397), No. 6720, pp. 579-83.

Bian, Y.; Alberio, R.; Allegrucci, C.; Campbell, K. H. and Johnson, A. D. (2009): Epigenetic marks in somatic chromatin are remodelled to resemble pluripotent nuclei by amphibian oocyte extracts, Epigenetics (vol. 4), No. 3, pp. 194-202.

Bibikova, M.; Laurent, L. C.; Ren, B.; Loring, J. F. and Fan, J. B. (2008): Unraveling epigenetic regulation in embryonic stem cells, Cell Stem Cell (vol. 2), No. 2, pp. 123-34.

Biniszkiewicz, D.; Gribnau, J.; Ramsahoye, B.; Gaudet, F.; Eggan, K.; Humpherys, D.; Mastrangelo, M. A.; Jun, Z.; Walter, J. and Jaenisch, R. (2002): Dnmt1 overexpression causes genomic hypermethylation, loss of imprinting, and embryonic lethality, Mol Cell Biol (vol. 22), No. 7, pp. 2124-35.

Bonifer, C.; Lefevre, P. and Tagoh, H. (2006): The regulation of chromatin and DNA-methylation patterns in blood cell development, Curr Top Microbiol Immunol (vol. 310), pp. 1-12.

Bourc'his, D.; Xu, G. L.; Lin, C. S.; Bollman, B. and Bestor, T. H. (2001): Dnmt3L and the establishment of maternal genomic imprints, Science (vol. 294), No. 5551, pp. 2536-9.

Busslinger, M. (2004): Transcriptional control of early B cell development, Annu Rev Immunol (vol. 22), pp. 55-79.

Chen, T.; Hevi, S.; Gay, F.; Tsujimoto, N.; He, T.; Zhang, B.; Ueda, Y. and Li, E. (2007): Complete inactivation of DNMT1 leads to mitotic catastrophe in human cancer cells, Nat Genet (vol. 39), No. 3, pp. 391-6.

Chen, X.; Liu, W.; Ambrosino, C.; Ruocco, M. R.; Poli, V.; Romani, L.; Quinto, I.; Barbieri, S.; Holmes, K. L.; Venuta, S. and Scala, G. (1997): Impaired generation of bone marrow B lymphocytes in mice deficient in C/EBPbeta, Blood (vol. 90), No. 1, pp. 156-64.

Cheshier, S. H.; Morrison, S. J.; Liao, X. and Weissman, I. L. (1999): In vivo proliferation and cell cycle kinetics of long-term self-renewing hematopoietic stem cells, Proc Natl Acad Sci U S A (vol. 96), No. 6, pp. 3120-5.

Cho, S. K.; Webber, T. D.; Carlyle, J. R.; Nakano, T.; Lewis, S. M. and Zuniga-Pflucker, J. C. (1999): Functional characterization of B lymphocytes generated in vitro from embryonic stem cells, Proc Natl Acad Sci U S A (vol. 96), No. 17, pp. 9797-802.

Chuang, L. S.; Ian, H. I.; Koh, T. W.; Ng, H. H.; Xu, G. and Li, B. F. (1997): Human DNA-(cytosine-5) methyltransferase-PCNA complex as a target for p21WAF1, Science (vol. 277), No. 5334, pp. 1996-2000.

Comb, M. and Goodman, H. M. (1990): CpG methylation inhibits proenkephalin gene expression and binding of the transcription factor AP-2, Nucleic Acids Res (vol. 18), No. 13, pp. 3975-82.

Congdon, K. L. and Reya, T. (2008): Divide and conquer: how asymmetric division shapes cell fate in the hematopoietic system, Curr Opin Immunol (vol. 20), No. 3, pp. 302-7.

Cooke, M. S.; Evans, M. D.; Dizdaroglu, M. and Lunec, J. (2003): Oxidative DNA damage: mechanisms, mutation, and disease, Faseb J (vol. 17), No. 10, pp. 1195-214.

Cumano, A. and Godin, I. (2001): Pluripotent hematopoietic stem cell development during embryogenesis, Curr Opin Immunol (vol. 13), No. 2, pp. 166-71.

de Pooter, R. F.; Schmitt, T. M.; de la Pompa, J. L.; Fujiwara, Y.; Orkin, S. H. and Zuniga-Pflucker, J. C. (2006): Notch signaling requires GATA-2 to inhibit myelopoiesis from embryonic stem cells and primary hemopoietic progenitors, J Immunol (vol. 176), No. 9, pp. 5267-75.

Decker, T.; Pasca di Magliano, M.; McManus, S.; Sun, Q.; Bonifer, C.; Tagoh, H. and Busslinger, M. (2009): Stepwise activation of enhancer and promoter regions of the B cell commitment gene Pax5 in early lymphopoiesis, Immunity (vol. 30), No. 4, pp. 508-20.

Dick, J. E.; Magli, M. C.; Huszar, D.; Phillips, R. A. and Bernstein, A. (1985): Introduction of a selectable gene into primitive stem cells capable of long-term reconstitution of the hemopoietic system of W/Wv mice, Cell (vol. 42), No. 1, pp. 71-9.

Domen, J.; Gandy, K. L. and Weissman, I. L. (1998): Systemic overexpression of BCL-2 in the hematopoietic system protects transgenic mice from the consequences of lethal irradiation, Blood (vol. 91), No. 7, pp. 2272-82.

Domen, J. and Weissman, I. L. (2000): Hematopoietic stem cells need two signals to prevent apoptosis; BCL-2 can provide one of these, Kitl/c-Kit signaling the other, J Exp Med (vol. 192), No. 12, pp. 1707-18.

Ehlers, A.; Oker, E.; Bentink, S.; Lenze, D.; Stein, H. and Hummel, M. (2008): Histone acetylation and DNA demethylation of B cells result in a Hodgkin-like phenotype, Leukemia (vol. 22), No. 4, pp. 835-41.

Ehrich, M.; Nelson, M. R.; Stanssens, P.; Zabeau, M.; Liloglou, T.; Xinarianos, G.; Cantor, C. R.; Field, J. K. and van den Boom, D. (2005): Quantitative high-throughput analysis of DNA methylation patterns by base-specific cleavage and mass spectrometry, Proc Natl Acad Sci U S A (vol. 102), No. 44, pp. 15785-90.

Fan, G.; Beard, C.; Chen, R. Z.; Csankovszki, G.; Sun, Y.; Siniaia, M.; Biniszkiewicz, D.; Bates, B.; Lee, P. P.; Kuhn, R.; Trumpp, A.; Poon, C.; Wilson, C. B. and Jaenisch, R. (2001): DNA hypomethylation perturbs the function and survival of CNS neurons in postnatal animals, J Neurosci (vol. 21), No. 3, pp. 788-97.

Farthing, C. R.; Ficz, G.; Ng, R. K.; Chan, C. F.; Andrews, S.; Dean, W.; Hemberger, M. and Reik, W. (2008): Global mapping of DNA methylation in mouse promoters reveals epigenetic reprogramming of pluripotency genes, PLoS Genet (vol. 4), No. 6, p. e1000116.

Feldman, N.; Gerson, A.; Fang, J.; Li, E.; Zhang, Y.; Shinkai, Y.; Cedar, H. and Bergman, Y. (2006): G9a-mediated irreversible epigenetic inactivation of Oct-3/4 during early embryogenesis, Nat Cell Biol (vol. 8), No. 2, pp. 188-94.

Flotho, C.; Claus, R.; Batz, C.; Schneider, M.; Sandrock, I.; Ihde, S.; Plass, C.; Niemeyer, C. M. and Lubbert, M. (2009): The DNA methyltransferase inhibitors azacitidine, decitabine and zebularine exert differential effects on cancer gene expression in acute myeloid leukemia cells, Leukemia (vol. 23), No. 6, pp. 1019-28.

Fujiwara, Y.; Browne, C. P.; Cunniff, K.; Goff, S. C. and Orkin, S. H. (1996): Arrested development of embryonic red cell precursors in mouse embryos lacking transcription factor GATA-1, Proc Natl Acad Sci U S A (vol. 93), No. 22, pp. 12355-8.

Gaspar-Maia, A.; Alajem, A.; Polesso, F.; Sridharan, R.; Mason, M. J.; Heidersbach, A.; Ramalho-Santos, J.; McManus, M. T.; Plath, K.; Meshorer, E. and Ramalho-Santos, M. (2009): Chd1 regulates open chromatin and pluripotency of embryonic stem cells, Nature.

Gaudet, F.; Hodgson, J. G.; Eden, A.; Jackson-Grusby, L.; Dausman, J.; Gray, J. W.; Leonhardt, H. and Jaenisch, R. (2003): Induction of tumors in mice by genomic hypomethylation, Science (vol. 300), No. 5618, pp. 489-92.

Gaudet, F.; Rideout, W. M., 3rd; Meissner, A.; Dausman, J.; Leonhardt, H. and Jaenisch, R. (2004): Dnmt1 expression in pre- and postimplantation embryogenesis and the maintenance of IAP silencing, Mol Cell Biol (vol. 24), No. 4, pp. 1640-8.

Gehring, M.; Reik, W. and Henikoff, S. (2009): DNA demethylation by DNA repair, Trends Genet (vol. 25), No. 2, pp. 82-90.

Goll, M. G. and Bestor, T. H. (2005): Eukaryotic cytosine methyltransferases, Annu Rev Biochem (vol. 74), pp. 481-514.

Goll, M. G.; Kirpekar, F.; Maggert, K. A.; Yoder, J. A.; Hsieh, C. L.; Zhang, X.; Golic, K. G.; Jacobsen, S. E. and Bestor, T. H. (2006): Methylation of tRNAAsp by the DNA methyltransferase homolog Dnmt2, Science (vol. 311), No. 5759, pp. 395-8.

Golshani, P.; Hutnick, L.; Schweizer, F. and Fan, G. (2005): Conditional Dnmt1 deletion in dorsal forebrain disrupts development of somatosensory barrel cortex and thalamocortical long-term potentiation, Thalamus Relat Syst (vol. 3), No. 3, pp. 227-233.

Goto, K.; Numata, M.; Komura, J. I.; Ono, T.; Bestor, T. H. and Kondo, H. (1994): Expression of DNA methyltransferase gene in mature and immature neurons as well as proliferating cells in mice, Differentiation (vol. 56), No. 1-2, pp. 39-44.

Grosveld, F.; van Assendelft, G. B.; Greaves, D. R. and Kollias, G. (1987): Position-independent, high-level expression of the human beta-globin gene in transgenic mice, Cell (vol. 51), No. 6, pp. 975-85.

Gruenbaum, Y.; Cedar, H. and Razin, A. (1982): Substrate and sequence specificity of a eukaryotic DNA methylase, Nature (vol. 295), No. 5850, pp. 620-2.

Hackanson, B.; Bennett, K. L.; Brena, R. M.; Jiang, J.; Claus, R.; Chen, S. S.; Blagitko-Dorfs, N.; Maharry, K.; Whitman, S. P.; Schmittgen, T. D.; Lubbert, M.; Marcucci, G.; Bloomfield, C. D. and Plass, C. (2008): Epigenetic modification of CCAAT/enhancer binding protein alpha expression in acute myeloid leukemia, Cancer Res (vol. 68), No. 9, pp. 3142-51.

Hacker, C.; Kirsch, R. D.; Ju, X. S.; Hieronymus, T.; Gust, T. C.; Kuhl, C.; Jorgas, T.; Kurz, S. M.; Rose-John, S.; Yokota, Y. and Zenke, M. (2003): Transcriptional profiling identifies Id2 function in dendritic cell development, Nat Immunol (vol. 4), No. 4, pp. 380-6.

Han, L.; Lin, I. G. and Hsieh, C. L. (2001): Protein binding protects sites on stable episomes and in the chromosome from de novo methylation, Mol Cell Biol (vol. 21), No. 10, pp. 3416-24.

Hansen, J. D. and Zapata, A. G. (1998): Lymphocyte development in fish and amphibians, Immunol Rev (vol. 166), pp. 199-220.

Hata, K.; Okano, M.; Lei, H. and Li, E. (2002): Dnmt3L cooperates with the Dnmt3 family of de novo DNA methyltransferases to establish maternal imprints in mice, Development (vol. 129), No. 8, pp. 1983-93.

Hendrich, B.; Hardeland, U.; Ng, H. H.; Jiricny, J. and Bird, A. (1999): The thymine glycosylase MBD4 can bind to the product of deamination at methylated CpG sites, Nature (vol. 401), No. 6750, pp. 301-4.

Hobeika, E.; Thiemann, S.; Storch, B.; Jumaa, H.; Nielsen, P. J.; Pelanda, R. and Reth, M. (2006): Testing gene function early in the B cell lineage in mb1-cre mice, Proc Natl Acad Sci U S A (vol. 103), No. 37, pp. 13789-94.

Hochedlinger, K. and Plath, K. (2009): Epigenetic reprogramming and induced pluripotency, Development (vol. 136), No. 4, pp. 509-23.

Holler, M.; Westin, G.; Jiricny, J. and Schaffner, W. (1988): Sp1 transcription factor binds DNA and activates transcription even when the binding site is CpG methylated, Genes Dev (vol. 2), No. 9, pp. 1127-35.

Hollick, J. B.; Dorweiler, J. E. and Chandler, V. L. (1997): Paramutation and related allelic interactions, Trends Genet (vol. 13), No. 8, pp. 302-8.

Howlett, S. K. and Reik, W. (1991): Methylation levels of maternal and paternal genomes during preimplantation development, Development (vol. 113), No. 1, pp. 119-27.

Ikawa, T.; Fujimoto, S.; Kawamoto, H.; Katsura, Y. and Yokota, Y. (2001): Commitment to natural killer cells requires the helix-loop-helix inhibitor Id2, Proc Natl Acad Sci U S A (vol. 98), No. 9, pp. 5164-9.

Inamdar, N. M.; Ehrlich, K. C. and Ehrlich, M. (1991): CpG methylation inhibits binding of several sequence-specific DNA-binding proteins from pea, wheat, soybean and cauliflower, Plant Mol Biol (vol. 17), No. 1, pp. 111-23.

Inlay, M. and Xu, Y. (2003): Epigenetic regulation of antigen receptor rearrangement, Clin Immunol (vol. 109), No. 1, pp. 29-36.

Iwasaki, H.; Mizuno, S.; Wells, R. A.; Cantor, A. B.; Watanabe, S. and Akashi, K. (2003): GATA-1 converts lymphoid and myelomonocytic progenitors into the megakaryocyte/erythrocyte lineages, Immunity (vol. 19), No. 3, pp. 451-62.

Jackson-Grusby, L.; Beard, C.; Possemato, R.; Tudor, M.; Fambrough, D.; Csankovszki, G.; Dausman, J.; Lee, P.; Wilson, C.; Lander, E. and Jaenisch, R. (2001): Loss of genomic methylation causes p53-dependent apoptosis and epigenetic deregulation, Nat Genet (vol. 27), No. 1, pp. 31-9.

Janeway, Charles A.; Travers, Paul; Walport, Mark; Shlomchik, Mark (2001): Immunobiology, Garland Science, New York and London.

Jia, D.; Jurkowska, R. Z.; Zhang, X.; Jeltsch, A. and Cheng, X. (2007): Structure of Dnmt3a bound to Dnmt3L suggests a model for de novo DNA methylation, Nature (vol. 449), No. 7159, pp. 248-51.

Jones, P. L.; Veenstra, G. J.; Wade, P. A.; Vermaak, D.; Kass, S. U.; Landsberger, N.; Strouboulis, J. and Wolffe, A. P. (1998): Methylated DNA and MeCP2 recruit histone deacetylase to repress transcription, Nat Genet (vol. 19), No. 2, pp. 187-91.

Kaiho, S. and Mizuno, K. (1985): Sensitive assay systems for detection of hemoglobin with 2,7-diaminofluorene: histochemistry and colorimetry for erythrodifferentiation, Anal Biochem (vol. 149), No. 1, pp. 117-20.

Kaushansky, K. (2006): Lineage-specific hematopoietic growth factors, N Engl J Med (vol. 354), No. 19, pp. 2034-45.

Keller, G.; Paige, C.; Gilboa, E. and Wagner, E. F. (1985): Expression of a foreign gene in myeloid and lymphoid cells derived from multipotent haematopoietic precursors, Nature (vol. 318), No. 6042, pp. 149-54.

Keller, G. and Snodgrass, R. (1990): Life span of multipotential hematopoietic stem cells in vivo, J Exp Med (vol. 171), No. 5, pp. 1407-18.

Kiel, M. J.; Yilmaz, O. H.; Iwashita, T.; Yilmaz, O. H.; Terhorst, C. and Morrison, S. J. (2005): SLAM family receptors distinguish hematopoietic stem and progenitor cells and reveal endothelial niches for stem cells, Cell (vol. 121), No. 7, pp. 1109-21.

Klug, M. and Rehli, M. (2006): Functional analysis of promoter CpG methylation using a CpG-free luciferase reporter vector, Epigenetics (vol. 1), No. 3, pp. 127-30.

Kodama, H.; Nose, M.; Niida, S.; Nishikawa, S. and Nishikawa, S. (1994): Involvement of the c-kit receptor in the adhesion of hematopoietic stem cells to stromal cells, Exp Hematol (vol. 22), No. 10, pp. 979-84.

Koschmieder, S.; Rosenbauer, F.; Steidl, U.; Owens, B. M. and Tenen, D. G. (2005): Role of transcription factors C/EBPalpha and PU.1 in normal hematopoiesis and leukemia, Int J Hematol (vol. 81), No. 5, pp. 368-77.

Kovesdi, I.; Reichel, R. and Nevins, J. R. (1987): Role of an adenovirus E2 promoter binding factor in E1A-mediated coordinate gene control, Proc Natl Acad Sci U S A (vol. 84), No. 8, pp. 2180-4.

Krivtsov, A. V.; Twomey, D.; Feng, Z.; Stubbs, M. C.; Wang, Y.; Faber, J.; Levine, J. E.; Wang, J.; Hahn, W. C.; Gilliland, D. G.; Golub, T. R. and Armstrong, S. A. (2006): Transformation from committed progenitor to leukaemia stem cell initiated by MLL-AF9, Nature (vol. 442), No. 7104, pp. 818-22.

Kuhn, R.; Schwenk, F.; Aguet, M. and Rajewsky, K. (1995): Inducible gene targeting in mice, Science (vol. 269), No. 5229, pp. 1427-9.

Laiosa, C. V.; Stadtfeld, M. and Graf, T. (2006): Determinants of lymphoid-myeloid lineage diversification, Annu Rev Immunol (vol. 24), pp. 705-38.

Laird, P. W.; Jackson-Grusby, L.; Fazeli, A.; Dickinson, S. L.; Jung, W. E.; Li, E.; Weinberg, R. A. and Jaenisch, R. (1995): Suppression of intestinal neoplasia by DNA hypomethylation, Cell (vol. 81), No. 2, pp. 197-205.

Landgrebe, J.; Wurst, W. and Welzl, G. (2002): Permutation-validated principal components analysis of microarray data, Genome Biol (vol. 3), No. 4, p. RESEARCH0019.

Lee, P. P.; Fitzpatrick, D. R.; Beard, C.; Jessup, H. K.; Lehar, S.; Makar, K. W.; Perez-Melgosa, M.; Sweetser, M. T.; Schlissel, M. S.; Nguyen, S.; Cherry, S. R.; Tsai, J. H.; Tucker, S. M.; Weaver, W. M.; Kelso, A.; Jaenisch, R. and Wilson, C. B. (2001): A critical role for Dnmt1 and DNA methylation in T cell development, function, and survival, Immunity (vol. 15), No. 5, pp. 763-74.

Lei, H.; Oh, S. P.; Okano, M.; Juttermann, R.; Goss, K. A.; Jaenisch, R. and Li, E. (1996): De novo DNA cytosine methyltransferase activities in mouse embryonic stem cells, Development (vol. 122), No. 10, pp. 3195-205.

Lemischka, I. R.; Raulet, D. H. and Mulligan, R. C. (1986): Developmental potential and dynamic behavior of hematopoietic stem cells, Cell (vol. 45), No. 6, pp. 917-27.

Leonhardt, H.; Page, A. W.; Weier, H. U. and Bestor, T. H. (1992): A targeting sequence directs DNA methyltransferase to sites of DNA replication in mammalian nuclei, Cell (vol. 71), No. 5, pp. 865-73.

Li, E. (2002): Chromatin modification and epigenetic reprogramming in mammalian development, Nat Rev Genet (vol. 3), No. 9, pp. 662-73.

Li, E.; Beard, C. and Jaenisch, R. (1993): Role for DNA methylation in genomic imprinting, Nature (vol. 366), No. 6453, pp. 362-5.

Li, E.; Bestor, T. H. and Jaenisch, R. (1992): Targeted mutation of the DNA methyltransferase gene results in embryonic lethality, Cell (vol. 69), No. 6, pp. 915-26.

Lin, H. and Grosschedl, R. (1995): Failure of B-cell differentiation in mice lacking the transcription factor EBF, Nature (vol. 376), No. 6537, pp. 263-7.

Lorenz, E.; Uphoff, D.; Reid, T. R. and Shelton, E. (1951): Modification of irradiation injury in mice and guinea pigs by bone marrow injections, J Natl Cancer Inst (vol. 12), No. 1, pp. 197-201.

Lyko, F.; Ramsahoye, B. H.; Kashevsky, H.; Tudor, M.; Mastrangelo, M. A.; Orr-Weaver, T. L. and Jaenisch, R. (1999): Mammalian (cytosine-5) methyltransferases cause genomic DNA methylation and lethality in Drosophila, Nat Genet (vol. 23), No. 3, pp. 363-6.

Mansson, R.; Hultquist, A.; Luc, S.; Yang, L.; Anderson, K.; Kharazi, S.; Al-Hashmi, S.; Liuba, K.; Thoren, L.; Adolfsson, J.; Buza-Vidas, N.; Qian, H.; Soneji, S.; Enver, T.; Sigvardsson, M. and Jacobsen, S. E. (2007): Molecular evidence for hierarchical transcriptional lineage priming in fetal and adult stem cells and multipotent progenitors, Immunity (vol. 26), No. 4, pp. 407-19.

Medina, K. L. and Singh, H. (2005): Genetic networks that regulate B lymphopoiesis, Curr Opin Hematol (vol. 12), No. 3, pp. 203-9.

Meissner, A.; Mikkelsen, T. S.; Gu, H.; Wernig, M.; Hanna, J.; Sivachenko, A.; Zhang, X.; Bernstein, B. E.; Nusbaum, C.; Jaffe, D. B.; Gnirke, A.; Jaenisch, R. and Lander, E. S. (2008): Genome-scale DNA methylation maps of pluripotent and differentiated cells, Nature (vol. 454), No. 7205, pp. 766-70.

Melki, J. R. and Clark, S. J. (2002): DNA methylation changes in leukaemia, Semin Cancer Biol (vol. 12), No. 5, pp. 347-57.

Mikkola, I.; Heavey, B.; Horcher, M. and Busslinger, M. (2002): Reversion of B cell commitment upon loss of Pax5 expression, Science (vol. 297), No. 5578, pp. 110-3.

Miyamoto, T.; Iwasaki, H.; Reizis, B.; Ye, M.; Graf, T.; Weissman, I. L. and Akashi, K. (2002): Myeloid or lymphoid promiscuity as a critical step in hematopoietic lineage commitment, Dev Cell (vol. 3), No. 1, pp. 137-47.

Mlynarczyk, S. K. and Panning, B. (2000): X inactivation: Tsix and Xist as yin and yang, Curr Biol (vol. 10), No. 24, pp. R899-903.

Moens, U.; Subramaniam, N.; Johansen, B. and Aarbakke, J. (1993): The c-fos cAMP-response element: regulation of gene expression by a beta 2-

adrenergic agonist, serum and DNA methylation, Biochim Biophys Acta (vol. 1173), No. 1, pp. 63-70.

Mohn, F.; Weber, M.; Rebhan, M.; Roloff, T. C.; Richter, J.; Stadler, M. B.; Bibel, M. and Schubeler, D. (2008): Lineage-specific polycomb targets and de novo DNA methylation define restriction and potential of neuronal progenitors, Mol Cell (vol. 30), No. 6, pp. 755-66.

Mohn, F.; Weber, M.; Schubeler, D. and Roloff, T. C. (2009): Methylated DNA immunoprecipitation (MeDIP), Methods Mol Biol (vol. 507), pp. 55-64.

Morita, S.; Kojima, T. and Kitamura, T. (2000): Plat-E: an efficient and stable system for transient packaging of retroviruses, Gene Ther (vol. 7), No. 12, pp. 1063-6.

Morrison, S. J.; Uchida, N. and Weissman, I. L. (1995): The biology of hematopoietic stem cells, Annu Rev Cell Dev Biol (vol. 11), pp. 35-71.

Nakano, T.; Kodama, H. and Honjo, T. (1994): Generation of lymphohematopoietic cells from embryonic stem cells in culture, Science (vol. 265), No. 5175, pp. 1098-101.

Nan, X.; Ng, H. H.; Johnson, C. A.; Laherty, C. D.; Turner, B. M.; Eisenman, R. N. and Bird, A. (1998): Transcriptional repression by the methyl-CpG-binding protein MeCP2 involves a histone deacetylase complex, Nature (vol. 393), No. 6683, pp. 386-9.

Ng, H. H.; Jeppesen, P. and Bird, A. (2000): Active repression of methylated genes by the chromosomal protein MBD1, Mol Cell Biol (vol. 20), No. 4, pp. 1394-406.

Ng, H. H.; Zhang, Y.; Hendrich, B.; Johnson, C. A.; Turner, B. M.; Erdjument-Bromage, H.; Tempst, P.; Reinberg, D. and Bird, A. (1999): MBD2 is a transcriptional repressor belonging to the MeCP1 histone deacetylase complex, Nat Genet (vol. 23), No. 1, pp. 58-61.

Ng, R. K.; Dean, W.; Dawson, C.; Lucifero, D.; Madeja, Z.; Reik, W. and Hemberger, M. (2008): Epigenetic restriction of embryonic cell lineage fate by methylation of Elf5, Nat Cell Biol (vol. 10), No. 11, pp. 1280-90.

Niehrs, C. (2009): Active DNA demethylation and DNA repair, Differentiation (vol. 77), No. 1, pp. 1-11.

Nutt, S. L.; Heavey, B.; Rolink, A. G. and Busslinger, M. (1999): Commitment to the B-lymphoid lineage depends on the transcription factor Pax5, Nature (vol. 401), No. 6753, pp. 556-62.

Ogawa, M. (1993): Differentiation and proliferation of hematopoietic stem cells, Blood (vol. 81), No. 11, pp. 2844-53.

Okano, M.; Bell, D. W.; Haber, D. A. and Li, E. (1999): DNA methyltransferases Dnmt3a and Dnmt3b are essential for de novo methylation and mammalian development, Cell (vol. 99), No. 3, pp. 247-57.

Okano, M.; Xie, S. and Li, E. (1998): Dnmt2 is not required for de novo and maintenance methylation of viral DNA in embryonic stem cells, Nucleic Acids Res (vol. 26), No. 11, pp. 2536-40.

Pevny, L.; Simon, M. C.; Robertson, E.; Klein, W. H.; Tsai, S. F.; D'Agati, V.; Orkin, S. H. and Costantini, F. (1991): Erythroid differentiation in chimaeric mice blocked by a targeted mutation in the gene for transcription factor GATA-1, Nature (vol. 349), No. 6306, pp. 257-60.

Pongubala, J. M.; Northrup, D. L.; Lancki, D. W.; Medina, K. L.; Treiber, T.; Bertolino, E.; Thomas, M.; Grosschedl, R.; Allman, D. and Singh, H. (2008): Transcription factor EBF restricts alternative lineage options and promotes B cell fate commitment independently of Pax5, Nat Immunol (vol. 9), No. 2, pp. 203-15.

Prendergast, G. C.; Lawe, D. and Ziff, E. B. (1991): Association of Myn, the murine homolog of max, with c-Myc stimulates methylation-sensitive DNA binding and ras cotransformation, Cell (vol. 65), No. 3, pp. 395-407.

Prendergast, G. C. and Ziff, E. B. (1991): Methylation-sensitive sequence-specific DNA binding by the c-Myc basic region, Science (vol. 251), No. 4990, pp. 186-9.

Prinz, M.; Schmidt, H.; Mildner, A.; Knobeloch, K. P.; Hanisch, U. K.; Raasch, J.; Merkler, D.; Detje, C.; Gutcher, I.; Mages, J.; Lang, R.; Martin, R.; Gold, R.; Becher, B.; Bruck, W. and Kalinke, U. (2008): Distinct and nonredundant in vivo functions of IFNAR on myeloid cells limit autoimmunity in the central nervous system, Immunity (vol. 28), No. 5, pp. 675-86.

Prokhortchouk, A.; Hendrich, B.; Jorgensen, H.; Ruzov, A.; Wilm, M.; Georgiev, G.; Bird, A. and Prokhortchouk, E. (2001): The p120 catenin partner Kaiso is a DNA methylation-dependent transcriptional repressor, Genes Dev (vol. 15), No. 13, pp. 1613-8.

Purton, L. E. and Scadden, D. T. (2007): Limiting factors in murine hematopoietic stem cell assays, Cell Stem Cell (vol. 1), No. 3, pp. 263-70.

Radtke, F.; Wilson, A.; Stark, G.; Bauer, M.; van Meerwijk, J.; MacDonald, H. R. and Aguet, M. (1999): Deficient T cell fate specification in mice with an induced inactivation of Notch1, Immunity (vol. 10), No. 5, pp. 547-58.

Rai, K.; Huggins, I. J.; James, S. R.; Karpf, A. R.; Jones, D. A. and Cairns, B. R. (2008): DNA demethylation in zebrafish involves the coupling of a deaminase, a glycosylase, and gadd45, Cell (vol. 135), No. 7, pp. 1201-12.

Razin, A. and Szyf, M. (1984): DNA methylation patterns. Formation and function, Biochim Biophys Acta (vol. 782), No. 4, pp. 331-42.

Reik, W. and Walter, J. (2001): Genomic imprinting: parental influence on the genome, Nat Rev Genet (vol. 2), No. 1, pp. 21-32.

Rhee, I.; Bachman, K. E.; Park, B. H.; Jair, K. W.; Yen, R. W.; Schuebel, K. E.; Cui, H.; Feinberg, A. P.; Lengauer, C.; Kinzler, K. W.; Baylin, S. B. and Vogelstein, B. (2002): DNMT1 and DNMT3b cooperate to silence genes in human cancer cells, Nature (vol. 416), No. 6880, pp. 552-6.

Rickert, R. C.; Roes, J. and Rajewsky, K. (1997): B lymphocyte-specific, Cre-mediated mutagenesis in mice, Nucleic Acids Res (vol. 25), No. 6, pp. 1317-8.

Riddle, N. C. and Elgin, S. C. (2008): A role for RNAi in heterochromatin formation in Drosophila, Curr Top Microbiol Immunol (vol. 320), pp. 185-209.

Robertson, K. D. (2005): DNA methylation and human disease, Nat Rev Genet (vol. 6), No. 8, pp. 597-610.

Robertson, K. D.; Ait-Si-Ali, S.; Yokochi, T.; Wade, P. A.; Jones, P. L. and Wolffe, A. P. (2000): DNMT1 forms a complex with Rb, E2F1 and HDAC1 and represses transcription from E2F-responsive promoters, Nat Genet (vol. 25), No. 3, pp. 338-42.

Robertson, K. D. and Wolffe, A. P. (2000): DNA methylation in health and disease, Nat Rev Genet (vol. 1), No. 1, pp. 11-9.

Rosenbauer, F. and Tenen, D. G. (2007): Transcription factors in myeloid development: balancing differentiation with transformation, Nat Rev Immunol (vol. 7), No. 2, pp. 105-17.

Rougier, N.; Bourc'his, D.; Gomes, D. M.; Niveleau, A.; Plachot, M.; Paldi, A. and Viegas-Pequignot, E. (1998): Chromosome methylation patterns during mammalian preimplantation development, Genes Dev (vol. 12), No. 14, pp. 2108-13.

Sauvageau, M. and Sauvageau, G. (2008): Polycomb group genes: keeping stem cell activity in balance, PLoS Biol (vol. 6), No. 4, p. e113.

Schlissel, M. S. (2004): Regulation of activation and recombination of the murine Igkappa locus, Immunol Rev (vol. 200), pp. 215-23.

Schmitt, T. M.; de Pooter, R. F.; Gronski, M. A.; Cho, S. K.; Ohashi, P. S. and Zuniga-Pflucker, J. C. (2004): Induction of T cell development and establishment of T cell competence from embryonic stem cells differentiated in vitro, Nat Immunol (vol. 5), No. 4, pp. 410-7.

Schmitt, T. M. and Zuniga-Pflucker, J. C. (2002): Induction of T cell development from hematopoietic progenitor cells by delta-like-1 in vitro, Immunity (vol. 17), No. 6, pp. 749-56.

Schneider, R. and Grosschedl, R. (2007): Dynamics and interplay of nuclear architecture, genome organization, and gene expression, Genes Dev (vol. 21), No. 23, pp. 3027-43.

Scott, E. W.; Simon, M. C.; Anastasi, J. and Singh, H. (1994): Requirement of transcription factor PU.1 in the development of multiple hematopoietic lineages, Science (vol. 265), No. 5178, pp. 1573-7.

Shen, X.; Liu, Y.; Hsu, Y. J.; Fujiwara, Y.; Kim, J.; Mao, X.; Yuan, G. C. and Orkin, S. H. (2008): EZH1 mediates methylation on histone H3 lysine 27 and complements EZH2 in maintaining stem cell identity and executing pluripotency, Mol Cell (vol. 32), No. 4, pp. 491-502.

Slack, A.; Pinard, M.; Araujo, F. D. and Szyf, M. (2001): A novel regulatory element in the dnmt1 gene that responds to co-activation by Rb and c-Jun, Gene (vol. 268), No. 1-2, pp. 87-96.

Slotkin, R. K. and Martienssen, R. (2007): Transposable elements and the epigenetic regulation of the genome, Nat Rev Genet (vol. 8), No. 4, pp. 272-85.

Smallwood, A.; Esteve, P. O.; Pradhan, S. and Carey, M. (2007): Functional cooperation between HP1 and DNMT1 mediates gene silencing, Genes Dev (vol. 21), No. 10, pp. 1169-78.

Srinivas, S.; Watanabe, T.; Lin, C. S.; William, C. M.; Tanabe, Y.; Jessell, T. M. and Costantini, F. (2001): Cre reporter strains produced by targeted insertion of EYFP and ECFP into the ROSA26 locus, BMC Dev Biol (vol. 1), p. 4.

Suzuki, M. M. and Bird, A. (2008): DNA methylation landscapes: provocative insights from epigenomics, Nat Rev Genet (vol. 9), No. 6, pp. 465-76.

Szyf, M. and Detich, N. (2001): Regulation of the DNA methylation machinery and its role in cellular transformation, Prog Nucleic Acid Res Mol Biol (vol. 69), pp. 47-79.

Tadokoro, Y.; Ema, H.; Okano, M.; Li, E. and Nakauchi, H. (2007): De novo DNA methyltransferase is essential for self-renewal, but not for differentiation, in hematopoietic stem cells, J Exp Med (vol. 204), No. 4, pp. 715-22.

Takahashi, S.; Shimizu, R.; Suwabe, N.; Kuroha, T.; Yoh, K.; Ohta, J.; Nishimura, S.; Lim, K. C.; Engel, J. D. and Yamamoto, M. (2000): GATA factor transgenes under GATA-1 locus control rescue germline GATA-1 mutant deficiencies, Blood (vol. 96), No. 3, pp. 910-6.

Tanaka, T.; Akira, S.; Yoshida, K.; Umemoto, M.; Yoneda, Y.; Shirafuji, N.; Fujiwara, H.; Suematsu, S.; Yoshida, N. and Kishimoto, T. (1995): Targeted disruption of the NF-IL6 gene discloses its essential role in bacteria killing and tumor cytotoxicity by macrophages, Cell (vol. 80), No. 2, pp. 353-61.

Turek-Plewa, J. and Jagodzinski, P. P. (2005): The role of mammalian DNA methyltransferases in the regulation of gene expression, Cell Mol Biol Lett (vol. 10), No. 4, pp. 631-47.

Urieli-Shoval, S.; Gruenbaum, Y.; Sedat, J. and Razin, A. (1982): The absence of detectable methylated bases in Drosophila melanogaster DNA, FEBS Lett (vol. 146), No. 1, pp. 148-52.

Ushijima, T.; Morimura, K.; Hosoya, Y.; Okonogi, H.; Tatematsu, M.; Sugimura, T. and Nagao, M. (1997): Establishment of methylation-sensitive-representational difference analysis and isolation of hypo- and hypermethylated genomic fragments in mouse liver tumors, Proc Natl Acad Sci U S A (vol. 94), No. 6, pp. 2284-9.

Vermes, I.; Haanen, C.; Steffens-Nakken, H. and Reutelingsperger, C. (1995): A novel assay for apoptosis. Flow cytometric detection of phosphatidylserine expression on early apoptotic cells using fluorescein labelled Annexin V, J Immunol Methods (vol. 184), No. 1, pp. 39-51.

Vire, E.; Brenner, C.; Deplus, R.; Blanchon, L.; Fraga, M.; Didelot, C.; Morey, L.; Van Eynde, A.; Bernard, D.; Vanderwinden, J. M.; Bollen, M.; Esteller, M.; Di Croce, L.; de Launoit, Y. and Fuks, F. (2006): The Polycomb group protein EZH2 directly controls DNA methylation, Nature (vol. 439), No. 7078, pp. 871-4.

Waddington, C.H. (1942), Endeavour, No. 1, pp. 18-20.

Waddington, C.H. (1957): The Strategy of the Genes; a Discussion of Some Aspects of Theoretical Biology, London: Allen & Unwin.

Wakimoto, B. T. (1998): Beyond the nucleosome: epigenetic aspects of position-effect variegation in Drosophila, Cell (vol. 93), No. 3, pp. 321-4.

Walsh, J. C.; DeKoter, R. P.; Lee, H. J.; Smith, E. D.; Lancki, D. W.; Gurish, M. F.; Friend, D. S.; Stevens, R. L.; Anastasi, J. and Singh, H. (2002): Cooperative and antagonistic interplay between PU.1 and GATA-2 in the specification of myeloid cell fates, Immunity (vol. 17), No. 5, pp. 665-76.

Weber, M.; Hellmann, I.; Stadler, M. B.; Ramos, L.; Paabo, S.; Rebhan, M. and Schubeler, D. (2007): Distribution, silencing potential and evolutionary impact of promoter DNA methylation in the human genome, Nat Genet (vol. 39), No. 4, pp. 457-66.

Wilson, A.; Murphy, M. J.; Oskarsson, T.; Kaloulis, K.; Bettess, M. D.; Oser, G. M.; Pasche, A. C.; Knabenhans, C.; Macdonald, H. R. and Trumpp, A. (2004): c-

Myc controls the balance between hematopoietic stem cell self-renewal and differentiation, Genes Dev (vol. 18), No. 22, pp. 2747-63.

Wilson, A. and Trumpp, A. (2006): Bone-marrow haematopoietic-stem-cell niches, Nat Rev Immunol (vol. 6), No. 2, pp. 93-106.

Wolffe, A. P. (2000): Transcriptional control: imprinting insulation, Curr Biol (vol. 10), No. 12, pp. R463-5.

Xie, H.; Ye, M.; Feng, R. and Graf, T. (2004): Stepwise reprogramming of B cells into macrophages, Cell (vol. 117), No. 5, pp. 663-76.

Yoder, J. A.; Soman, N. S.; Verdine, G. L. and Bestor, T. H. (1997): DNA (cytosine-5)-methyltransferases in mouse cells and tissues. Studies with a mechanism-based probe, J Mol Biol (vol. 270), No. 3, pp. 385-95.

Yokota, Y.; Mansouri, A.; Mori, S.; Sugawara, S.; Adachi, S.; Nishikawa, S. and Gruss, P. (1999): Development of peripheral lymphoid organs and natural killer cells depends on the helix-loop-helix inhibitor Id2, Nature (vol. 397), No. 6721, pp. 702-6.

Yu, F.; Thiesen, J. and Stratling, W. H. (2000): Histone deacetylase-independent transcriptional repression by methyl-CpG-binding protein 2, Nucleic Acids Res (vol. 28), No. 10, pp. 2201-6.

Zhang, D. E.; Zhang, P.; Wang, N. D.; Hetherington, C. J.; Darlington, G. J. and Tenen, D. G. (1997): Absence of granulocyte colony-stimulating factor signaling and neutrophil development in CCAAT enhancer binding protein alpha-deficient mice, Proc Natl Acad Sci U S A (vol. 94), No. 2, pp. 569-74.

Zhang, J.; Grindley, J. C.; Yin, T.; Jayasinghe, S.; He, X. C.; Ross, J. T.; Haug, J. S.; Rupp, D.; Porter-Westpfahl, K. S.; Wiedemann, L. M.; Wu, H. and Li, L. (2006): PTEN maintains haematopoietic stem cells and acts in lineage choice and leukaemia prevention, Nature (vol. 441), No. 7092, pp. 518-22.

Zhang, P.; Iwasaki-Arai, J.; Iwasaki, H.; Fenyus, M. L.; Dayaram, T.; Owens, B. M.; Shigematsu, H.; Levantini, E.; Huettner, C. S.; Lekstrom-Himes, J. A.; Akashi, K. and Tenen, D. G. (2004): Enhancement of hematopoietic stem cell repopulating capacity and self-renewal in the absence of the transcription factor C/EBP alpha, Immunity (vol. 21), No. 6, pp. 853-63.

Abbreviations

% percentage
Aa amino acid
AID activation induced deaminase
AP2 activating protein 2
APC allophycocyanin
APC-β-catenin-TCF adenomatous polyposis coli-beta-catenin-T cell factor
ATRX cysteine-rich zinc finger
bcl-2 B-cell lymphoma 2
BM bone marrow
BP B-cell progenitor
bp base pair(s)
BSA bovine serum albumin
C cytosine
C/EBP CCAATT/enhancer binding protein
cAMP response element CRE
c-fms or **csf1r** colony stimulating factor 1 receptor
c-myc myelocytomatosis viral oncogene homolog
CpG cytosine guanine dinucleotide
Cre cyclization recombination protein
DAPI 4',6-diamidino-2-phenylindole
DMEM Dulbecco's modified Eagle medium
DMSO dimethylsulfoxid
DNA desoxyribonucleic acid
DNA desoxyribonucleic acid
dNTP deoxynucleotide triphosphate
DTT dithiotreitol
E embryonic day
e.g. exempli gratia
E2F early gene 2 factor
Ebf1 early B cell factor 1
EDTA ethylenediaminetetraacetate
Env envelope protein
EPO erythropoietin
ES cells embryonic stem cells
EYFP enhanced yellow fluorescent protein
EZH2 enhancer of zeste homolog 2
FACS fluorescent activated cell sorting
FCS fetal calf serum

FITC fluoresceinisothiocyanat
FL fetal liver
Flt3 Fms- related tyrosine kinase 3
Flt3L Flt3 ligand
g gravity
G/M-CSF granulocyte/macrophage stimulating factor
G9A also known as **EHMT2** euchromatic histone-lysine N-methyltransferase 2
Gadd45 growth arrest and DNA damage
Gag-pol group antigen protein - polymerase
Gata1 GATA binding protein 1 or globin transcription factor 1
GFP green-fluorescent protein
h hour
H3K9met3 Tri-methylated Lysine 9 of Histone H3
HCT116 human colon epithelial cell line
HDAC histone deacetylase
HMTase histone methyltransferase
HP1 heterochromatin protein 1
HSC hematopoietic stem cell
IAP intracisternal A particle
ICF immunodeficiency, centromeric instability and facial anomalies syndrome
Id2 inhibitor of DNA binding 2
Igf2 insulin-like growth factor 2
IL interleukin
Ires internal ribosomal entry site
Kb kilobase
KCl potassium chloride
KH_2PO_4 potassium phosphate monobasic
Klf4 kruppel like factor 4
Lif leukemia inducing factor
LM-PCR clinker mediated polymerase chain reaction
M molar
MEM modified Eagle's Medium
MFI mean fluorescence intensity
mg milligram
min minutes
Mk megakaryocyte
Mk megakaryocytic
ml milliliter
mM milli molar
mM millimolar
MP myeloid progenitor

mRNA messenger ribonucleic acid
Mx1 myxovirus (influenza virus) resistance 1
n number
Na_2HPO_4 Sodium phosphate dibasic
NaCl Sodiumchloride
NF-κB nuclear factor 'kappa-light-chain-enhancer' of activated B-cells
Oct3/4 octamer binding transcription factor 3/4
P probability value
Pax5 paired box gene 5
PBS phosphate buffered saline
PCA principal components analysis
PcG polycomb group
PCR polymerase-chain-reaction
PE Phycoerythrin
Polybrene hexadimethrine bromide
PRC polycomb complex
pSP para-aorta splanchnopleura
ptcrα pre T cell antigen receptor alpha
Pten Phosphatase and tensin homologue
R26R Rosa locus
RNA ribonucleic acid
rpm rotations per minute
RT room teperature
RT-PCR reverse transcription real time polymerase chain reaction
s.d. standard deviation
SAM *S*-adenosylmethionin
SCF stem cell factor
Scl/tal1 stem cell leukemia/T cell acute lymphoblastic leukemia 1
SDS Natriumdodecylsulfat
Sox2 sex determining region Y box 2
T thymidine
T4 T4 DNA polymerase
TAE Tris/acetate/EDTA buffer
Taq Taqman DNA polymerase
TE Tris/EDTA
TPO thrombopoisis stimulating factor
tRNA transfer RNA
UV Ultraviolet
WT wild type
X X chromosome
µg microgram

µl microliter
µM micromolar
µM micromolar

Selbständigkeitserklärung

Ich versichere hiermit, dass die von mir vorgelegte Dissertation eigenständig und ohne Benutzung anderer als der angegebenen Hilfsmittel angefertigt wurde. Ich versichere, dass alle aus anderen Quellen übernommenen Daten und Konzepte, sowie Ergebnisse aus Kooperationsprojekten unter Angabe der Referenz gekennzeichnet sind.
Außerdem versichere ich, dass mir die aktuelle Promotionsordnung bekannt ist und ich mich nicht anderwärts um einen Doktorgrad bewerbe, bzw. noch keinen entsprechenden Doktorgrad besitze. Diese Arbeit wurde in gleicher oder ähnlicher Form nicht einer anderen Prüfungsbehörde vorgelegt.

Berlin, den 14.10.2009

Ann-Marie Elisabeth Bröske

Acknowledgements

In the first place, I would like to thank Dr. Frank Rosenbauer for providing the opportunity to perform my PhD project in his laboratory, for his financial support and permanent scientific support.
Furthermore, I want to thank Dr. Marina Scheller for answering all questions concerning mouse work and her encouragement. Additionally, I want to thank all members of the AG Leutz for unhesitant helpfulness with experiments and constructive criticism in shared seminars.
I want to thank Prof. Dr. S. E. Jacobsen for the knowledge I have acquired in his laboratory and Shabnam Kharazi for her great help in Lund.
Thanks to Dr. Miguel Andrade-Navarro and Matthew Huska for the help with all bioinformatics and to Prof. Dr. Marco Prinz for his help with histology work.
I want to thank Victoria Malchin, Christine Graubmann, Lotte Huismann and Nancy Endruhn for their excellent mouse work. Moreover, I would like to thank all AG Rosenbauer members for their technical advices, fruitful discussions and constant practical and mental support.
I want to thank the program for equal opportunity of the Humboldt University Berlin, the HGS-MCB travel support of the Max-Delbrück-Center, the Deutsche Krebhilfe and the Berliner Krebsgesellschaft e.V. for their financial support.

My biggest thank goes to Lena Vockentanz for working together with me on this enormous project, sharing every up and down in the last three years and getting a close friend.
Needless to say that nothing of this work would have been possible without the love of my friends, my family and Kai.